



# PPNW 2023

## International workshop on Physical Processes in Natural Waters

---

19-23 June 2023  
Brescia (Italy)



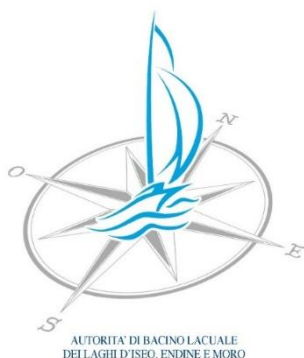
UNIVERSITÀ  
DEGLI STUDI  
DI BRESCIA

*Organized with the support of:*

**Acque Bresciane**  
Servizio Idrico Integrato

**Hortus**  
Monitoring Solutions & Software Applications

**Navigazione**  
Lago d'Iseo



**RISERVA  
NATURALE  
TORBIERE  
DEL SEBINO**

**FONDAZIONE  
MUSEI**  
BRESCIA



**ROCKLAND  
SCIENTIFIC**



UNIVERSITÀ  
DEGLI STUDI  
DI BRESCIA

*Con la collaborazione:*



**Siamo  
Capitale  
Italiana  
della Cultura  
2023**

BERGAMO  
BRESCIA

# Program

**19/6 18:30-20:30 *Complesso dei Chiostri del Carmine*  
Vicolo dell'Anguilla, 8**  
Registration and welcome aperitif

**20/6 08:00-18:00 *Room 1 of Law Department*  
Via S. Faustino, 41**  
Registration and welcome  
Regular session

**21/6 08:30-15:00 *Room 1 of Law Department*  
Via S. Faustino, 41**  
Regular session

**21/6 16:20-22:30 *Brescia, old town*  
Historical tour (Via dei Musei, 55)  
Social dinner (Via dei Musei, 25)**

**22/6 08:30-17:30 *Room 1 of Law Department*  
Via S. Faustino, 41**  
Regular session

**23/6 08:30-13:00 *Room 1 of Law Department*  
Via S. Faustino, 41**  
Regular session

**23/6 14:30-23:30 *Lake Iseo*  
Field trip to Torbiere del Sebino and to Lake Iseo  
Social dinner in Monte Isola**

# Program overview and venue

## Monday 19/06/2023

Time	Event	Location	Directions
18:30 – 20:30	Welcome Aperitif	Vicolo dell'Anguilla, 8	<a href="#">Google Maps Link</a>

## Tuesday 20/06/2023

Time	Event	Location	Directions
08:00 – 18:00	Session	Via San Faustino, 41, Giurisprudenza Room 1	<a href="#">Google Maps Link</a>

## Wednesday 21/06/2023

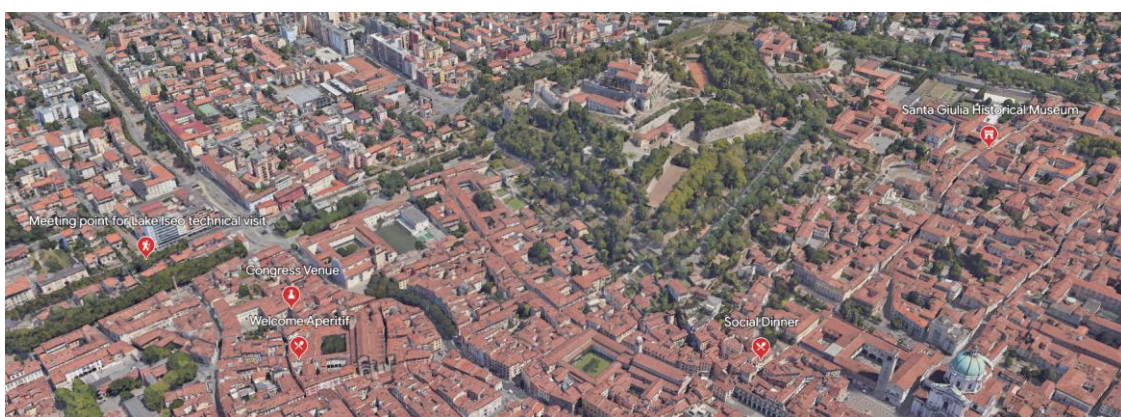
Time	Event	Location	Directions
08:30 – 15:00	Session	Via San Faustino, 41, Giurisprudenza Room 1	<a href="#">Google Maps Link</a>
16:20 – 18:30	Historical Tour	Museo di Santa Giulia, Via dei Musei, 55	<a href="#">Google Maps Link</a>
19:30 – 22:30	Social Dinner	Restaurante "Al Frate", Via dei Musei, 25	<a href="#">Google Maps Link</a>

## Thursday 22/06/2023

Time	Event	Location	Directions
08:30 – 17:30	Session	Via San Faustino 41, Giurisprudenza Room 1	<a href="#">Google Maps Link</a>

## Friday 23/06/2023

Time	Event	Location	Directions
08:30 – 13:00	Session	Via San Faustino, 41, Giurisprudenza Room 1	<a href="#">Google Maps Link</a>
14:30 – 19:30	Technical visit	Meeting point, Via Leonardo da Vinci, 9	<a href="#">Google Maps Link</a>



# Detailed program

## MONDAY 19/06/2023

18:30	20:30	Welcome aperitif and registration
-------	-------	-----------------------------------

## TUESDAY 20/06/2023

08:00	08:45	Registration
08:45	09:00	Welcome
09:00	09:30	Lorke A. Physical limnology of ponds: knowledge gaps and research perspectives
09:30	10:00	Henderson S.M. Advection and mixing in ponds
10:00	10:30	Ostrovsky I. Vertical distribution and dynamics of gas-containing cyanobacteria in relation to stratification and turbulence: insights from acoustical observations
10:30	11:00	Coffee break
11:00	11:30	Shikhani M. Composition of photosynthetic gas bubbles from submerged macrophytes
11:30	12:00	Mammarella I. Long term flux measurements of carbon dioxide and methane over a small boreal lake using eddy covariance technique
12:00	12:30	Boehrer B. Sound speed in limnic waters and its application for the detection of extreme concentrations of carbon dioxide in Lake Nyos
12:30	13:30	Lunch
13:30	14:30	<b>Rouwet D.</b> <i>Keynote lecture: Volcanic lake research: a 240(0)-year long explosive history</i>
14:30	15:00	Sherman B. The impact of extreme hydrological events on reservoir methane emissions.
15:00	15:30	Doda T. Impact of methane extraction on stratification in Lake Kivu
15:30	16:00	Coffee break
16:00	16:30	Ordonez C. Magnitude, temporal dynamics, and drivers of oxic methane production across a trophic state gradient
16:30	17:00	Thirkill R. What the sediment holds - hydroacoustic quantification of reservoir methane emissions
17:00	17:05	Bonomelli R. Far field simulation of a landslide-generated tsunami in Lake Iseo
17:05	17:10	Ramón C. L. Ebullition rates and drivers in a shallow eutrophic Mediterranean reservoir
17:10	17:15	Tedford E. Methane bubbles under ice in Base Mine Lake
17:15	17:20	Zamani B. 3D Modeling of climate change impacts on a groundwater-fed lake in Berlin area
17:20	17:25	Valerio G. Dynamics of lakes heatwaves in summer 2022: interplay between wind mixing and surface heating
17:25	18:00	Poster discussion

## WEDNESDAY 21/06/2023

08:30	09:00	Valbuena S. Rotational effects in lake upwelling and the thresholds for conceptual models
09:00	09:30	Bouffard D. Differential cooling in lakes
09:30	10:00	Serra Putellas M.T. Stem stiffness behaviour in an oscillatory flow submerged canopy patch
10:00	10:30	Kirillin G. Thermal conditions and lake metabolism in the ice-covered North Aral Sea
10:30	11:00	Coffee break
11:00	11:30	Laval B. Physical Transport in a thermobarically stratified fjord-type lake
11:30	12:00	Peng N. Identifying and quantifying deepwater-renewal processes during winter cooling in a large, deep lake (Lake Geneva)
12:00	12:30	Lilover M. J. Hunting for submesoscale temperature, salinity and current velocity signal from CTD and ADCP/RDCP profilers data in the Gulf of Finland, the Baltic Sea
12:30	13:30	Lunch
13:30	14:00	Amadori M. Analysis of spatiotemporal variability of remotely sensed variables to investigate thermal and morphological heterogeneity beneath lakes surface

14:00	14:30	Calamita E.	Satellite Earth Observation to monitor lake mixing anomalies worldwide
14:30	15:00	Pinardi M.	The Lakes_cci project: presenting the satellite-derived lakes variables for climate studies
16:20	18:30		Historical tour in Brescia
19:30	22:30		Social dinner

**THURSDAY 22/06/2023**

08:30	09:00	Spank U.	Mobile eddy covariance measurements as a key to improve estimates of momentum, mass and energy fluxes between atmosphere and inland waters
09:00	09:30	Mullarney J. C.	In-situ observations of the acoustic scattering characteristics from a suspension of flocculated particles
09:30	10:00	Pieters R.	Turbid inflow into a drinking water reservoir
10:00	10:30	Monti P.	Turbulent Schmidt number measurements in a density current flowing over surface roughness
10:30	11:00		Coffee break
11:00	11:30	Sharifi F. S.	Three-dimensional modelling of gravity currents in an idealized stratified ice-covered lake
11:30	12:30	Adduce C.	<b>Keynote lecture: Entrainment and mixing in gravity currents over complex boundaries</b>
12:30	13:30		Lunch
13:30	14:00	Piccolroaz S.	A simple model for predicting ice timing and thickness in lakes
14:00	14:30	Wang J.	Modeling two-way ice-wave interactions in the Great Lakes using FVCOM_ice+wave model
14:30	15:00	Toffolon M.	Energy considerations to understand the impact of cooling and wind on freeze-up in lakes
15:00	15:30		Coffee break
15:30	16:00	Donini G.	Simulation of short-term effects of pumped-storage hydropower on stratification and ice cover in two Norwegian reservoirs
16:00	16:30	Schmid M.	Unexpected inflow behaviour complicates assessment of heat usage potential for an ice-covered lake
16:30	16:35	Maggi M.R.	Mixing properties of steady gravity currents flowing over sloping terrain
16:35	16:40	Piotti M.	Science communication and teaching in secondary schools through limnology
16:40	16:45	Jansen J.	Weakening of inverse stratification in northern lakes
16:45	16:50	De Vincenzi M.	Role of aquatic vegetation and meteorological forcing on the hydrodynamics of Mantua Lakes: insights from a bathymetric survey and hydraulic modelling
16:50	16:55	Cortés A.	Inter-basin exchange in a multi-basin polymictic lake
16:55	17:00	Forrest A.L.	Under-ice cyclonic gyre formation in a narrow, elongated lake
17:00	17:30		Poster discussion

**FRIDAY 23/06/2023**

08:30	09:00	Hinegk F.	Role of lake water balance on the intensity of surface cyanobacterial bloom
09:00	09:30	Larrieu K.	Suspended particulate aggregation in a large, oligotrophic, freshwater lake following wildfire deposition
09:30	10:00	Rose K.	Climate change impacts on aquatic deoxygenation
10:00	10:30		Coffee break
10:30	11:30	Pinardi N.	<b>Keynote lecture: Observing and predicting the global coastal ocean</b>
11:30	12:00	Schwefel R.	Physical and ecological effects of climate change on a eutrophic lake
12:00	12:30	Yousefi A.	Ranking the meteorological factors influencing lake surface water temperature across different climates
12:30	13:00	Hinegk L.	Long-term evolution of the European perialpine lakes water resources under climatic and management factors
13:00	14:30		Lunch
14:30	19:30		Technical visit to Torbiere del Sebino and to Lake Iseo
19:30	22:30		Social dinner

# Invited lectures



## Dr. Dimitri Rouwet

Researcher in Volcanology at INGV-Bologna and Adjunct professor at Bologna University.

His main interest is the chemistry and the dynamics of active volcanic lakes. His aim is to shed light on the functioning of the lake-surrounding volcano-hydrothermal system, with a special emphasis on variations in volcanic activity and tracking its state of unrest.

<https://www.unibo.it/sitoweb/dmitri.rouwet/publications>



## Prof. Claudia Adduce

Full professor of Hydraulics at Università degli Studi Roma tre.

Her main interests are sediment transport, stratified and rotating flows, investigated both with laboratory experiments and with 3D Large Eddy Simulations.

<https://www.uniroma3.it/persone/WXA4cXRFc1kxVWdndnZ5b05FNTJ1c1ZnS1ZNR0xXbjlueS9ydm9wUDc5dz0=/ricerca/>



## Prof. Nadia Pinardi

Full professor of Oceanography at Bologna University.

Her interests range from ocean numerical modelling and predictions to data assimilation, numerical modelling of the marine physical-biological interactions and pollutants at sea. She has written more than hundred and seventy papers in peer reviewed journals on a wide range of subjects.

<https://www.unibo.it/sitoweb/nadia.pinardi/en>

# Local organizing committee



## Prof. Marco Pilotti

Full Professor at  
Università degli Studi  
di Brescia



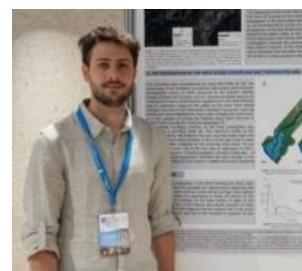
## Prof. Giulia Valerio

Professor at Università  
degli Studi di Brescia



## Dr. Riccardo Bonomelli

Ph.D. student at  
Università degli Studi di  
Brescia



## Dr. Gabriele Farina

Ph.D. student at  
Università degli Studi  
di Brescia

# Scientific committee

- *Chairman* — **Bertram Boehrer**, Helmholtz Centre for Environmental Research (UFZ), Germany
- **Josef Ackerman**, University of Guelph, Canada
- **Hrund Andradóttir**, University of Iceland, Reykjavik, Iceland
- **Lars Bengtsson**, Lund University, Sweden
- **Damien Bouffard**, EAWAG, Kastanienbaum, Switzerland
- **Lee Bryant**, University of Bath, U.K.
- **Xavier Castamitjana**, University of Girona, Spain
- **Giuseppe Ciraolo**, University of Palermo, Italy
- **Nikolai Filatov**, Karelian Research Centre of RAS, Petrosavodsk, Russia
- **Andrew Folkard**, Lancaster University, United Kingdom
- **Georgiy Kirillin**, Institute of Freshwater Ecology IGB, Berlin, Germany
- **Charles Lemckert**, University of Canberra, Australia
- **Madis-Jaak Lilover**, Marine Systems Institute, Tallinn, Estonia
- **Andreas Lorke**, University of Koblenz-Landau, Germany
- **Daniel McGinnis**, University de Genève, Switzerland
- **Marco Pilotti**, University of Brescia, Italy
- **Francisco Rueda**, University of Granada, Spain
- **Geoffrey Schladow**, University of California, Davis, U.S.
- **Adolf Stips**, European Commission, Italy
- **Arkady Terzhevnik**, Karelian Research Centre of RAS, Russia
- **Marco Toffolon**, University of Trento, Italy
- **Lars Umlauf**, Leibniz-Institute for Baltic Sea Research IOW, Warnemuende, Germany
- **Giulia Valerio**, University of Brescia, Italy
- **Timo Vesala**, University of Helsinki, Finland
- **Danielle J. Wain**, 7 Lakes Alliance, Belgrade Lakes, U.S.
- **Alfred Wüest**, EPFL, Lausanne, Switzerland
- **Ram Yerubandi**, Canada Centre for Inland Waters, Burlington, Canada

# List of participants

- **Claudia Adduce**, Roma Tre University, Roma, Italy, [claudia.adduce@uniroma3.it](mailto:claudia.adduce@uniroma3.it)
- **Marina Amadori**, National Research Council, Milan, Italy, [amadori.m@irea.cnr.it](mailto:amadori.m@irea.cnr.it)
- **Bertram Boehrer**, Helmholtz Centre for Environmental Research, Magdeburg, Germany, [Bertram.Boehrer@ufz.de](mailto:Bertram.Boehrer@ufz.de)
- **Riccardo Bonomelli**, Università degli Studi di Brescia, Brescia, Italy, [r.bonomelli@unibs.it](mailto:r.bonomelli@unibs.it)
- **Damien Bouffard**, Eawag, Kastanienbaum, Switzerland, [damien.bouffard@eawag.ch](mailto:damien.bouffard@eawag.ch)
- **Elisa Calamita**, Eawag, Switzerland, [elisa.calamita@eawag.ch](mailto:elisa.calamita@eawag.ch)
- **Alicia Cortés**, Tahoe Environmental Research Center, University of California Davis, California, USA, [alicortes@ucdavis.edu](mailto:alicortes@ucdavis.edu)
- **Matteo De Vincenzi**, University of Trento, Trento, Italy, [matteo.devincenzi@unitn.it](mailto:matteo.devincenzi@unitn.it)
- **Tomy Doda**, Eawag, Kastanienbaum, Switzerland, [tomy.doda@eawag.ch](mailto:tomy.doda@eawag.ch)
- **Gaia Donini**, University of Trento, Trento, Italy, [gaia.donini@unitn.it](mailto:gaia.donini@unitn.it)
- **Gabriele Farina**, University of Brescia, Brescia, Italy, [gabriele.farina@unibs.it](mailto:gabriele.farina@unibs.it)
- **Alexander Forrest**, University of California Davis, California, USA, [alforrest@ucdavis.edu](mailto:alforrest@ucdavis.edu)
- **Stephen Henderson**, Washington State University, Vancouver, USA., [steve.henderson@wsu.edu](mailto:steve.henderson@wsu.edu)
- **Francesca Hinegk**, University of Trento, Trento, Italy, [francesca.hinegk@unitn.it](mailto:francesca.hinegk@unitn.it)
- **Luigi Hinegk**, University of Trento, Trento, Italy, [luigi.hinegk@unitn.it](mailto:luigi.hinegk@unitn.it)
- **Joachim Jansen**, Uppsala University, Uppsala, Sweden, [joachim.jansen@ebc.uu.se](mailto:joachim.jansen@ebc.uu.se)
- **Georgiy Kirillin**, Leibniz-Institute of Freshwater Ecology and Inland Fisheries, Berlin, Germany, [georgiy.kirillin@igb-berlin.de](mailto:georgiy.kirillin@igb-berlin.de)
- **Kenneth Larrieu**, UC Davis, Davis, California, USA, [kglarrieu@ucdavis.edu](mailto:kglarrieu@ucdavis.edu)
- **Bernard Laval**, University of British Columbia, Vancouver, BC, Canada, [bernard.laval@ubc.ca](mailto:bernard.laval@ubc.ca)
- **Madis-Jaak Lilover**, Tallinn University of Technology, Tallinn, Estonia, [madis.lilover@taltech.ee](mailto:madis.lilover@taltech.ee)
- **Andreas Lorke**, University of Kaiserslautern-Landau (RPTU), Landau, Germany, [lorke@uni-landau.de](mailto:lorke@uni-landau.de)
- **Maria Rita Maggi**, National Research Council, Rome, Italy, [mariarita.maggi@uniroma3.it](mailto:mariarita.maggi@uniroma3.it)
- **Ivan Mammarella**, University of Helsinki, Helsinki, Finland, [ivan.mammarella@helsinki.fi](mailto:ivan.mammarella@helsinki.fi)
- **Paolo Monti**, Sapienza University of Rome, Rome, Italy, [paolo.monti@uniroma1.it](mailto:paolo.monti@uniroma1.it)
- **Julia Mullarney**, University of Waikato, Hamilton, New Zealand, [julia.mullarney@waikato.ac.nz](mailto:julia.mullarney@waikato.ac.nz)
- **Cesar Ordóñez**, University of Geneva, Geneva, Switzerland, [cesar.ordonez@unige.ch](mailto:cesar.ordonez@unige.ch)
- **Ilia Ostrovsky**, Kinneret Limnological Laboratory, Migdal, Israel, [ostrovsky@ocean.org.il](mailto:ostrovsky@ocean.org.il)
- **Naifu Peng**, Ecole Polytechnique Federal de Lausanne (EPFL), 1015 Lausanne, Switzerland, [naifu.peng@epfl.ch](mailto:naifu.peng@epfl.ch)
- **Sebastiano Piccolroaz**, University of Trento, Trento, Italy, [s.piccolroaz@unitn.it](mailto:s.piccolroaz@unitn.it)
- **Roger Pieters**, University of British Columbia, Vancouver, Canada, [rpieters@eoas.ubc.ca](mailto:rpieters@eoas.ubc.ca)
- **Marco Pilotti**, University of Brescia, Brescia, Italy, [marco.pilotti@unibs.it](mailto:marco.pilotti@unibs.it)
- **Monica Pinardi**, National Research Council, Milan, Italy, [pinardi.m@irea.cnr.it](mailto:pinardi.m@irea.cnr.it)
- **Nadia Pinardi**, University of Bologna, Bologna, Italy, [nadia.pinardi@unibo.it](mailto:nadia.pinardi@unibo.it)

- **Cintia Ramón**, University of Granada, Granada, Spain, [crcasanas@ugr.es](mailto:crcasanas@ugr.es)
- **Kevin Rose**, Rensselaer Polytechnic Institute in New York, [rosek4@rpi.edu](mailto:rosek4@rpi.edu)
- **Dmitri Rouwet**, Istituto Nazionale di Geofisica e Vulcanologia, Sezione di Bologna, Bologna, Italy , [dmitri.rouwet@ingv.it](mailto:dmitri.rouwet@ingv.it)
- **Martin Schmid**, Eawag, Kastanienbaum, Switzerland, [martin.schmid@eawag.ch](mailto:martin.schmid@eawag.ch)
- **Robert Schwefel**, Leibniz-Institute of Freshwater Ecology and Inland Fisheries, Berlin, Germany, [robert.schwefel@igb-berlin.de](mailto:robert.schwefel@igb-berlin.de)
- **Maria Teresa Serra Putellas**, University of Girona, Girona, Spain, [teresa.serra@udg.edu](mailto:teresa.serra@udg.edu)
- **Fatemeh Sadat Sharifi**, Leibniz Institute of Freshwater Ecology and Inland Fisheries (IGB), Berlin, Germany, [fatemeh.sharifi@igb-berlin.de](mailto:fatemeh.sharifi@igb-berlin.de)
- **Bradford Sherman**, CSIRO Land and Water, Canberra, ACT, Australia, [reservoir.doctor@icloud.com](mailto:reservoir.doctor@icloud.com)
- **Muhammed Shikhani**, Helmholtz Centre for Environmental Research, Magdeburg, Germany, [Muhammed.shikhani@ufz.de](mailto:Muhammed.shikhani@ufz.de)
- **Uwe Spank**, Technische Universität Dresden, Tharandt, Germany, [uwe.spank@tu-dresden.de](mailto:uwe.spank@tu-dresden.de)
- **Edmund Tedford**, University of British Columbia, Vancouver, Canada, [ttedford@eos.ubc.ca](mailto:ttedford@eos.ubc.ca)
- **Ruth Thirkill**, University of California Davis, CA, USA, [rthirkill@ucdavis.edu](mailto:rthirkill@ucdavis.edu)
- **Marco Toffolon**, University of Trento, Trento, Italy, [marco.toffolon@unitn.it](mailto:marco.toffolon@unitn.it)
- **Sergio Valbuena**, University of California, Davis, California, USA, [savalbuena@ucdavis.edu](mailto:savalbuena@ucdavis.edu)
- **Giulia Valerio**, University of Brescia, Brescia, Italy, [giulia.valerio@unibs.it](mailto:giulia.valerio@unibs.it)
- **Jia Wang**, Great Lakes Environmental Research Laboratory, NOAA, Ann Arbor, MI 48108, USA, [jia.wang@noaa.gov](mailto:jia.wang@noaa.gov)
- **Azadeh Yousefi**, University of Trento, Trento, Italy, [azadeh.yousefi@unitn.it](mailto:azadeh.yousefi@unitn.it)
- **Behnam Zamani**, Technical University of Berlin, Berlin, [b.zamani.gharehchaman@tu-berlin.de](mailto:b.zamani.gharehchaman@tu-berlin.de)

# *Proceedings*



## *Editors:*

*Prof. Marco Pilotti*

*Prof. Giulia Valerio*

*Dr. Riccardo Bonomelli*

*Dr. Gabriele Farina*

# Index

## A. Lorke\*

Physical limnology of ponds: knowledge gaps and research perspectives pag. 1

**S.M. Henderson\*, J.R. Nielson, S. R. Mayne, J.A. Manning and C.S. Goldberg**

Advection and mixing in ponds pag. 2

## I. Ostrovsky\*, A. Hozumi, H. Gildor, J.C. Wells, E. Uzhanskii and B. Katsnelson

Vertical distribution and dynamics of gas-containing cyanobacteria in relation to stratification and turbulence: insights from acoustical observations pag. 4

**M. Shikhani\*, L. Reinschke, P. Aurich, C. Waldemer, M. Koschorreck and B. Boehrer**

Composition of photosynthetic gas bubbles from submerged macrophytes pag. 6

## I. Mammarella\*, J. Ala-Konni, J. Heiskanen, K.M. Kohonen, S. MacIntyre, A. Ojala, A. Vähä and T. Vesala

Long term flux measurements of carbon dioxide and methane over a small boreal lake using eddy covariance technique pag. 8

## L. Hrdlicka and B. Boehrer\*

Sound speed in limnic waters and its application for the detection of extreme concentrations of carbon dioxide in Lake Nyos pag. 10

## D. Rouwet\*

### *Keynote lecture: Volcanic lake research: a 240(0)-year long explosive history*

pag. 12

## B.S. Sherman\*, P.W. Ford

The impact of extreme hydrological events on reservoir methane emissions. pag. 13

**T. Doda\*, A. Mugisha, E.R. Mudakikwa, F. Darchambeau and M. Schmid**

Impact of methane extraction on stratification in Lake Kivu pag. 15

**C. Ordóñez\*, T. DelSontro, T. Langenegger, D. Donis and D.F. McGinnis**

Magnitude, temporal dynamics, and drivers of oxic methane production across a trophic state gradient pag. 17

**R. Thirkill\*, W. Gray IV, C. Clemons, J. Porraz, H. Oldroyd, A.L. Forrest and M. Seelos**

What the sediment holds - hydroacoustic quantification of reservoir methane emissions pag. 19

**R. Bonomelli\*, G. Farina and M. Pilotti**

Far field simulation of a landslide-generated tsunami in Lake Iseo pag. 21

**C.L. Ramón\*, E. Rodríguez-Velasco, C. Clemons., I. Reche, H.J. Oldroyd, A.L. Forrest, and F.J. Rueda**

Ebullition rates and drivers in a shallow eutrophic Mediterranean reservoir pag. 23

**E. Tedford\*, R. Pieters, L. Ing and G. Lawrence**

Methane bubbles under ice in Base Mine Lake pag. 25

**B. Zamani\* and F. Hellweger**

3D Modeling of climate change impacts on a groundwater-fed lake in Berlin area pag. 27

**G. Valerio\* and M. Pilotti**

Dynamics of lakes heatwaves in summer 2022: interplay between wind mixing and surface heating pag. 29

**S. Valbuena\*, F. Bombardelli, J. Largiera and G. Schladow**

Rotational effects in lake upwelling and the thresholds for conceptual models pag. 31

<b>D. Bouffard*, T. Doda, C. Ramón and H.N. Ulloa</b>	
Differential cooling in lakes	pag. 33
<b>A. Barcelona, J. Colomer and M.T. Serra Putellas*</b>	
Stem stiffness behaviour in an oscillatory flow submerged canopy patch	pag. 35
<b>G. Kirillin*, A. Izhitsky and A. Kurbaniyazov</b>	
Thermal conditions and lake metabolism in the ice-covered North Aral Sea	pag. 37
<b>B. Laval*, L. Smith, S. Vagle and E. Carmack</b>	
Physical transport in a thermobarically stratified fjord-type lake	pag. 39
<b>N. Peng*, U. Lemmin, F. Mettra, R. S. Reiss and D. A. Barry</b>	
Identifying and quantifying deepwater-renewal processes during winter cooling in a large, deep lake (Lake Geneva)	pag. 41
<b>M.J. Lilover*, U. Lips, T. Liblik, I. Suhhova and G. Väli</b>	
Hunting for submesoscale temperature, salinity and current velocity signal from CTD and ADCP/RDCP profilers data in the Gulf of Finland, the Baltic Sea	pag. 43
<b>M. Amadori*, M. Bresciani, C. Giardino and H.A. Dijkstra</b>	
Analysis of spatiotemporal variability of remotely sensed variables to investigate thermal and morphological heterogeneity beneath the lakes surface	pag. 45
<b>E. Calamita*, M. Brechbühler, I. Woolway, C. Albergel and D. Odermatt</b>	
Satellite Earth observation to monitor lake mixing anomalies worldwide	pag. 47
<b>M. Pinardi*, M. Bresciani, R. Caroni, G. Tellina, J.F Crétaux, S. Simis, C. Duguay, C.J. Merchant, Laura Carrea, H. Yesou, A. Andral and C. Giardino</b>	
The Lakes_cci project: presenting the satellite-derived lakes variables for climate studies	pag. 49
<b>U. Spank,*, M. Mauder, J. Matschullat, G. Licht and M. Koschorreck</b>	
Mobile eddy covariance measurements as a key to improve estimates of momentum, mass and energy fluxes between atmosphere and inland waters	pag. 51
<b>J.C. Mullarney*, I.T. MacDonald and C.A. Eager</b>	
In-situ observations of the acoustic scattering characteristics from a suspension of flocculated particles	pag. 53
<b>R. Pieters*, L. Gu and G. Lawrence</b>	
Turbid inflow into a drinking water reservoir	pag. 55
<b>A. Di Bernardino, P. Monti*, G. Leuzzi and G. Querzoli</b>	
Turbulent Schmidt number measurements in a density current flowing over surface roughness	pag. 57
<b>F.S. Sharifi*, R. Hinkelmann, T. Hattermann and G. Kirillin</b>	
Three-dimensional modelling of gravity currents in an idealized stratified ice-covered lake	pag. 59
<b>C. Adduce*</b>	
<b>Keynote lecture: Entrainment and mixing in gravity currents over complex boundaries</b>	pag. 61
<b>M. Fregona, M. Leppäranta, I. Mammarella and S. Piccolroaz*</b>	
A simple model for predicting ice timing and thickness in lakes	pag. 63
<b>J. Wang*, D. Cannon, A. Fujisaki-Manome, D. Beletsky, S. Constant, S. Ruberg and S. Orendorf</b>	
Modeling two-way ice-wave interactions in the Great Lakes using FVCOM_ice+wave model	pag. 65
<b>M. Toffolon*, L. Cortese and D. Bouffard</b>	
Energy considerations to understand the impact of cooling and wind on freeze-up in lakes	pag. 67

**G. Donini\*, A. Adeva Bustos, and M. Toffolon**

Simulation of short-term effects of pumped-storage hydropower on stratification and ice cover in two Norwegian reservoirs

pag. 69

**M. Schmid\* and T. Lorimer**

Unexpected inflow behaviour complicates assessment of heat usage potential for an ice-covered lake

pag. 71

**M.R. Maggi\*, M.E. Negretti, E.J. Hopfinger and C. Adduce**

Mixing properties of steady gravity currents flowing over sloping terrain

pag. 73

**M. Pilotti\* and G. Valerio**

Science communication and teaching in secondary schools through limnology

pag. 75

**J. Jansen\*, R. I. Woolway, Z. Tan**

Weakening of inverse stratification in northern lakes

pag. 77

**M. De Vincenzi\*, M. Amadori, L. Adami, M. Tubino**

Role of aquatic vegetation and meteorological forcing on the hydrodynamics of Mantua Lakes: insights from a bathymetric survey and hydraulic modelling

pag. 79

**A. Cortés\*, S.A. Valvuna, A.L. Forrest and S.G. Schladow**

Inter-basin exchange in a multi-basin polymictic lake

pag. 81

**K. Hughes, A.L. Forrest\*, A. Cortés, H.J. Oldroyd and F. Bombardelli**

Under-ice cyclonic gyre formation in a narrow, elongated lake

pag. 83

**F. Hinegk\*, S. Piccolroaz, S. Speltoni, M. Amadori, S. Pozzi and M. Toffolon**

Role of lake water balance on the intensity of surface cyanobacterial bloom

pag. 85

**K. Larrieu\*, Y. Song, M. Rau, A. Forrest and S.G. Schladow**

Suspended particulate aggregation in a large, oligotrophic, freshwater lake following wildfire deposition

pag. 87

**K. Rose\* and S. Jane**

Climate change impacts on aquatic deoxygenation

pag. 89

**N. Pinardi\***

***Keynote lecture: Observing and predicting the global coastal ocean***

pag. 91

**R. Schwefel\*, S. Jordan, S. Krishna and M. Hupfer**

Physical and ecological effects of climate change on a eutrophic lake

pag. 92

**A. Yousefi\*, S. Piccolroaz, M. Amadori and M. Toffolon**

Ranking the meteorological factors influencing lake surface water temperature across different climates

pag. 94

**L. Hinegk\*, L. Adami and M. Tubino**

Long-term evolution of the European perialpine lakes water resources under climatic and management factors

pag. 96

# Physical limnology of ponds: knowledge gaps and research perspectives

A. Lorke<sup>1\*</sup>

<sup>1</sup>*IES Landau, Institute for Environmental Sciences, University of Kaiserslautern-Landau (RPTU), Landau, Germany*

\*Corresponding author; e-mail [lorke@uni-landau.de](mailto:lorke@uni-landau.de)

## KEYWORDS

shallow flows; density-driven flow; thermal stratification; optical flow measurement.

Small lentic ('stagnant') aquatic ecosystems, often referred to as ponds, comprise the majority of global lakes by number. They play a critical role in global biogeochemical cycling and are hotspots of biodiversity. The high microbial activity and biodiversity in ponds are challenged by extreme environmental variability, with strong diel changes in temperature, inorganic carbon, and oxygen, which can pose severe challenges to the survival of organisms. These processes interact intimately with prevailing hydrodynamic conditions, which control the transport of heat, solutes, and organisms and affect their exposure to light and trophic interactions. Flow regimes and thermal stratification have been extensively studied in larger lakes, and reservoirs, but surprisingly little is known about the physical conditions in ponds, their temporal dynamics, spatial variability, and relation to geographic and climatic conditions. Unlike lakes and reservoirs, flows in ponds are predominantly driven by horizontal density gradients caused by differential heating and cooling. The latter can arise from partial shading of the ponds, varying water depth, vegetation coverage, and different bed material properties. Using measurements from replicated outdoor pond mesocosms, I illustrate the challenges associated with observing these flows, their driving forces, and their interactions with biota. I propose that combining distributed temperature observations with optical flow measurements using low-cost cameras can become a valuable tool for improving the current understanding of pond physics.

## Advection and mixing in ponds

S.M. Henderson<sup>1\*</sup>, J.R. Nielson<sup>2</sup>, S. R. Mayne<sup>3</sup>, J.A. Manning<sup>3</sup> and C.S. Goldberg<sup>3</sup>

<sup>1</sup> School of the Environment, Washington State University (Vancouver), Vancouver, USA.

<sup>2</sup> College of Natural Resources, Utah State University, Logan, USA.

<sup>3</sup> School of the Environment, Washington State University, Pullman, USA.

\*Corresponding author, e-mail [steve\\_henderson@wsu.edu](mailto:steve_henderson@wsu.edu)

### KEYWORDS

Ponds; stratification; mixing; advection; seiches

### Introduction

Ponds (area<1000 m<sup>2</sup>) are characterized by high biodiversity and intense biogeochemical cycling. Ponds may contribute 37% of global methane emissions from all lakes (Rosentreter et al., 2021) and at high latitudes contribute to permafrost melting. Ponds often suffer significant anthropogenic impacts, and many are deliberately engineered for treatment of polluted waters. To examine patterns of advection and quantify turbulent mixing, we present high resolution observations of water velocity and stratification in two ~50 m long temperate ponds.

### Materials and methods

Velocity and temperature were measured in Wyatt pond (50 m × 26 m × 2.7 m, WA, USA) from 15 July to 30 August 2021. Eight pulse-coherent 2MHz Nortek Aquadopps were suspended at intermediate depths, looking upward to measure velocity profiles (1.5 cm vertical bins, spanning depths 0.17-1.53 m and 0.04-0.23 m respectively for deep and shallow instruments). A 1 MHz Aquadopp measured (4.5 cm bins) between 0.23 and 2.27 m depth. Vertical stacks of RBR Solo-T loggers measured temperature. A Hobo weather station measured winds.

Higher resolution measurements were obtained in a New Zealand pond from 27 to 29 April 2022. Solo-T loggers recorded temperature. Three Nortek Vectrinos recorded 50 Hz velocity profiles (1 mm bins) at depths 0.006-0.023 m, 0.035-0.065 m, and 0.155-0.185 m.

### Results and discussion

Each night, free convection created a surface mixed layer with depth  $h$  extending about 1 m below the surface. Each day, mixed layer depth was greatly reduced as solar heating re-established temperature stratification. The turbulent dissipation rate  $\epsilon$  (Figure 1, top), estimated from velocity structure functions, ranged from  $<10^{-8}$  W/kg (below the mixed layer) to about  $1.5 \times 10^{-6}$  W/kg (about 1 cm below the surface), with values observed near the downwind shore exceeding those observed upwind. Daytime mixed-layer depths often exceeded half a meter at the downwind shore, but were greatly reduced upwind. Consistent with an established, vertically integrated momentum balance,  $h \sim x^{1/2}$ , where  $x$ =distance from upwind shore. Below the mixed layer, downwind water velocity  $u$  was usually just a few millimetres per second. However, velocity oscillations (amplitude ~1 cm/s, period 40 – 70 minutes) were observed most afternoons, owing to internal seiching (Figure 1, middle and bottom). In the mixed layer during the day, velocities of a few centimetres per second often flowed downwind near the surface, and returned upwind near the mixed-layer base. Significant shear was observed within 1-2 cm of the surface. Advective acceleration  $u(du/dx)$  was a significant component in the near-surface momentum balance. The timescale for vertical mixing of the mixed-layer [ $8.5(h^2/\epsilon)^{1/3}$ ] was about 15-60 minutes, with the smallest values observed during the day. This mixing timescale was comparable to the lateral advection time  $L/u$ , where  $L$ =pond length. In many lakes, vertical profile models that neglect lateral advection are useful for estimating near-surface mixing and surface fluxes. However, neglect of lateral advection may not have been justified for the ponds considered here, given the observed leading-order role for advective

acceleration, the downwind increase in near-surface dissipation, and the similarity of timescales for vertical mixing and lateral advection.

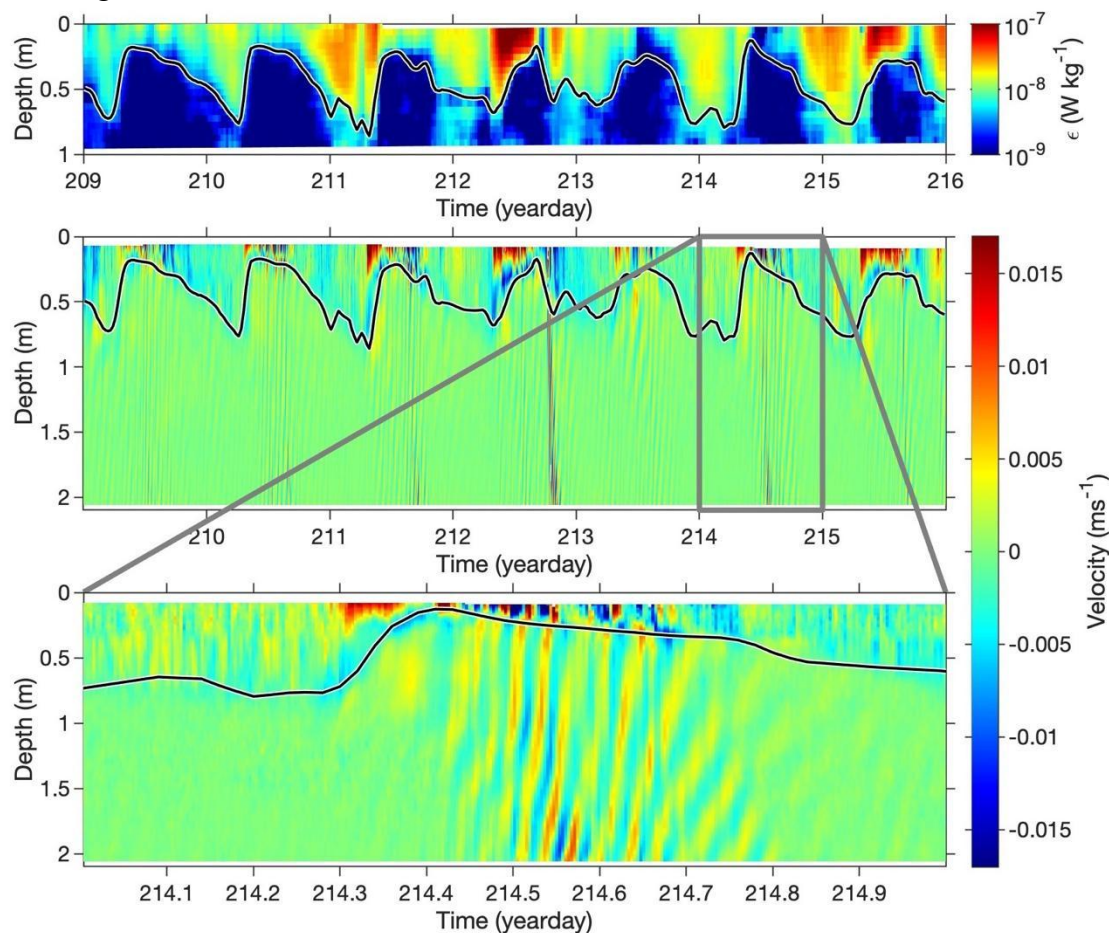


**Figure 1:** Turbulent dissipation rate  $\epsilon$  (top) and along-pond velocity (middle, bottom) measured near the centre of Wyatt Pond. Surface mixed layer depth increased at night, and reduced during the day (black curve). Within the mixed-layer, turbulence was intense and flows often exceeded 1 cm/s, with downwind flow near the surface and upwind return flow near the mixed layer base. Below the mixed layer, turbulence was unmeasurably weak, and flows exceeded 1 cm/s only during afternoon seiche-induced oscillations.

## REFERENCES

- Rosentreter, Judith A. et al. (2021), Half of global methane emissions come from highly variable aquatic ecosystem sources, *Nature Geoscience*, **14**, 225-230, <https://doi.org/10.1038/s41561-021-00715-2>.

# Vertical distribution and dynamics of gas-containing cyanobacteria in relation to stratification and turbulence: insights from acoustical observations

I. Ostrovsky <sup>1\*</sup>, A. Hozumi <sup>1,2</sup>, H. Gildor<sup>2</sup>, J.C. Wells <sup>3</sup>, E. Uzhanskii <sup>4</sup> and B. Katsnelson <sup>4</sup>

<sup>1</sup> Israel Oceanographic and Limnological Research, Kinneret Limnological Laboratory, Migdal, Israel

<sup>2</sup> Institute of Earth Sciences, The Hebrew University of Jerusalem, Jerusalem, Israel

<sup>3</sup> Ritsumeikan University, Civil and Environmental Engineering, Kusatsu, Japan

<sup>4</sup> L. Charney School of Marine Sciences, University of Haifa, Haifa, Israel

\*Corresponding author; e-mail [ostrovsky@ocean.org.il](mailto:ostrovsky@ocean.org.il)

## KEYWORDS

Stratification; turbulence; echosounder; ADCP; cyanobacteria.

## Introduction

Harmful Algal Blooms (HAB), which are blooms of toxic phytoplankton (dinoflagellates, diatoms, cyanobacteria), become of common occurrence in freshwater and marine environments. The blooms disrupt the functioning of aquatic ecosystems, water use and threaten human and animal health. HABs are a rapidly expanding global problem. Harmful effects may occur even when visible signs of a bloom are absent. Cyanobacteria can live and proliferate in different environments and are considered one of the indicators of eutrophication. Monitoring programs are widely implemented to detect the early stages of HAB. The main difficulty in monitoring stems from the huge lateral heterogenic distribution of cyanobacteria, and their rapid vertical migrations/dispersions resulting in the episodic formations of high biomass near the water surface in relation to hydrodynamic processes at various scales. The floating cells and colonies can be accumulated at certain locations when they are driven by wind and water motions. Here, we present the advantages of *in situ* observations using non-invasive remote-sensing acoustic and laser instruments to investigate the dynamics and spatial organization of the bloom-forming cyanobacterium *Microcystis* sp. We also examine the role of physical factors in *Microcystis* bloom formation.

## Materials and methods

Volume backscattering strength ( $S_v$ ) of *Microcystis* was measured with 120-kHz Simrad EY60 echosounder and 500-kHz Sentinel V50 ADCP in Lake Kinneret (the Sea of Galilee), Israel. The ADCP was moored at station F located ~2 km off the western side of the lake at a depth of 18 m. The depth bin length was 0.6 m. 256 individual pings were recorded at 15- or 30-minute intervals. The ADCP data were used for the calculation of the mean volume backscattering strength,  $S_v$  (dB), from the recorded echo intensity (counts) and transducer parameters by using the sonar equation (Lorke et al 2004). The  $S_v$  measured with EY60 was calibrated against chlorophyll-*a* concentration and colony volumetric concentration, which can serve as proxies for cyanobacteria biomass during bloom. Quantifications of *Microcystis* colony volumetric concentration were done with a submersible laser-diffraction based particle size analyzer LISST-100x (Sequoia Scientific, Inc) LISST-100x – an instrument allowing measurements of particle size distribution and concentration (e.g. Wu et al. 2020).

## Results and discussion

We found that gas-containing *Microcystis* colonies are strong acoustic backscatterers at ultrasound frequencies. They can be detected and monitored using acoustic methods. Observations on the spatiotemporal variability of backscattering strength measured with ADCP showed a close linkage between the distribution of cyanobacterial biomass with thermal stratification. Thermal stratification and turbulence levels influence the vertical distribution of *Microcystis* colonies and surface scum

formation. During periods of weak turbulence (vertical turbulent eddy diffusivity  $[K_z] < 1 \text{ cm}^2 \text{ s}^{-1}$ ) the volume concentration of buoyant *Microcystis* colonies near the surface increased fast. High turbulence after the initiation of strong wind or night cooling abruptly disperses the colonies vertically. Simulations of the vertical distribution of *Microcystis* colonies under different turbulence levels showed that the thickness of the surface layer, where most cyanobacteria biomass is concentrated, increased when  $K_z > 3 \text{ cm}^2 \text{ s}^{-1}$ .

Distinct patterns of *Microcystis* horizontal distributions and areas of high near-surface concentration of colonies (patches) can be well seen on satellite images (Dev et al. 2022). Such structures are formed by water motions on various spatial scales. The high density of *Microcystis* biomass at the water surface absorbs solar radiation and induces additional heating of the topmost water layer. This creates optimal ambient conditions for photosynthesis. We argue that the development of surface patches is crucial for the acceleration of *Microcystis* production and the rapid development of HAB at nutrient availability.

Our study shows that high-frequency acoustic instruments can be used for the accurate detection and monitoring of toxic cyanobacteria in lakes (Ostrovsky et al. 2020). Implementation of remote and non-invasive methods allows for studying the interdependency between the distribution and dynamics of cyanobacteria biomass and ambient factors, which should help to model and forecast HAB and surface scum formation.

### Acknowledgments

This work was supported by Japan-Israel Cooperative Scientific Research Program of the Ministry of Science and Technology (MOST), grant 3-14952.

### REFERENCES

- Dev P.J., Sukenik A., Mishra D.R., Ostrovsky I. (2022). Cyanobacterial pigment concentrations in inland waters: Novel semi-analytical algorithms for multi- and hyperspectral remote sensing data, *Sci. Total Environ.* **805**, 150423. <https://doi.org/10.1016/j.scitotenv.2021.150423>
- Lorke, A., McGinnis, D. F., Spaak, P. and Wüest A. (2004), Acoustic observations of zooplankton in lakes using a Doppler current profiler, *Freshwater Biol.* **49**, 1280–1292, 2004. <https://doi.org/10.1111/j.1365-2427.2004.01267.x>
- Ostrovsky, I., Wu, S., Li, L., Song, L. (2020). Bloom-forming toxic cyanobacterium *Microcystis*: Quantification and monitoring with a high-frequency echosounder, *Water Research* **183**, 116091. <https://doi.org/10.1016/j.watres.2020.116091>
- Wu, X., Yang, T., Feng, S., Li, L., Xiao, B., Song, L., Sukenik, A., Ostrovsky, I. (2020) Recovery of *Microcystis* surface scum following a mixing event: insights from a tank experiment. *Sci. Total Environ.* **728**. <https://doi.org/10.1016/j.scitotenv.2020.138727>

# Composition of photosynthetic gas bubbles from submerged macrophytes

M. Shikhani<sup>1\*</sup>, L. Reinschke<sup>1</sup>, P. Aurich<sup>1</sup>, C. Waldemer<sup>1</sup>, M. Koschorreck<sup>1</sup>, B. Boehrer<sup>1</sup>

<sup>1</sup> Department of Lake Research, Helmholtz Centre for Environmental Research – UFZ, Magdeburg, Germany

\*Corresponding and presenting author; e-mail [muhammed.shikhani@ufz.de](mailto:muhammed.shikhani@ufz.de)

## KEYWORDS

Ebullition; oxygen; bubble formation; bubble composition; dissolved gases .

## Introduction

The interaction between lake waters and the atmosphere, particularly the exchange of gases, is integral to understanding the carbon cycle and its implications for global warming. The ebullition of oxygen had widely been ignored, but studies have reported although it is relevant and can reach up to about 30% of the net diffusive exchange of oxygen. This study focuses on initiating a quantitative understanding of oxygen ebullition from photosynthesis, an aspect largely overlooked despite its relevance to the carbon cycle. Prior research has used gas pressure arguments to predict bubble composition. However, no known study has experimentally tested the gas composition in relation to the gas pressure considerations for bubble formation in environments comparable to lakes. Our research aimed to fill this gap by examining the composition of bubbles originating from photosynthetically active macrophytes in a controlled laboratory setting and providing a quantitative understanding of oxygen ebullition from photosynthesis.

## Materials and methods

If a water surface is exposed to a gas space, gas concentrations in the water change

towards the equilibrium concentration defined by the Henry law:

$$c = k_h p \quad (1)$$

where  $p$  represents the partial pressure of the respective gas in the gas phase. When photosynthesis takes place, the oxygen gas pressure would rise in the water around the plant and once the total gas pressure exceeded the outside pressure, bubbles formed. The absolute pressure is the sum of atmospheric pressure and hydrostatic pressure.

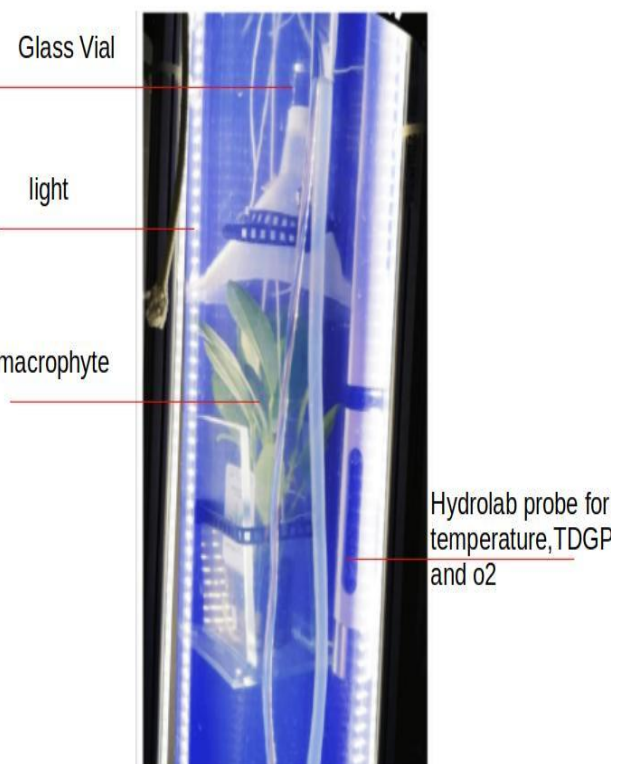


Figure 1. Experiment setup

$$p_{O_2} + p_{N_2} + p_{Ar} + p_{CO_2} + p_{H_2O} = p_{tot} = p_{absolute} \quad (2)$$

The experiments were conducted in a 5m high PVC tube filled with tap water to simulate a limnic environment. A plant was placed on a platform inside the water column and illuminated on a 12h/12h light cycle. The ascending bubbles were collected in small containers. O<sub>2</sub>, CH<sub>4</sub>, CO<sub>2</sub>, N<sub>2</sub>, and Ar were measured in the bubbles that formed at varying depths. The exposure depth of the

plant varied between 0.3 m and 4.5 m below the water surface, expecting that depth would affect the bubble composition. Gas samples were collected, and their composition was analyzed using both optical sensors and gas chromatographs.

### Results and discussion

In the main experimental series, we conducted 29 experiments at various depths between 0.3 and 4.5m. The oxygen concentration in the collected gas samples varied between 28% and 45%. Despite the data scatter, we noted a correlation between oxygen concentration and depth. Fast experiments, defined by the quick filling of the vial with gas, consistently produced bubbles with O<sub>2</sub> contents at or above the theoretical line derived from minimum gas pressure considerations. Oxygen concentrations exceeded 40% at all depths and surpassed 38.5% for all samples collected at depths greater than 4m. Intriguingly, bubbles with high O<sub>2</sub> content were produced at all depths, with a clear upper limit of 45% O<sub>2</sub> content.

The study demonstrated that bubbles forming at macrophytes are not pure oxygen bubbles but contain other gases, primarily N<sub>2</sub>, Ar, and CO<sub>2</sub>. The actual bubble composition varied significantly, with many bubbles containing more O<sub>2</sub> than required by minimum gas pressure considerations.

High O<sub>2</sub> levels were attributed to the rapid formation of bubbles that depleted N<sub>2</sub> at the site of bubble formation faster than it could be replenished. We also noted the critical role of CO<sub>2</sub> in bubble formation, which requires further exploration.

In conclusion, this study provides a quantitative understanding of oxygen ebullition from photosynthesis, a vital yet often overlooked aspect of the carbon cycle. The oxygen content of photosynthetic bubbles ranged between 28% and 45%, with intensive bubble formation leading to an increase in oxygen content above the theoretical minimum. However, no concentrations above 45% were measured, suggesting a depth-independent empirical maximum for oxygen content.

### REFERENCES

- Shikhani, M., Reinschke, L., Aurich, P., Waldemer, C., Koschorreck, M., & Boehrer, B. (2023). Composition of photosynthetic gas bubbles from submerged macrophytes. (**under review**).

# Long term flux measurements of carbon dioxide and methane over a small boreal lake using eddy covariance technique

I. Mammarella<sup>1\*</sup>, J. Ala-Konni<sup>1</sup>, J. Heiskanen<sup>2</sup>, K.M. Kohonen<sup>1,3</sup>, S. MacIntyre<sup>4</sup>, A. Ojala<sup>5</sup>, A. Vähä<sup>1</sup> and T. Vesala<sup>1,6</sup>

<sup>1</sup> Institute for Atmospheric and Earth System Research (INAR) / Physics, University of Helsinki, Helsinki, Finland

<sup>2</sup> Faculty of Biological and Environmental Sciences, University of Helsinki, Helsinki, Finland

<sup>3</sup> Department of Environmental Systems Science, ETH Zurich, Zürich, Switzerland

<sup>4</sup> Earth Research Institute, University of California, Santa Barbara, California

<sup>5</sup> Natural Resources Institute Finland (Luke), Helsinki, Finland

<sup>6</sup> Institute for Atmospheric and Earth System Research (INAR) / Forest Sciences, University of Helsinki, Helsinki, Finland

\*Corresponding author; e-mail: [ivan.mammarella@helsinki.fi](mailto:ivan.mammarella@helsinki.fi)

## KEYWORDS

Lakes; Eddy covariance; Carbon dioxide and methane fluxes; Lake internal dynamics.

## Introduction

Advancing our understanding on physical and biogeochemical processes controlling turbulent exchange of energy, carbon dioxide (CO<sub>2</sub>), methane (CH<sub>4</sub>) and other trace gases over lacustrine systems is crucial in order to improve climate and weather forecast models. Lakes are able to process large amounts of organic carbon and their importance in terrestrial carbon cycle and climate change issues is well recognised (Battin et al., 2009). Nevertheless, the amount of carbon dioxide and methane released into the atmosphere is largely uncertain (Bastviken et al., 2011). Here we analyse eleven years (for CO<sub>2</sub>) and three years (for CH<sub>4</sub>) of eddy covariance flux measurements over the Lake Kuivajärvi, a small boreal lake in Finland. The aims of this study are: i) to provide new insights on EC methodologies applied to lake ecosystems, based on long term flux measurements; ii) to determine the seasonal and interannual variations of CO<sub>2</sub> and CH<sub>4</sub> fluxes; iii) to assess the relative contribution of shear and buoyancy-induced water turbulence on air-water gas exchange.

## Materials and methods

Energy and CO<sub>2</sub> exchange has been monitored in Lake Kuivajärvi, located close to the Hyytiälä Forest Field Station, since 2009. Lake Kuivajärvi is a small humic boreal lake extending about 2.6 km in North/West-South/East direction and it is a few hundred meters wide (Fig. 1). The measurement platform is located approximately 1.8 km and 0.8 km from the Northern and Southern shorelines, respectively. The lake has a maximum depth of 13.2 m, and the depth at the location of the platform is 12.5 m.

The eddy covariance (EC) system on the platform includes an ultrasonic anemometer (Metek USA-1, GmbH, Germany) to measure the three wind velocity components and sonic temperature, and the enclosed-path infrared gas analyser Licor 7200 (LiCor Inc., Lincoln, NE, US) that measures CO<sub>2</sub> and H<sub>2</sub>O concentrations. Starting from June 2012, the CH<sub>4</sub> turbulent fluctuations are also measured by using the fast response gas analyser G1301-f (Picarro Inc., USA). All data were sampled at 10 Hz and the gas inlets were located at 1.5 m above the water surface close to the sonic anemometer.

The eddy covariance fluxes were calculated as 30 min block averaged co-variances between the scalars (or horizontal wind speed) and vertical wind velocity according to commonly accepted procedures (Aubinet et al. 2000). Fluxes were corrected for high frequency loss, due to the limited frequency response of the EC system. In this study we used the theoretical approach (Aubinet et al. 2000), for correcting the momentum and buoyancy fluxes. Instead, the CO<sub>2</sub> and H<sub>2</sub>O fluxes were corrected by using experimentally estimated co-spectral transfer functions, as described in

Mammarella et al. (2009). Auxiliary data are continuously measured in proximity of the platform (5 sec sampling frequency), and they are water CO<sub>2</sub> and temperature profiles, radiation components, air temperature and relative humidity.

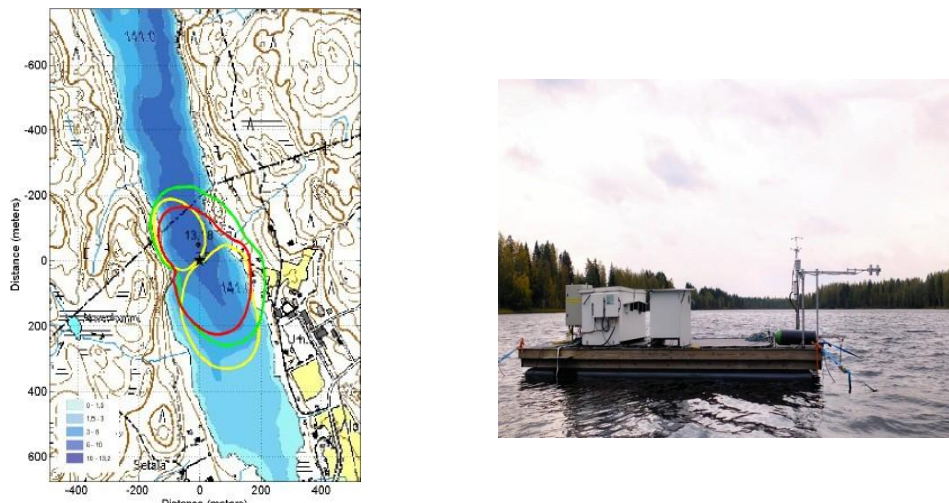


**Figure 1. Left.** Bathymetric map of the lake. The location of the raft (**Right**) is indicated by a star. Contour lines represent the 80% flux footprint for different atmospheric stability and all wind direction. Red line ( $z/L < -0.0625$ ), green line ( $-0.0625 < z/L < 0$ ) and yellow line ( $0 < z/L < 0.03$ ), where  $z$  is the measurement height and  $L$  is the Obukhov length.

## Results and discussion

The lake ecosystem mostly acted as a net CO<sub>2</sub> source ( $0.42 \pm 1.56 \text{ mmol m}^{-2} \text{ s}^{-1}$ ) throughout the ice-free periods and having a relatively high interannual variability when compared to surrounding forests and wetlands. On average, the lake is also a net source of CH<sub>4</sub> ( $0.63 \pm 2.44 \text{ nmol m}^{-2} \text{ s}^{-1}$ ), but the measured annual emissions are lower than for CO<sub>2</sub>, revealing that most of CH<sub>4</sub> produced at the lake bottom is oxidized in the water column. Carbon dioxide and methane emissions are largely affected by the weather forcing through the effects of wind shear and nocturnal water cooling, deepening the mixed layer and enhancing the gas exchange at air-water interface.

## REFERENCES

- Aubinet, M., Grelle, A., Ibrom, A., Rannik U., Moncrieff, J., Foken, T., Kowalski A. S., Martin, P.H., Berbigier,P., Bernhofer, C., Clement, R., Elbers, J., Granier, A., Grunwald, T., Morgenstern, K., Pilegaard, K., Rebmann, C., Snijders, W., Valentini, R., and Vesala, T. (2000). Estimates of the annual net carbon and water exchange of forests: The EUROFLUX methodology, *Adv. Ecol. Res.*, 30, 113–175.
- Bastviken, D., L. Tranvik, J. Downing, P. Crill, and A. Enrich-Prast (2011), Freshwater Methane Emissions Offset the Continental Carbon Sink, *Science*, 331(6013), 50-50, doi:10.1126/science.1196808.
- Battin, T.J., S. Luyssaert, L.A. Kaplan, A.K. Aufdenkampe, A. Richter L.J. and Tranvik (2009). The boundless carbon cycle. *Nature Geoscience*, 2, 598-600.
- Mammarella I., S. Launiainen, T. Gronholm, P. Keronen, J. Pumpanen, Ü. Rannik and T. Vesala (2009). Relative humidity effect on the high frequency attenuation of water vapour flux measured by a closed-path eddy covariance system, *Journal of Atmospheric and Oceanic Technology*, 26(9), 1856-186.

# Sound speed in limnic waters and its application for the detection of extreme concentrations of carbon dioxide in lake Nyos

L. Hrdlicka<sup>1</sup>, B. Boehrer<sup>1\*</sup>

<sup>1</sup>Helmholtz Centre for Environmental Research - UFZ, Magdeburg, Germany

\*Corresponding and presenting author; e-mail [Bertram.Boehrer@ufz.de](mailto:Bertram.Boehrer@ufz.de)

## KEYWORDS

Sound speed; properties of limnic waters; carbon dioxide, Lake Nyos

## Introduction

Sound speed is important for echo sounding and for acoustic current measurements. Beyond this, sound propagation in stratified waters depends sensitively on gradients of sound speed and hence exact knowledge is required for the detection of sources of noise in the water. Finally, sound speed can be used for acoustic tomography and it serves as a proxy for other properties of water, such as density or solutes.



## Materials and methods

Sound speed in a fluid can be derived as:

$$c = \frac{1}{\sqrt{\rho_{in-situ} \cdot K}}$$

with  $\rho_{in-situ}$  and  $K$  representing in-situ density and adiabatic compressibility of water. Hence sound speed turns out to be dependent on temperature, dissolved substances and pressure. For ocean water, the effect of solutes can be included by electrical conductivity. Temperature and pressure can be measured directly. Some people claim that calculations of sound speed in the ocean are more exact than direct measurements with probes. In lakes, this is different due to the variable composition of solutes.

**Figure 1.** Probe used for measuring CTD And sound speed in Lake Nyos (from Boehrer et al. 2021).

## Results and discussion

We present measurements from Lake Nyos with a multiparameter probe, including measurements of pressure, temperature, electrical conductivity and sound speed from the surface to the ground. Based on the ocean formula for sound speed we calculate sound speed based on pressure, temperature and electrical conductivity. We compare this calculated sound speed with sound speed measured as time-of-flight with the same instrument. The comparison shows that sound speed in the deep water is higher than calculated values.

It is known that carbon dioxide contributes positively to sound speed. No other solute is available at similar concentrations in the deep waters of Lake Nyos. Most other solutes are ions and their contributions have been covered by including electrical conductivity in the calculation of sound speed. Using a coefficient connecting sound speed excess to carbon dioxide concentration from Sanemasa et al., the difference between the profiles can directly converted into carbon dioxide concentrations and compared to earlier measurements (Kusakabe et al. 2008, Saiki et al., 2018).

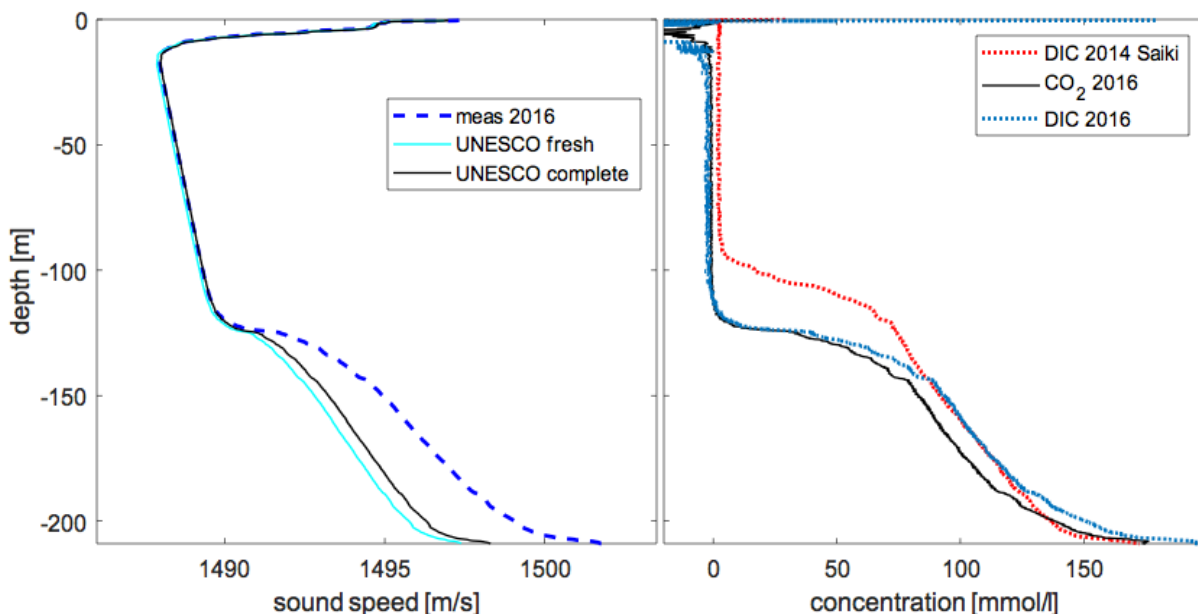


**Figure 2.** Measured and calculated (from pressure, temperature and electrical conductivity) sound speed in Lake Nyos and the calculated carbon dioxide profile (from Boehrer et al. 2021).

From this good result, the question arises, whether this approach is transferable to other lakes. A candidate of special interest is Lake Kivu, which also shows enormous concentrations of carbon dioxide. A fast trial shows that the large salt background requires a more exact inclusion of the solutes in the calculation compared to how it is done in the ocean formula.

The literature does not provide much material on this. There is no systematic investigation of specific sound speed contributions of salts. As a consequence, we started such an investigation and we are going to present first results.

#### REFERENCES

- Boehrer, B., Saiki, K., Ohba, T., Tanyileke, G., Rouwet, D., Kusakabe, M. (2021): Carbon dioxide in Lake Nyos, Cameroon, estimated quantitatively from sound speed measurements. *Front. Earth Sci.* **9**, art. 645011
- Kusakabe, M., Ohba, T., Issa, Yoshida, Y., Satake, H., Ohizumi, T., Evans, W.C., Tanyileke, G., and Kling, G.W. (2008). Evolution of CO<sub>2</sub> in Lakes Monoun and Nyos, Cameroon, before and during controlled degassing. *Geochem. J.* **42**, 93-118.
- Saiki, K., Kaneko, K., Ohba, T., Sanemasa, M., Kusakabe, M., Ntchantcho, R., Fouépé, A.T., Tanyileke, G., and Hell, J. (2018). Vertical distribution of dissolved CO<sub>2</sub> in lakes Nyos and Monoun (Cameroon) as estimated by sound speed in water. In: Ohba, T., Capaccioni, B. & Caudron, C. (eds) *Geochemistry and Geophysics of Active Volcanic Lakes*. Geological Society, London, Special Publications **437**, 185-192
- Sanemasa, M., Saiki, K., Kaneko K., Ohba T., Kusakabe M., Ntschantscho R., Foupe A., Tanyileke G. and Hell J.V. (2017). A new method to determine dissolved CO<sub>2</sub> concentration of lakes Nyos and Monoun using the sound speed and electrical conductivity of lake water. In: Ohba, T., Capaccioni, B., and Caudron, C. (eds.) *Geochemistry and Geophysics of Active Volcanic Lakes*. Geological Society, London, Special Publications **437**. <http://doi.org/10.1144/SP437.5>.

# Volcanic lake research: a 240(0)-year long explosive history

D. Rouwet<sup>1\*</sup>

<sup>1</sup>Istituto Nazionale di Geofisica e Vulcanologia, Sezione di Bologna, Viale Berti Pichat 6/2, Bologna, Italy

\*Corresponding author, e-mail: [dmitri.rouwet@ingv.it](mailto:dmitri.rouwet@ingv.it)

The quest for sulfur has often been a major scope during colonisation, as it also was for the Dutch who arrived in Eastern Java, Indonesia, when establishing in Banyuwangi, at the foot of Kawah Ijen volcano. A scientific exploration of the majestic Kawah Ijen crater lake in 1789 was arguably the first in its kind preluding modern volcanic lake research. Shortly after, the cataclysmic 1815 Tambora (Sumbawa, Indonesia) eruption was followed by an eruption at Kawah Ijen itself in 1817, modifying its crater morphology and lake basin. A century later, following the 1917 unrest at Ijen, Dutch engineers understood that keeping the hyperacid lake in its basin during phreatic eruptions or overflow events was essential to safeguard the surrounding population; they reinforced the lower west rim of the crater lake by a dam in 1919-1920.

Meanwhile in Japan in the early 1900s, sulfur spherules floating on Yugama crater lake, Kusatsu-Shirane volcano, central Honshu, were sketched and described by Kawasaki (1903); the model on how they were formed nailed it and still stands today. This other iconic crater lake, Yugama, erupted in 1932 and became the subject of early lake studies. Elemental sulfur, phreatic eruptions and mitigation strategies of these pioneering visions not coincidentally set the trend that is extrapolated into volcanic lake research today. Geochemical monitoring of some of the most active crater lakes initiated in the mid-1960s, at Yugama and Ruapehu, New Zealand/Aotearoa, and in 1978 at Poás volcano, Costa Rica. In the early 1990s instead, the geochemical research was picked up at Kawah Ijen and El Chichón, in Chiapas, Mexico, where a crater lake was formed after the 1982 Plinian eruptions.

A few years after the El Chichón eruption, two lakes in Cameroon exploded: Lake Monoun in 1984 and Lake Nyos in 1986, killing 37 and 1800 people, respectively. A CO<sub>2</sub> cloud was released from the bottom waters, but there was no evidence of a volcanic eruption: “the limnic gas burst” entered the scene. Especially the Lake Nyos event fueled a fiery discussion and gave rise to the International Working Group on Crater Lakes, that was rebaptised in the Commission on Volcanic Lakes (CVL), absorbed into IAVCEI. Since the late 1980s and 1990s, many researches were executed on apparently innocuous lakes with the fear that dissolved CO<sub>2</sub> could be stored in deep lake layers, ready to burst and kill. One such lake, our Lago Albano, seemed to be such a “Nyos-type” lake, eventually doesn’t seem to be, but potentially could become one in the future being stressed by Climate Change and anthropic impact. The emissario, a drainage tunnel arguably built by the Romans 400 years AC, might evidence that risk mitigation at volcanic lakes was already a hot topic 2400 years ago.

This presentation does not only deal with the history of volcanic lake research, but, en route, also sheds light on many chemical and physical processes reigning inside and around the lakes, with the scope to better assess the hazard related to these “blue windows” into volcano-hydrothermal systems.

# The impact of extreme hydrological events on reservoir methane emissions

B.S. Sherman<sup>1,2\*</sup>, P.W. Ford<sup>1</sup>

<sup>1</sup>CSIRO Environment, Canberra, ACT, Australia

<sup>2</sup>Reservoir Doctors Pty Ltd, Canberra, ACT, Australia

\*Corresponding author, e-mail [reservoir.doctor@icloud.com](mailto:reservoir.doctor@icloud.com)

## KEYWORDS

Methane; Stratification; Hydrology; Reservoir.

## Introduction

As the hydrologic cycle intensifies while the planet warms, periods of drought are expected to become more intense and to last longer. Rainfall events are expected to intensify as well, increasing the magnitude of extreme river flows. During droughts, fallen leaves, twigs, and branches accumulate in the landscape. This pool of reactive organic matter (OM) is then transported to reservoirs via the first heavy drought-breaking rains. In addition, intense precipitation will increase the supply of eroded soil to provide additional OM as well as nutrients that may contribute to larger algal populations. Allochthonous (catchment) loads of terrestrial organic carbon and autochthonous supply of locally-produced algae to the sediments are expected to increase CH<sub>4</sub> emissions from reservoirs.

The evidence for the involvement of allochthonous carbon in CH<sub>4</sub> emission from reservoirs is presently limited to relatively few systems. High rates of ebullition generally dominate total areal fluxes of CH<sub>4</sub> (Sherman et al., 2012; Aben et al., 2017), and high C burial rates are associated with high rates of ebullition (Sobek, et al., 2012). Ebullition has frequently been observed to be highest in areas of greatest sediment deposition such as the deltaic region of Lake Kariba (DelSontro et al., 2011) and the downstream ends of a series of shallow impoundments (forebays) in the Saar River (Maeck et al., 2013). Large upstream/downstream gradients in CH<sub>4</sub> ebullition fluxes have been observed in a small reservoir (McClure et al., 2020) and by the authors in two subtropical reservoirs in Australia, and analogous gradients in dissolved CH<sub>4</sub> have been reported in 3 subtropical reservoirs with different morphologies and catchment conditions by Musenze et al., (2014).

Here we report spatially-resolved measurements of diffusive and ebullitive CH<sub>4</sub> emissions, dissolved CH<sub>4</sub>, and reservoir stratification at Cotter Reservoir (Canberra, Australia) during 2010-2012. This period included two extreme hydrological events that produced the largest runoff in 26 years and followed the driest 3 years on record as well as a devastating bushfire in 2003 that burned a significant portion of the lower catchment.

## Materials and methods

Methane (and CO<sub>2</sub>) fluxes were measured by recirculating air at 5.5 ± 0.5 L/min through the headspace of a floating chamber and passing the air through a Picarro G1301 CRDS (which recorded CO<sub>2</sub>/CH<sub>4</sub>/H<sub>2</sub>O every 5 s) during a deployment of minimum duration 15-minutes. The chamber was deployed from a boat and replicate measurements were performed at 6 - 9 sites during each of 5 field trips. Water column physical parameters were measured with a YSI 6600v2 sonde. Full details of the project are in Sherman and Ford (2022).

## Results and discussion

The large inflow events caused by drought breaking rains profoundly altered reservoir stratification and delivered exceptionally large loads of OM to Cotter Dam. These inflows were followed by a substantial increase in methane emissions across the entire reservoir and the

establishment of a pronounced upstream/downstream gradient in flux. The late spring 2010 flood mixed the entire water column and raised the hypolimnion temperature from the typical seasonal value of ca. 10 °C to 18 °C. The early autumn 2012 flood raised the hypolimnion temperature to 13 °C. The observed changes in hypolimnion temperature could increase methane production by factors of up to 7 and 2, respectively, based on measured thermal regulation of methanogenesis (Duc et al., 2010). The total observed methane flux increased by factors of 23 and 7, respectively, suggesting that an additional factor of 3.3-3.5 was attributable to increased organic matter supply from the catchment during both years.

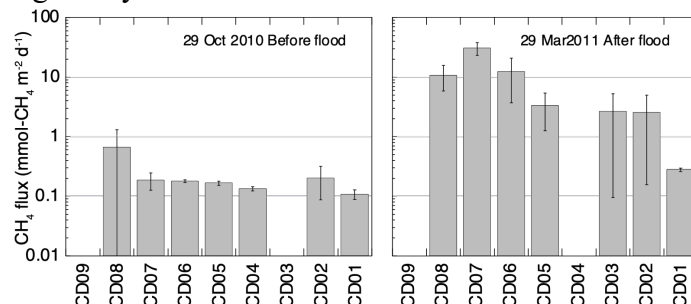


**Figure 1.** Methane flux measured before and after first flood event. CD01 is near the dam, CD09 is most upstream site. Note log scale used for y-axis.

## REFERENCES

- Aben, R.C.H. et al. (2017) Cross continental increase in methane ebullition under climate change. *Nature Communications*, **8**, 1682.
- Deemer, B.R. & Holgerson, M.A. (2021) Drivers of Methane Flux Differ Between Lakes and Reservoirs, Complicating Global Upscaling Efforts. *Biogeosciences*, **126**, e2019JG005600.
- DelSontro, T. et al. (2011) Spatial Heterogeneity of Methane Ebullition in a Large Tropical Reservoir. *Environmental Science & Technology*, **45**, 9866-9873.
- Duc, N.T., Crill, P. & Bastviken, D. (2010) Implications of temperature and sediment characteristics on methane formation and oxidation in lake sediments. *Biogeochemistry*, **100**, 185-196.
- Maeck, A. et al. (2013) Sediment Trapping by Dams Creates Methane Emission Hot Spots. *Environmental Science & Technology*, **47**, 8130-8137.
- McClure, R.P. et al. (2020) The Magnitude and Drivers of Methane Ebullition and Diffusion Vary on a Longitudinal Gradient in a Small Freshwater Reservoir. *Journal of Geophysical Research: Biogeosciences*, **125**, e2019JG005205.
- Musenze, R.S. et al. (2014) Assessing the spatial and temporal variability of diffusive methane and nitrous oxide emissions from subtropical freshwater reservoirs. *Environmental Science and Technology*, **48**, 14499-14507.
- Sobek, S. et al. (2012) Extreme organic carbon burial fuels intense methane bubbling in a temperate reservoir. *Geophysical Research Letters*, **39**, L01401.
- Sherman, B.S. & Ford, P.W. (2022) Extreme Hydrological Events and Reservoir Methane Emissions. *Frontiers in Environmental Science*, **10**, 893180.

# Impact of methane extraction on stratification in lake Kivu

T. Doda<sup>1\*</sup>, A. Mugisha<sup>2</sup>, E.R. Mudakikwa<sup>2</sup>, F. Darchambeau<sup>3</sup>, M. Schmid<sup>1</sup>

<sup>1</sup> Eawag, Swiss Federal Institute of Aquatic Science and Technology, Surface Waters - Research and Management, Kastanienbaum, Switzerland

<sup>2</sup> Environment Analytics and Lake Kivu Monitoring Division, Rwanda Environment Management Authority (REMA), Kigali, Rwanda

<sup>3</sup> ContourGlobal/KivuWatt Ltd., Kigali, Rwanda

\*Corresponding author; e-mail [tomy.doda@eawag.ch](mailto:tomy.doda@eawag.ch)

## KEYWORDS

Lake Kivu; stratification; chemocline; dissolved gases; CTD profiles.

## Introduction

Lake Kivu is a large, 485 m deep East African Rift lake containing important reservoirs of methane ( $62 \text{ km}^3$ ) and carbon dioxide ( $285 \text{ km}^3$ ) in its deep waters. The lake remains permanently stratified below 60 m depth with a main chemocline at 260 m depth. Due to hydrothermal groundwater springs, dissolved methane and carbon dioxide accumulate below the main chemocline, with concentrations reaching 18 and 90 mmol L<sup>-1</sup>, respectively (Bärenbold et al., 2020). Such high concentrations represent a risk of limnic eruption that would be dramatic for the dense population living on the shore of Lake Kivu. Although the stable lake stratification currently acts as a natural barrier against the upward transport of dissolved gases, it is unclear whether the vertical density structure evolves over time. In particular, the operation of the KivuWatt methane extraction plant since 2016 might modify the density gradients by pumping dense water at 350 m depth and re-injecting the degassed water above the main chemocline at 240 m depth.

Our study aims at better understanding the natural development of the lake stratification and determining the effects of methane extraction on lake stability to improve prediction of potential limnic eruption in the future.

## Materials and methods

We analysed 2370 Conductivity-Temperature-Depth (CTD) profiles collected in Lake Kivu between 2008 and 2022 by the Lake Kivu Monitoring Activities under the Rwanda Environment Management Authority (REMA) and the KivuWatt monitoring program. The 1030 profiles deeper than the main chemocline were used to characterise the lake vertical density structure. We obtained water density profiles  $\rho(z)$  by estimating  $\rho$  from temperature, conductivity, and concentrations of CO<sub>2</sub> and CH<sub>4</sub> from Bärenbold et al. (2020). We averaged the profiles over three periods to determine temporal changes in stratification: a reference period defining the initial conditions (2008-2010), the following five years without methane extraction (2011-2015) and the last seven years with methane extraction (2016-2022).

## Results and discussion

Averaged profiles of temperature, conductivity and density reveal temporal changes in stratification before and after the start of methane extraction (Fig. 1). Temperature profiles show a natural warming of  $\sim 0.01 \text{ }^\circ\text{C.yr}^{-1}$  at all depths (Fig. 1a), as already reported by previous studies (Lorke et al., 2004; Schmid & Wüest, 2012; Katsev et al., 2014). A slight rise of the main chemocline also seems to occur before 2016 (Fig. 1c). In contrast, the chemocline has deepened on average by  $\sim 2 \text{ m}$  during the methane extraction period compared to 2011-2015. The reinjection of degassed water above the chemocline has increased the density between 240 and 255 m depth by  $\sim 0.15 \text{ kg.m}^{-3}$ , which has weakened the upper limit of the main density gradient. We will discuss in this talk additional effects of methane extraction on lake stratification and the spatial extent of such modifications.

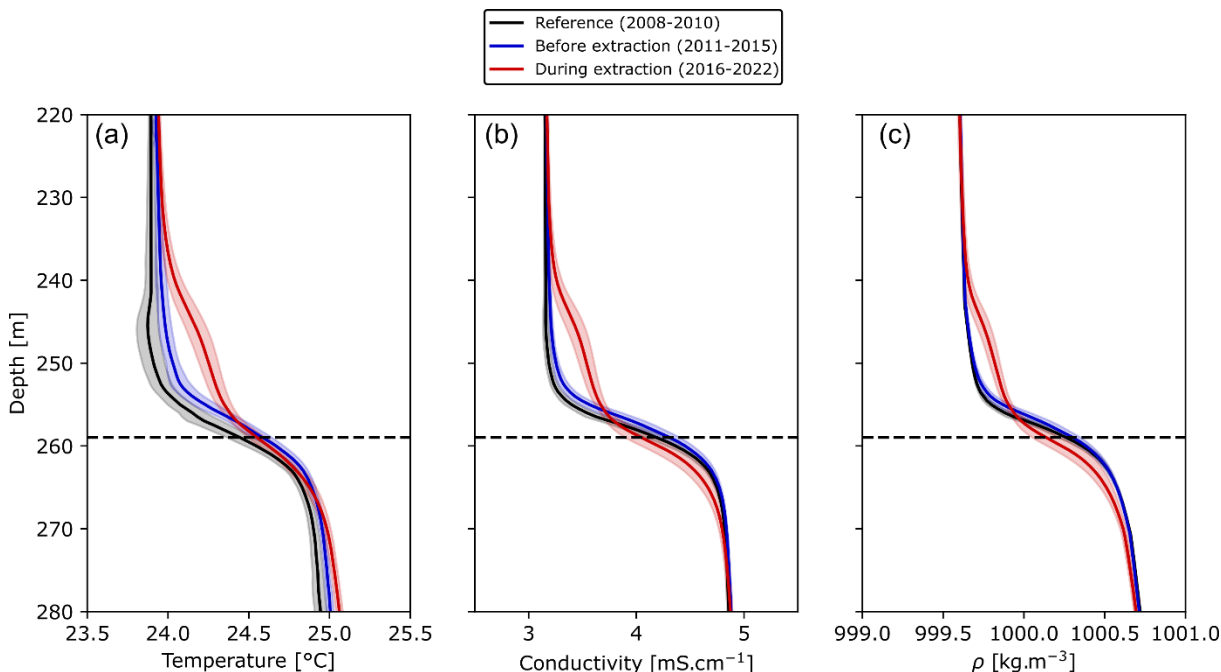


**Figure 1.** Temporal changes in stratification near the main chemocline of Lake Kivu for (a) temperature, (b) conductivity and (c) water density. The profiles are averaged over three periods: a reference period (black), before methane extraction (blue) and during methane extraction (red). The shaded area represents the standard deviation for each profile. The horizontal dashed line depicts the average depth of the main chemocline.

## REFERENCES

- Bärenbold, F., Boehrer, B., Grilli, R., Mugisha, A., von Tümpeling, W., Umutoni, A., & Schmid, M. (2020). No increasing risk of a limnic eruption at Lake Kivu: Intercomparison study reveals gas concentrations close to steady state. *PLoS ONE*, **15**(8), e0237836. <https://doi.org/10.1371/journal.pone.0237836>.
- Katsev, S., Aaberg, A. A., Crowe, S. A., & Hecky, R. E. (2014). Recent warming of Lake Kivu. *PLoS ONE*, **9**(10), e109084. <https://doi.org/10.1371/journal.pone.0109084>
- Lorke, A., Tietze, K., Halbwachs, M., & Wüest, A. (2004). Response of Lake Kivu stratification to lava inflow and climate warming. *Limnol. Oceanogr.*, **49**(3), 778–783. <https://doi.org/10.4319/lo.2004.49.3.00778>
- Schmid, M., & Wüest, A. (2012). Stratification, Mixing and Transport Processes in Lake Kivu. In J.-P. Descy, F. Darchambeau, & M. Schmid (Eds.), *Lake Kivu* (pp. 13–29). Springer Netherlands. [https://doi.org/10.1007/978-94-007-4243-7\\_2](https://doi.org/10.1007/978-94-007-4243-7_2)

# Magnitude, temporal dynamics, and drivers of oxic methane production across a trophic state gradient

C. Ordóñez<sup>1\*</sup>, T. DelSontro<sup>1,2</sup>, T. Langenegger<sup>1</sup>, D. Donis<sup>1</sup> and D.F. McGinnis<sup>1</sup>

<sup>1</sup> Department F.-A. Forel for Environmental and Aquatic Sciences, University of Geneva, Geneva, Switzerland

<sup>2</sup> now at Department of Earth and Environmental Sciences, University of Waterloo, Ontario, Canada

\*Corresponding author, e-mail [cesar.ordonez@unige.ch](mailto:cesar.ordonez@unige.ch)

## KEYWORDS

Lakes; methane; modelling; oxic methane production; greenhouse gases.

## Introduction

Contrasting the current paradigms that biogenic CH<sub>4</sub> is only produced under anoxic conditions, several studies have shown that oxic methane production (OMP) occurs in surface waters in the ocean and lakes (Karl et al. 2008; Tang et al. 2014). Although it is still under debate, several studies have shown a substantial contribution of OMP to diffusive CH<sub>4</sub> emissions from lakes. Several mechanisms have been proposed for OMP, however correlations between CH<sub>4</sub>, oxygen and phytoplankton concentrations suggest a direct role of phytoplankton in OMP (Bižić et al. 2020). Moreover, recent studies have also shown that OMP follow light-dark cycles in various phytoplankton cultures (Bižić et al. 2020). Therefore, it is probable that the production of CH<sub>4</sub> on oxic conditions may vary seasonally, based on trophic properties of each lake and due to different light conditions.

Lakes CH<sub>4</sub> emissions are responsible for about 25% of the natural atmospheric CH<sub>4</sub> global budget (Rosentreter et al. 2021). Since OMP occurs in surface waters, it can be quickly emitted to the atmosphere. Therefore, to predict future CH<sub>4</sub> emissions from lakes, it is crucial to understand the OMP dynamics and its mains drivers. In this study we estimate the net production rate of CH<sub>4</sub> ( $P_{\text{net}}$ ) defined as the balance between OMP (adds CH<sub>4</sub>) and methane oxidation (MOx, removes CH<sub>4</sub>) in the surface mixed layer (SML). We studied the main biochemical and physical parameters that could drive  $P_{\text{net}}$  across a trophic gradient and daily and seasonal dynamic during the stratified season in five lakes.

## Materials and methods

Our research was divided in three main strategies: First, to study the OMP magnitude and its drivers across trophic gradient, we conducted three sampling campaigns over the stratified season in four pre-alpine lakes (~1800 m.a.s.l) – Lac de Bretaye, Lac des Chavonnes, Lac Lioson and Lac Noir located in the Swiss Alps. Then we investigated the OMP seasonality in Soppensee, a eutrophic lake located in Canton Lucerne. We monitored this lake monthly during four years. And finally, we conducted a 24-h campaign over three days in Lac de Bretaye to study the daily variation of OMP in the SML.

In all these sampling campaigns, we measured surface concentrations and water column profiles of CH<sub>4</sub> and the stable carbon isotopic signature of CH<sub>4</sub>. We estimated the net production of CH<sub>4</sub> ( $P_{\text{net}}$ ) in all the lakes in the surface mixed layer (SML) using different mass balance approaches, where all sources and sinks of CH<sub>4</sub> were measured (Fig. 1), i.e., surface

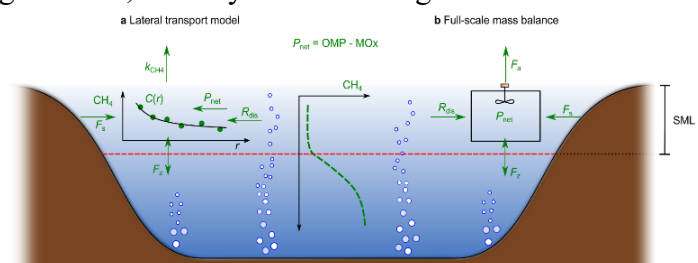


**Figure 1.** Conceptual schematic of the CH<sub>4</sub> budget components in the surface mixed layer and methodological approaches (Ordóñez et al. 2023).

$\text{CH}_4$  diffusive fluxes to the atmosphere ( $F_a$ ), sediment diffusive fluxes of  $\text{CH}_4$  from littoral sediment ( $F_s$ ),  $\text{CH}_4$  bubble dissolution in the SML ( $R_{\text{dis}}$ ) and vertical transport at the base of the SML ( $F_z$ ).

## Results and discussion

In most of the studied lakes, average  $P_{\text{net}}$  rates during the stratified season were positive, indicating that OMP rates were higher than MOx rates, therefore  $P_{\text{net}}$  acted as a source of  $\text{CH}_4$  in the SML.  $P_{\text{net}}$  and  $F_s$  were the two main sources of  $\text{CH}_4$  in the SML. On average  $P_{\text{net}}$  contributed about 60% of the diffusive  $\text{CH}_4$  emissions to the atmosphere in our lakes. Higher  $P_{\text{net}}$  rates were observed in more eutrophic lakes compared to oligotrophic lakes. While no clear tendency was observed in the oligotrophic lakes, higher  $P_{\text{net}}$  rates were estimated at the beginning of the summer in the eutrophic lakes. Towards the end of the stratified season  $P_{\text{net}}$  rates were negative, indicating that MOx was dominant over  $P_{\text{net}}$ , which was verified with isotopically less enriched  $\text{CH}_4$ . During our 24h campaign in Lac de Bretaye, preliminary results show that  $P_{\text{net}}$  followed the light-dark cycle, suggesting a role of photoautotrophs on OMP. Including literature  $P_{\text{net}}$  rates, we were able to observe that  $P_{\text{net}}$  can be mostly explained by changes in light climate (LC) at each specific lake. LC defines the average light intensity that phytoplankton can be exposed to in the SML. Since the relationship between LC and  $P_{\text{net}}$  strongly depends on the trophic state of each lake, we suggest an empirical approach using additional trophic variables (Ordóñez et al. 2023). While more studies are needed, this up-scaling approach provides an important step towards estimating the  $P_{\text{net}}$  contribution to the atmospheric  $\text{CH}_4$  budget. This study emphasizes that although OMP is common in the majority of lakes examined, there is a need for a more comprehensive understanding of the scope of OMP, its drivers, and its temporal patterns. This is important given the possible relationship between climate change, phytoplankton, and  $\text{CH}_4$  emissions into the atmosphere.

## REFERENCES

- Bižić, M. et al. (2020). Aquatic and terrestrial cyanobacteria produce methane. *Sci. Adv.* **6**: eaax5343. doi:10.1126/sciadv.aax5343
- Karl, D. M., L. Beversdorf, K. M. Björkman, M. J. Church, A. Martinez, and E. F. Delong (2008). Aerobic production of methane in the sea. *Nat. Geosci.* **1**: 473–478. doi:10.1038/ngeo234
- Ordóñez, C., T. DelSontro, T. Langenegger, D. Donis, E. L. Suarez, and D. F. McGinnis (2023). Evaluation of the methane paradox in four adjacent pre-alpine lakes across a trophic gradient. *Nat. Commun.* **14**: 1–13. doi:10.1038/s41467-023-37861-7
- Rosentreter, J. A. et al. (2021). Half of global methane emissions come from highly variable aquatic ecosystem sources. *Nat. Geosci.* 1–6. doi:10.1038/s41561-021-00715-2

# What the sediment holds – hydroacoustic quantification of reservoir methane emissions

R. Thirkill<sup>1,2\*</sup>, W. Gray IV<sup>1</sup>, C. Clemons<sup>1</sup>, J. Porraz<sup>1</sup>, H. Oldroyd<sup>1,2</sup>, A.L. Forrest<sup>1,2</sup>, M. Seelos<sup>3</sup>

<sup>1</sup>Department of Civil and Environmental Engineering, University of California Davis, CA, USA

<sup>2</sup>Tahoe Environmental Research Center, University of California Davis, CA, USA

<sup>3</sup>Valley Water, San Jose, CA, USA

\*Corresponding author, e-mail [rthirkill@ucdavis.edu](mailto:rthirkill@ucdavis.edu)

## KEYWORDS

Hydroacoustics; ebullition; methane; sediments; gas storage.

## Introduction

Across all climate regions, reservoirs play an important, yet poorly understood role in the generation of greenhouse gases (GHGs). There is an ongoing debate regarding their net effect on atmospheric GHG concentrations as reservoirs can be both sources of high GHG emissions (23-142 Tg CH<sub>4</sub> yr<sup>-1</sup>) as well as strong CO<sub>2</sub> sinks resulting from carbon burial and algal photosynthesis (Rosentreter et al., 2021). This debate is largely due to the difficulties that exist in collecting spatiotemporal emissions data that include all the major pathways and are representative across many systems of the same category (i.e. reservoirs, lakes, wetlands). As a result, more effort is necessary from all stakeholders (water agencies, scientists, etc.) to better quantify CH<sub>4</sub> releases (which comprise the majority of reservoir GHG emissions) through these major pathways, which include ebullition and diffusion from the reservoir water surface. Quantifying flux rates of carbon is critical for water managers to reach net carbon neutrality, evaluate potential impacts of dam construction projects, and manage reservoir operations (e.g. oxygenation systems, reservoir releases). In Mediterranean climate areas specifically, where there exists a paucity of data and drought-related water level fluctuations are becoming significantly larger, understanding the biogeochemical processes that can aggravate or lessen CH<sub>4</sub> releases is increasingly critical.

## Materials and Methods

To develop a systematic approach for an extensive investigation of the GHG production and related parameters in a reservoir, hydroacoustic methods were combined with physiochemical sediment variables and surface gas measurements. Hydroacoustic measurements were made following Anderson and Martinez's 2015 methodology using a 200 kHz transducer connected to a BioSonics DT-X echosounder surface unit and a Garmin real-time differential GPS receiver. Echograms were analyzed and 15 different attributes of the bottom echo envelope (i.e. E1', E1, FD, Svmax, E1'/E1, etc.) were extracted. These acoustic signatures were then normalized, and a Fuzzy C cluster analysis was performed on the first 6 PCA components. The resultant clusters were plotted and compared to particle size distributions of grab samples to identify the distribution of different sediment types within each reservoir. Lastly, linear relationships between in-situ sediment gas volume measurements and the Svmax were made based on sediment type. These equations were then used to model the spatial distribution of gas volume within each of the reservoirs' bottom sediments.

## Results and discussion

Each reservoir shows a strong seasonal trend in CH<sub>4</sub> fluxes, with peak emissions occurring in the warmer months when the reservoir bottoms have low dissolved oxygen (DO) concentrations (anoxic) and oxidation-reduction potentials (ORP). Likewise, we observed strong diurnal variability in both CH<sub>4</sub> and CO<sub>2</sub>, with peak flux rates generally occurring during the daytime for CH<sub>4</sub> and during the nighttime for CO<sub>2</sub>. Water quality measurements taken concurrently with gas flux measurements show strong correlations exist between CH<sub>4</sub> emissions and both chlorophyll

(measured as chl-a) and water temperature. Echosounder sediment surveys suggest a spatial distribution of gas storage that changes across the seasons and provides a method of quantifying bubble plumes in the water (e.g., Fig. 1). A high quantity of bubble plumes measured in the dry season suggest that it is a key time period for ebullitive CH<sub>4</sub> emission. Furthermore, the surveys show strong intra- annual variability between low and high-water years suggesting that previously exposed sediments can be major sources of GHGs once they are rewetted (Fig. 1a). This process appears to be closely linked to the position of the thermocline layer within the reservoir (Fig. 2b). Conversely, the CH<sub>4</sub> surface fluxes were comparatively lower in spring 2022 than spring 2021, presumably a result of the longer travel time from the sediments to the water's surface resulting in more chances for oxidation to occur. This work represents important data and methodological contributions that better constrains CH<sub>4</sub> modeling and budget assessments for reservoirs, while also providing insight into the processes that regulate CH<sub>4</sub> emissions from inland waters.

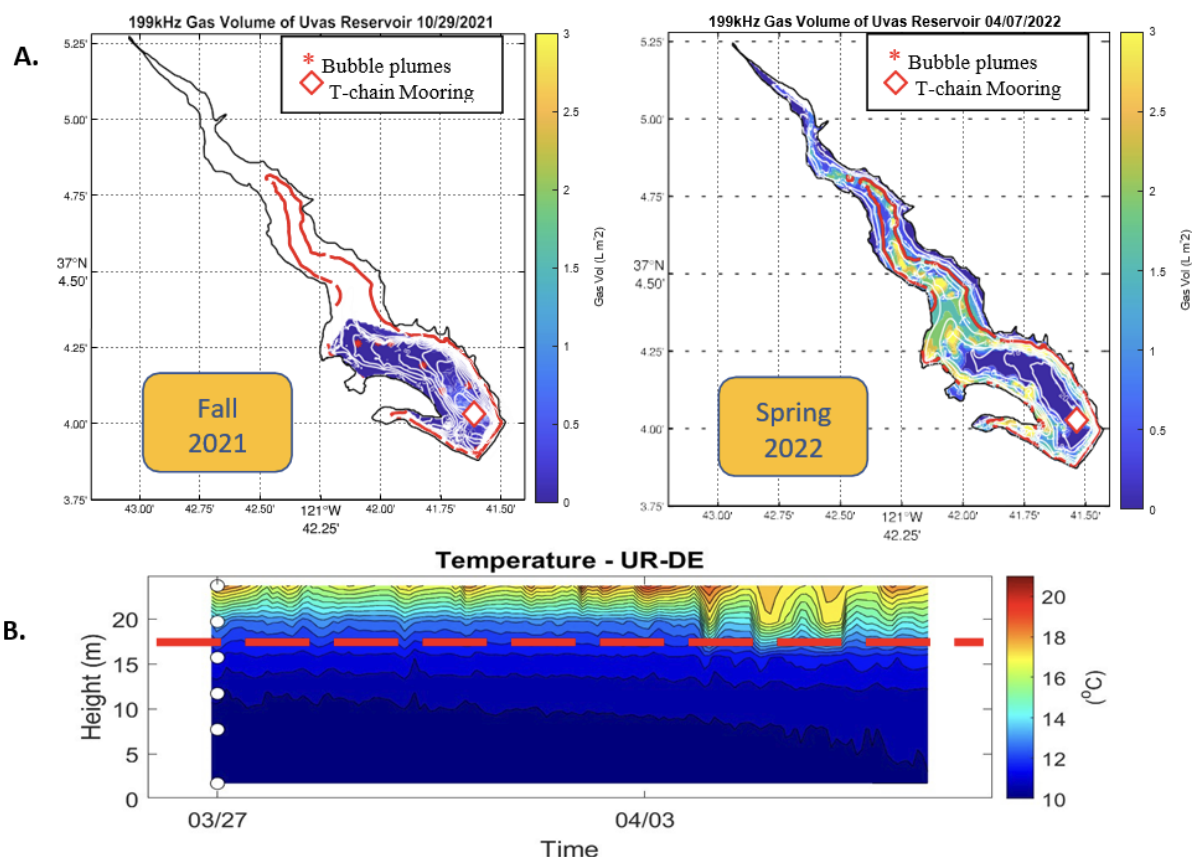


**Figure 1.** (a) Distribution of methane gas present in surficial sediments of Uvas Reservoir for fall 2021 (left) and winter/spring 2022 (right); (b) Continuous temperature profile from 03/27/2022 to 04/07/2022 at the deep site within Uvas Reservoir (white and red diamond). The red lines in contour plots indicates a depth of 8m from surface waters where the thermocline is indicated with dashed red line in figure b. White depth contours are included in meters.

## REFERENCES

- Anderson, M.A., Martinez, D., (2015). Methane gas in lake bottom sediments quantified using acoustic backscatter strength. *Journal of Soils and Sediments* **15**, 1246–1255. <https://doi.org/10.1007/s11368-015-1099-1>
- Rosentreter, J.A., Borges, A.V., Deemer, B.R., Holgerson, M.A., Liu, S., Song, C., Melack, J., Raymond, P.A., Duarte, C.M., Allen, G.H., Olefeldt, D., Poulter, B., Battin, T.I., Eyre, B.D., (2021). Half of global methane emissions come from highly variable aquatic ecosystem sources. *Nature Geoscience* **14**, 225–230. <https://doi.org/10.1038/s41561-021-00715-2>

# Far field simulation of a landslide-generated tsunami in Lake Iseo

R. Bonomelli<sup>1\*</sup>, G. Farina<sup>1</sup>, M. Pilotti<sup>1</sup>

<sup>1</sup> Department Civil, Environmental, Architectural Engineering and Mathematics, Università degli Studi di Brescia, Brescia, Italy

\*Corresponding author; e-mail [r.bonomelli@unibs.it](mailto:r.bonomelli@unibs.it)

## KEYWORDS

Landslide-generated waves; Numerical simulation; Shallow Water Equations; Exposure

## Introduction

Italian prealpine lake shores are characterized by heavily populated areas and valuable assets. In presence of steep slopes, they can be endangered by wave runup caused by possible landslides into the lake. The most notorious example in Italy is the Vajont event (1963) which claimed over 2000 lives in the neighboring villages, but similar events happened in other parts of the world (e.g. Lake Lohen, Norway & Lituya Bay, Alaska). The enclosed geometry of the lakes may focus the destructive effects of the waves. In the month of February 2021 the lake Iseo, located in northern Italy, was endangered by a similar event. A landslide mass initially estimated of over 2 million of m<sup>3</sup>, located near the town of Vigolo, manifested daily displacements in the order of centimeters, which triggered panic in the local population.

## Materials and methods

The first step is the simulation of the landslide movement along the slope. There are numerous numerical techniques to properly simulate the dynamics of granular flow (Yavari-Ramshe et al., 2015), with various levels of complexity. Landslides commonly exhibit a fluid-like flow behaviour with an appropriate rheology (Yavari-Ramshe & Ataie-Ashriani, 2016). In this contribution, we choose to model the motion of the landslide as a homogeneous fluid characterized by a Voellmy rheology (Salm, 1993) using a custom shock-capturing finite volume solver of the Shallow Water Equations presented in Bonomelli et al. (2023). Geological surveys in the field allowed to partially assess the shape of the failure surface of the landslide, fixing the amount of material that loses equilibrium, as well as the geotechnical properties (internal friction angle 20°) of the granular medium being modelled. A failure cylinder intersecting the slope at a maximum depth of 50 m and capable of mobilize 2 million of m<sup>3</sup> of granular material has been selected as the source of the granular material that suddenly loses equilibrium. The velocity profiles obtained from the first simulation are then imposed as a boundary condition to represent in a simplified way the interaction between the landslide body falling into the lake and the lake surface. As a following step an unstructured computational mesh of 1.6 million cells spanning the whole lake was used to properly assess the far field waves generated by such an impact. Inside the lake the mesh has an average dimension of 40 m while near the coastlines such step diminishes up to 5 m. The same numerical model based on the Shallow Water Equations (SWE) but with newtonian rheology was used for the modelled fluid. Lastly, the inundation map caused by the landslide-generated waves are used to compute both the risk to population and residential building using the MOVIDA procedure (Ballio et al. 2022, AdBpo 2021), focusing on the town of Iseo that would be one of the most impacted by the wave.

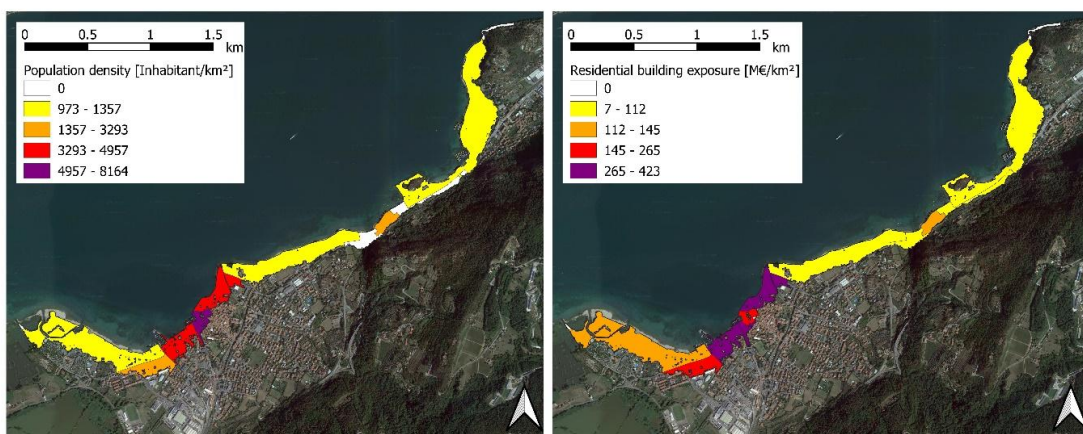


**Figure 1.** (Left) Population density distribution in the flooded areas in Iseo town. (Right) Residential building exposure distribution in the flooded areas in Iseo town. Both maps are computed using the MOVIDA procedure.

## Results and discussion

The described modelling chain has been used to assess the exposure of Iseo town to the consequences of a landslide into the lake. Despite the inadequacy of the SWE to represent complex wave patterns generated by a landslide near the impact (the so-called splash zone and near field), such equations can still provide a reliable answer for the wave propagation phase (far field). Predicted maximum wave height in Iseo town is around 2 m, with a maximum inundation extent of 200 m measured normally with respect to the coastline, covering an area of 0.5 km<sup>2</sup>. The MOVIDA procedure highlights the exposure associated with such waves, which reflects the heavily populated areas located along the shores. Given the impulsive nature of the event, (landslide-generated waves would reach Iseo town in less than 3 minutes) the uncertainties and the constant changing conditions associated with the complex nature of landslides, the current methodology (although simplified) may provide reasonably accurate results without elevated computational burdens (lake simulation finished in less than 5 hours on a regular laptop) that would be associated with more rigorous numerical simulations.

## REFERENCES

- AdBpo – (2021). Relazione metodologica: MOdello per la Valutazione Integrata del Danno Alluvionale (MOVIDA) Distretto del fiume Po dicembre 2021 ([www.pianoalluvioni.adbpo.it](http://www.pianoalluvioni.adbpo.it))
- Ballio et al. (2022). The MOVIDA Project to Support the Update of Flood Risk Maps in the Po River District: methodology for flood damage assessment, *Proceedings of the 39th IAHR World Congress, 19-24 June 2022 Granada, Spain.* <https://doi.org/10.3850/IAHR-39WC2521711920221136>
- Bonomelli, R., Farina, G., Pilotti, M., Molinari, D., Ballio, F., (2023) Historical comparison of the damage caused by the propagation of a dam break in a pre-alpine valley, *Journal of hydrology regional studies (under review)*
- Salm, B. (1993) Flow transition and runout distances of flowing avalanches. *Ann. Glaciol.* **18**, 221-226.
- Yavari-Ramshe S., Ataie-Ashtiani B. (2015) A robust finite volume model to simulate granular flows. *Comput. Geotech.* **66**:96-112 doi:[10.1016/j.compgeo.2015.01.015](https://doi.org/10.1016/j.compgeo.2015.01.015)
- Yavari-Ramshe, S., Ataie-Ashtiani, B. (2016) Numerical modeling of subaerial and submarine landslide-generated tsunami waves—recent advances and future challenges. *Landslides* **13**, 1325–1368. <https://doi.org/10.1007/s10346-016-0734-2>

# Ebullition rates and drivers in a shallow eutrophic Mediterranean reservoir

C.L. Ramón<sup>1\*</sup>, E. Rodríguez-Velasco<sup>2</sup>, C. Clemons.<sup>3</sup>, I. Reche<sup>2</sup>, H.J. Oldroyd<sup>3</sup>, A.L. Forrest<sup>3</sup>, and F.J. Rueda<sup>1</sup>

<sup>1</sup> Department of Civil Engineering and Water Institute, University of Granada, Granada, Spain

<sup>2</sup> Department of Ecology and Water Institute, University of Granada, Granada, Spain.

<sup>3</sup> Department of Civil and Environmental Engineering, University of California, Davis, USA

\*Corresponding author, e-mail [crcasanas@ugr.es](mailto:crcasanas@ugr.es)

## KEYWORDS

Methane; Ebullition; Mediterranean reservoir; drivers.

## Introduction

Current estimates indicate that lakes and reservoirs contribute to approximately 20% of global CH<sub>4</sub> emissions (e.g., Rosentreter et al., 2021). Unfortunately, these global estimates are still highly uncertain partly because emission estimates are not available for all biomes and lake/reservoir typologies. The lack of information is particularly the case of the Mediterranean biome from 30°N to 45°N (e.g., Deemer et al., 2016; Harrison et al., 2021), where reservoirs, with large seasonal-scale temperature and water level fluctuations, are the prevalent aquatic ecosystem. Here, we present data on CH<sub>4</sub> emissions from a small and shallow eutrophic reservoir in South Spain, Cubillas Reservoir, focusing on ebullition which is the most efficient natural transport pathway in the reservoir and represents ≥ 70% of ebullitive plus diffusive emissions in summer.

## Materials and methods

Cubillas (37.278°N, -3.672°E) is a small (surface area ≈ 2 km<sup>2</sup> and 13.5 hm<sup>3</sup> capacity) and shallow eutrophic reservoir, with a maximum depth of ≈ 14 m at full capacity. An eddy covariance EC tower was installed on top of a floating platform at the end of 2021, to measure high-frequency CH<sub>4</sub> emissions using an 'open path' infrared gas analyzer IRGA (Li 7700, LiCor). The wavelet-based partitioning method of Iwata et al. (2018) was used to calculate ebullition from the EC data. Automated bubble traps ABT (Senect) were also deployed in 2021 and 2022 in the lake, allowing for high temporal resolution ebullition rates estimates.

## Results and discussion

Ebullition rates ranged from ≈ 0 ml m<sup>-2</sup> day<sup>-1</sup> in winter up to 2000 ml m<sup>-2</sup> day<sup>-1</sup> in summer, or equivalently up to 1200 mg CH<sub>4</sub> m<sup>-2</sup> day<sup>-1</sup> for the average ≈ 90% CH<sub>4</sub> content of methane in the bubbles. Water temperature is the main driver of the seasonal evolution of ebullition, and daily rates, as measured by the bubble traps are well predicted by the modified Arrhenius equation ( $R^2 = 0.92$  for ABT data in Fig.1), although the longer time-signal of the EC tower shows hysteresis in the temperature response of the bubble flux (Fig. 1). On hourly scales, atmospheric pressure is also significantly negatively correlated with ebullition rates, and the daily pattern of ebullition shows two characteristic daily peaks.

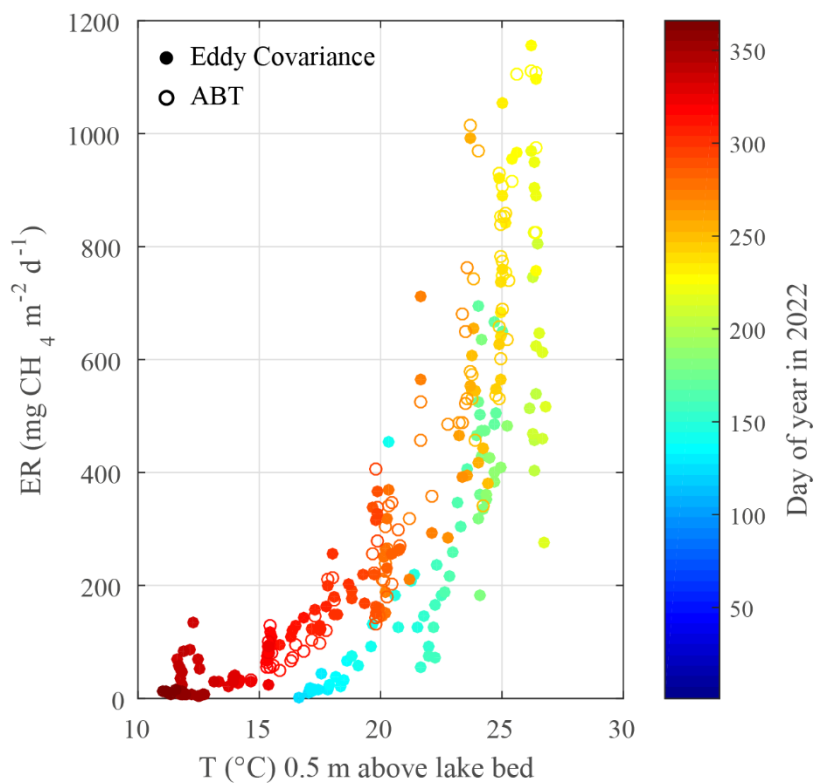


**Figure 1.** Daily ebullition rates in Cubillas reservoir as a function of water temperature close to the lake sediment. For the automated bubble trap (ABT), it was assumed a 90% content of methane in bubbles.

## REFERENCES

- Deemer, B. R., Harrison, J. A., Li, S., Beaulieu, J. J., DelSontro, T., Barros, N., et al. (2016). Greenhouse Gas Emissions from Reservoir Water Surfaces: A New Global Synthesis. *BioScience*, **66**(11), 949–964. <https://doi.org/10.1093/biosci/biw117>.
- Harrison, J. A., Prairie, Y. T., Mercier-Blais, S., & Soued, C. (2021). Year-2020 Global Distribution and Pathways of Reservoir Methane and Carbon Dioxide Emissions According to the Greenhouse Gas From Reservoirs (G-res) Model. *Global Biogeochemical Cycles*, **35**(6), e2020GB006888. <https://doi.org/10.1029/2020GB006888>.
- Iwata, H., Hirata, R., Takahashi, Y., Miyabara, Y., Itoh, M., & Iizuka, K. (2018). Partitioning Eddy-Covariance Methane Fluxes from a Shallow Lake into Diffusive and Ebullitive Fluxes. *Boundary-Layer Meteorology*, **169**(3), 413–428. <https://doi.org/10.1007/s10546-018-0383-1>.
- Rosentreter, J. A., Borges, A. V., Deemer, B. R., Holgerson, M. A., Liu, S., Song, C., et al. (2021). Half of global methane emissions come from highly variable aquatic ecosystem sources. *Nature Geoscience*, **14**(4), 225–230. <https://doi.org/10.1038/s41561-021-00715-2>.

# Methane bubbles under ice in Base Mine Lake

E. Tedford<sup>1\*</sup>, R. Pieters<sup>1,2</sup>, L. Ing<sup>1</sup>, G. Lawrence<sup>1</sup>

<sup>1</sup> Civil Engineering, University of British Columbia, Vancouver, Canada

<sup>2</sup> Earth, Ocean and Atmospheric Sciences, University of British Columbia, Vancouver, Canada

\*Corresponding author, e-mail [tedford@eos.ubc.ca](mailto:tedford@eos.ubc.ca)

## KEYWORDS

methane ebullition; ice; echosoundings; mine tailings, turbidity.

## Introduction

Base Mine Lake ( $7.9 \text{ km}^2$ ,  $57^\circ 1' \text{ N}$ ,  $112^\circ 31' \text{ W}$ ) is a pit lake in the oil sands region of northern Alberta, Canada. The lake consists of a 10 m water cap, on top of approximately 40 m of fluid fine tailings sequestered in the bottom of the lake. Within the underlying fluid fine tailings, methane bubbles are generated that rise through the water cap throughout the year. These bubbles can transport particles (turbidity) and residual hydrocarbon from the bottom tailings into the water column.

## Methods

We report on three different measurements of ebullition:

1. The first records of ebullition at Base Mine Lake were collected with autonomous echosounders (Echologger EA400) under ice. These measurements captured the temporal variability of ebullition.
2. The second set of ebullition records were collected with CT scans of ice cores collected from a grid of locations covering the whole lake. These cores provided horizontal and temporal (based on depth within the core) description of ebullition during the period of ice growth (approximately 90 days). An example of a CT scan of Base Mine Lake ice is shown in Figure 1.
3. The third set of ebullition records are from modified bubble traps similar to those of Varadharajan et al. (2010). These were deployed under the ice and in open water. This method provided a direct quantitative measure of ebullition based on the volume of trapped bubbles plus a continuous record of ebullition based on the difference in pressure measured inside and outside the trap.

## Results

All three types of measurements of ebullition showed intense ebullition events were correlated with troughs in atmospheric pressure.

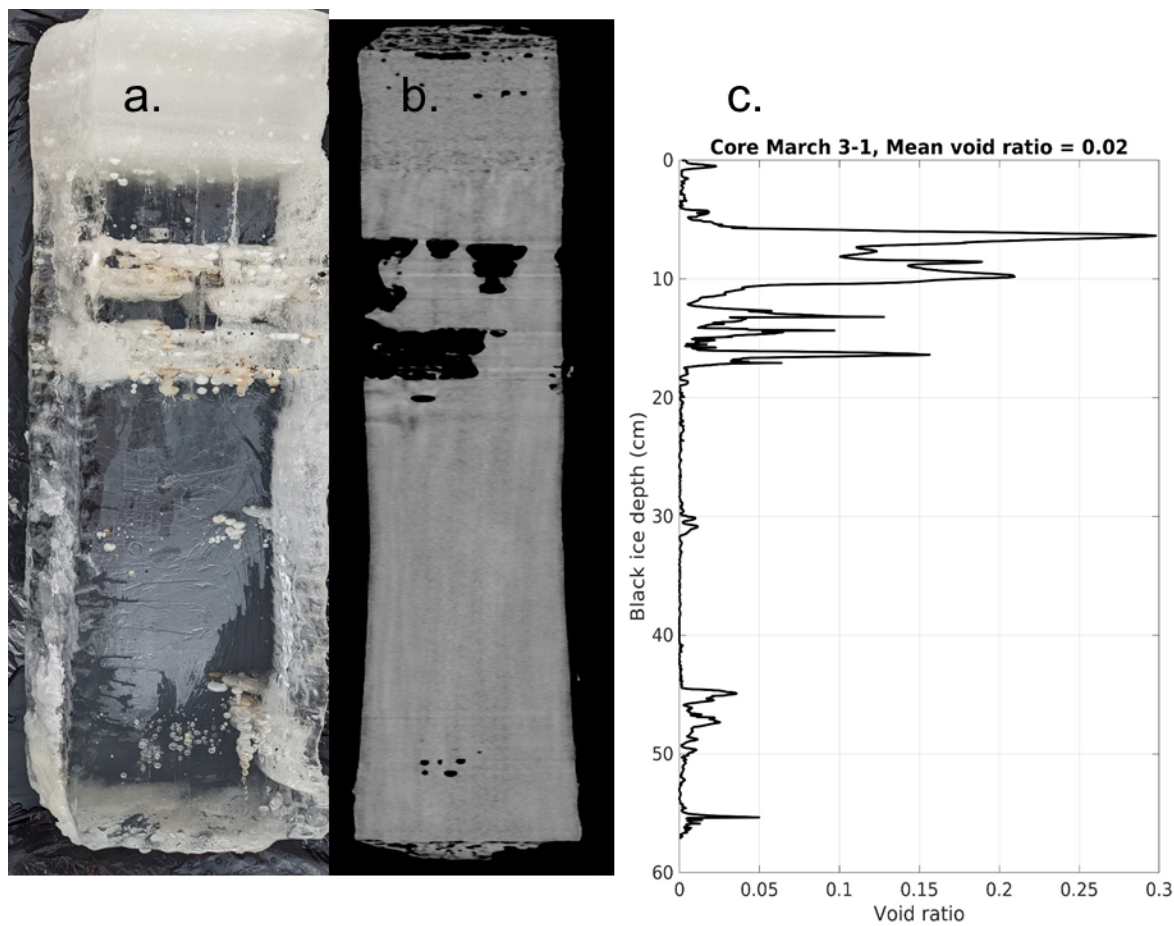


**Figure 1.** (a) Image of an ice core recovered from Base Mine Lake, consisting of approximately 15 cm of white (snow) ice at the top, and 57 cm of black (transparent) ice below. (b) Two-dimensional slice from the CT scan of the ice shown in panel (a). (c) Vertical profile of the void ratio for the black ice determined from the three-dimensional CT scan of the ice shown in panel (a).

#### REFERENCES

- Varadharajan, C., Hermosillo, R., & Hemond, H. F. (2010). A low-cost automated trap to measure bubbling gas fluxes. *Limnology and Oceanography: Methods*, 8(7), 363-375.

# 3D Modeling of climate change impacts on a groundwater-fed lake in Berlin area

B. Zamani<sup>1\*</sup>, F. Hellweger<sup>1</sup>

<sup>1</sup>*Department of water quality engineering, Technical University of Berlin, Germany*

\*Corresponding author; e-mail [b.zamani.gharehchaman@tu-berlin.de](mailto:b.zamani.gharehchaman@tu-berlin.de)

## KEYWORDS

hydrodynamic modeling; water quality; groundwater; phytoplankton, ecosystem

## Introduction

Groundwater-fed lakes with no surface inflow/outflows are very sensitive to any groundwater level changes in their catchment. This becomes a more critical issue in terms of water quality and phytoplankton when it comes to water level decline by climate change impacts. In this study, as a part of the CliWaC consortium project (Climate and Water under Change), we model the hydrodynamics and ecosystem of lake “Sacrower See”, a dimictic groundwater-fed lake in the Berlin/Potsdam region of Germany.

## The goal

The final goal of the current study is to model and study the outcomes of the climate change impacts on the phytoplankton and the ecosystem of the lakes in Berlin/Brandenburg area and provide decision makers and stakeholders with enough information on different possible scenarios to mitigate climate change impacts on the lake water quantity and quality. These scenarios include predicting the long-term effects of providing water from different external sources (to maintain lake water level) on the lake water quality and reactivating the aeration system within the lake.

## Materials and methods

The three-dimensional hydrodynamic and ecosystem model AEM3D, is employed to simulate the hydrodynamic processes (e.g. stratification and mixing), nutrients cycle, and phytoplankton to provide a modeling tool and act as a decision-making tool for stakeholders. The lake model is planned to be integrated with a groundwater model (developed by the hydrogeology group of CliWaC) to simulate the groundwater balance of the lake (as boundary conditions of the lake model). As the result of the hydrogeologic modeling is still under development, we developed a simple water balance model as a short-term solution for the lake’s watershed, including surface hydrology, evapotranspiration, and an active groundwater inflow/outflow model for the simulated lake (using the USGS segmented approach), which employs water table and hydraulic information of wells around the lake to simulate lake/aquifer water exchanges. For the case of Sacrower See, 8 active wells in the lake neighborhood were used, one of which includes groundwater temperature and nutrients measurements of the aquifer. The AEM3D model was run for the entire stratification and mixing season of 2017-18. In addition to groundwater data, other boundary conditions of the AEM3D model include bathymetry and meteorological data. The meteorological data were interpolated for the lake location using two nearby DWD (German weather service) stations in Potsdam and Berlin. The hydrodynamic model includes a horizontal structured grid of 20×20m with 36 vertical layers with 1m layer thickness.

## Results and discussion

The results of the segmented approach showed a relatively good agreement with the measured water levels of the lake (as a measure of the lake water balance), which allows us to use it as the inflow boundary conditions of the hydrodynamic model. As hydrodynamic processes are the driver for

biochemical processes, it was important to provide an accurate hydrodynamic model before coupling and calibrating the ecosystem (water quality) model of AEM3D. The hydrodynamic model, using meteorological data, interpolated for the lake Sacrower See showed a good consistency with the measured water temperature profiles, mimicking stratification and mixing of the water column.

Based on the mentioned hydrodynamic model, the calibration of the water quality model of AEM3D is now being performed and the results are expected to be published soon.

# Dynamics of lake heatwaves in summer 2022: interplay between wind mixing and surface heating

G. Valerio<sup>1\*</sup> and M. Pilotti<sup>1</sup>

<sup>1</sup> Department of Civil, Environmental, Architectural Engineering and Mathematics, Università degli Studi di Brescia, Italy

\*Corresponding author; e-mail [giulia.valerio@unibs.it](mailto:giulia.valerio@unibs.it)

## KEYWORDS

modelling; internal waves; wind, temperature, heatwave.

## Introduction

In a warming climate, it is virtually certain that warm extremes will become more frequent and intense. On a global scale, Woolway et al. (2021) attested that lakes will experience more intense and long-lasting heatwaves, which could contribute to threatening the key ecological and economic benefits that lakes provide to society, already endangered by the long-term increase in temperature. On a local scale, field studies putting light on the dynamics of extreme heating in lakes are generally lacking.

## Materials and methods

In summer 2022, in Lake Garda and Iseo (northern Italy), high-resolution data were provided by two floating stations equipped with meteorological sensors and thermistors sampling with  $\pm 0.01$  °C accuracy. These data allowed us to compute all the thermal and mechanical forcing at the water surface. Extreme thermal responses of the lakes were identified according to Hobday et al. (2016), referring to a climatology reconstructed by means of 1D models and satellite data made available by the CEDA CCI dataset. Measured data were interpreted at the light of the results of 3D simulations developed with the AEM3D hydrodynamic model.

## Results and discussion

Summer 2022 resulted exceptionally warm. The surface of Lake Garda and Lake Iseo experienced extreme monthly-averaged temperatures and two almost synchronous heatwaves in July and September. In the following, we discuss the features of the July heatwaves at light of the thermal fluxes and of the wind-induced hydrodynamics of the two lakes.

In Lake Iseo a moderate, 10-day-long heatwave was observed after the 17<sup>th</sup> of July, having a maximum intensity of 3.2°C and a mean intensity of 2.6°C. During the heatwave, surface temperature at the floating station increased at an average rate of 0.2°C/day, starting from the 10<sup>th</sup> of July for 10 days. The internal wave pattern evidenced by temperature in the upper 60 m was regular in time, with energy mostly concentrated in the 1-day period, corresponding to the 1st vertical and 1st horizontal (V1H1) mode already described by Valerio et al. (2012) during the stratified period. The thermocline thus oscillated in counter-phase at the northern and southern basin around an average depth of 12 m (see Fig.1). Enhanced warming rates resulted from the model in the southern basin, mostly favored by higher thermal fluxes due to the wind sheltering.

In the same period, Lake Garda experienced a moderate, 13 day-long heatwave, starting from the 13<sup>th</sup> of July, having a maximum intensity of 3.7°C and a mean intensity of 2.7°C. The temperature increased at an average rate of 0.3°C/day starting from on 10<sup>th</sup> of July. The temperature along the water column revealed a more complex structure with respect to Iseo, with strong variations in time and space, depending on the acting wind (Amadori et al., 2021).

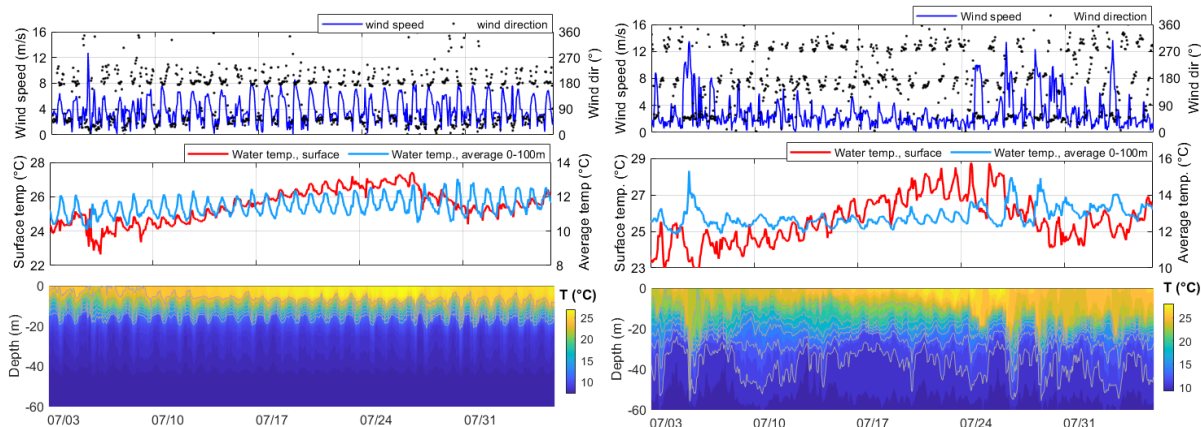


**Fig. 1.** Comparison of the response of Lake Iseo (left column) and Lake Garda (right column) to the exceptional heating in July 2022. The first row shows the time series of wind speed and direction measured at the floating stations; the second and the third rows show the measured time series of water temperature at the floating stations.

In response to the strong northerly winds, a downwelling occurred in the southern basin on the 4<sup>th</sup> of July. Afterward, the metalimnion thickness changed along the lake axis, reaching on the 10<sup>th</sup> of July

a configuration characterized by a squeezed metalimnion in the northern basin and a stretched one in the southern one, which had been maintained almost steady in the following 13 days under the southerly wind in the northern basin (see Fig. 2c). In such a condition, the warming was enhanced in the sheltered southern basin where the floating station was located. The average daily flux was 177 W/m<sup>2</sup> resulting in a surface warming rate on overall 28% higher than the northern one. We estimated that ~36% was due to the reduced latent flux and ~64% was due to the shallower surface layer which kept the incoming heat confined in the upper layers. During the heatwave, on the 18<sup>th</sup> of July, both the satellite images and the results of the 3D simulation confirmed that this factor made the southern basin a heatwave hotspot (see Fig. 2a-b). After the 24<sup>th</sup>, a regular and sustained northerly wind blew in the southern basin and mixed the upper 20 m of the water column, determining a V1H1 internal wave motion, having a period between 1.6 and 2.3 days. The strong mixing and vertical heat transport resulted in the interruption of the heatwave and in an overall warming of the water column.

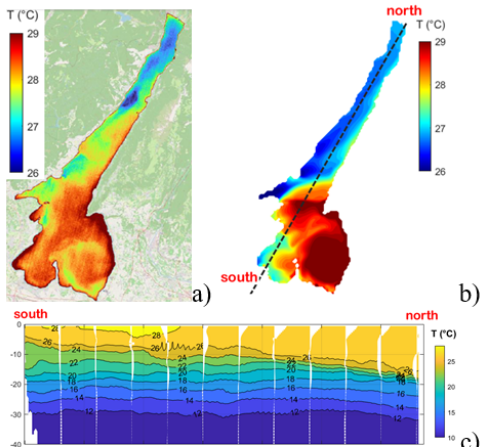


**Fig. 2.** Temperature field on 18/7/22 in Lake Garda: surface temperature measured by Landsat satellite (a), simulated temperature at the surface (b) and along the lake axis (c).

wave motion, having a period between 1.6 and 2.3 days. The strong mixing and vertical heat transport resulted in the interruption of the heatwave and in an overall warming of the water column.

## REFERENCES

- Amadori, M. et al. Multi-scale evaluation of a 3D lake model forced by an atmospheric model against standard monitoring data (2021). *Environmental Modelling and Software* 139, 105017
- Hobday, A. J. et al. A hierarchical approach to defining marine heatwaves (2016). *Progress in Oceanography* 141, 227–238
- Valerio, G., Pilotti, M., Marti, C.L., and Imberger J., The structure of basin scale internal waves in a stratified lake in response to lake bathymetry and wind spatial and temporal distribution: Lake Iseo, Italy (2012). *Limnology and Oceanography*, 57(3), 772-786
- Woolway, R. I. et al. Lake heatwaves under climate change (2021). *Nature* 589, 402–407

# Rotational effects in lake upwelling and the thresholds for conceptual models

S. Valbuena<sup>1,2\*</sup>, F. Bombardelli<sup>1</sup>, J. Largier<sup>3,4</sup>, G. Schladow<sup>1,2</sup>

<sup>1</sup>Department Civil and Environmental Engineering, University of California, Davis, California, USA

<sup>2</sup>UC Davis Tahoe Environmental Research Center (TERC), Incline Village, Nevada, USA

<sup>3</sup>Department of Environmental Science and Policy, University of California, Davis, California, USA

<sup>4</sup>UC Davis Coastal and Marine Science Institute, Bodega Bay, California, USA

\*Corresponding author, e-mail [savalbuena@ucdavis.edu](mailto:savalbuena@ucdavis.edu)

## KEYWORDS

Lake upwelling; Coriolis force; Burger number; modelling; Wedderburn number.

## Introduction

Lake upwelling generates vertical fluxes that redistribute constituents, nutrients, and the thermal structure of lakes (Csanady, 1975). Current conceptual models generally classify lake upwelling as either non-rotational 2D (Monismith, 1986) or rotational 3D (Csanady, 1975) response.

The lake response to wind forcing depend on factors such as density stratification, Coriolis force, bathymetry, and flow length scale. Basin-wide parameterizations have been used to define thresholds for specific flow types in lakes, and limits for upwelling, internal wave, and mixing have been reported (Monismith, 1986; Spigel & Imberger, 1980; Stocker & Imberger, 2003). The timing and magnitude of upwelling can be estimated using the Wedderburn and Lake numbers (Roberts et al., 2021), and rotational internal wave motions are expected when the Burger number  $S < 1$  (Antenucci & Imberger, 2001). However, the validity of the conceptual model has not been evaluated, and clear thresholds for delineating when lake upwelling is best described by the 2D closed basin or Ekman upwelling are yet to be defined. A recent numerical study of Lake Tahoe concluded that upwelling-induced flows exhibit rotational dynamics and upwelling expressions were a combination of both conceptual models (Valbuena et al., 2022). Therefore, there is a need to establish parameterizations and thresholds for the rotational influence on the flow and temperature patterns during lake upwelling. Here we define the combination of length scale, stratification conditions, and Coriolis force that determine the lake response during upwelling events. This work provides a new perspective of upwelling conceptual models, specifically at defining the thresholds of applicability of upwelling conceptual models.

## Material and methods

Stratified square and circular basins were modelled to represent lake upwelling for the combination of multiple stratification conditions, Coriolis force, and length scale. The wind forcing was estimated following the definition of the Wedderburn number under the consideration of the known limit for full lake upwelling expressions (i.e.,  $W = 0.5$ ). Length scales between 5 km and 70 km, latitudes between 5° and 40° and multiple stratification conditions were modelled, and over 300 numerical models were analyzed.

## Results and discussion

In all numerical simulations, full upwelling was observed. The influence of the Coriolis force on the lake response during upwelling was analyzed by studying the orientation of the surface temperature gradients in relation to wind forcing and flow patterns within the basin. Three conceptual models were identified to categorize the lake response: non-rotational, Ekman, and rotational upwelling. The latter identified response, exhibited moderate rotational effects, resulting in upwelling being observed at upwind boundaries and boundaries to the left of the wind direction – in the northern hemisphere (Figure 1).

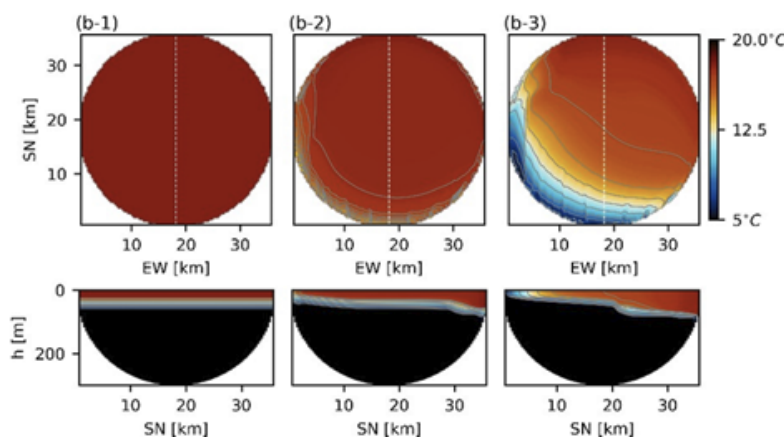


**Figure 1.** Snapshot of flow-induced patterns from southerly winds at  $0.25\text{Ti}$  for Rotational circular basin parameterized by  $S=0.46$ .

The Burger number  $S = 2R_o$  is a surrogate of the Rossby number, and thus is a basin-wide parameter that considers the ratio between the inertial and Coriolis forces. Thus, this parameterization provides insight into the potential rotational influence in the flow and temperature patterns. The combination of the  $S$  and the relative orientation of the temperature gradients and the wind forcing allowed us to define the threshold for the 3 types of conceptual lake upwelling response previously identified. Thus, it can be concluded that the non-rotational response is expected in basins with  $S \geq 0.8$ , the newly identified rotational model is expected when  $0.2 \leq S < 0.8$ , and the Ekman upwelling can be predicted in lakes parameterized with  $S < 0.2$ .

## REFERENCES

- Antenucci, J. P., & Imberger, J. (2001). Energetics of long internal gravity waves in large lakes. *Limnology and Oceanography*, **46**(7), 1760–1773. <https://doi.org/10.4319/lo.2001.46.7.1760>
- Csanady, G. T. (1975). Hydrodynamics of large lakes. *Journal of Fluid Mechanics*, **7**, 357–386.
- Monismith, S. (1986). An experimental study of the upwelling response of stratified reservoirs to surface shear stress. *Journal of Fluid Mechanics*, **171**, 407. <https://doi.org/10.1017/S0022112086001507>
- Roberts, D. C., Egan, G. C., Forrest, A. L., Largier, J. L., Bombardelli, F. A., Laval, B. E., Monismith, S. G., & Schladow, G. (2021). The setup and relaxation of spring upwelling in a deep, rotationally influenced lake. *Limnology and Oceanography*, **66**(4), 1168–1189. <https://doi.org/10.1002/limo.11673>
- Spigel, R. H., & Imberger, J. (1980). The classification of Mixed-Layer Dynamics of Lakes of Small to Medium Size. *Journal of Physical Oceanography*, **10**(7), 1104–1121. [https://doi.org/10.1175/1520-0485\(1980\)010<1104:TCOMLD>2.0.CO;2](https://doi.org/10.1175/1520-0485(1980)010<1104:TCOMLD>2.0.CO;2)
- Stocker, R., & Imberger, J. (2003). Energy Partitioning and Horizontal Dispersion in a Stratified Rotating Lake. *Journal of Physical Oceanography*, **33**(3), 512–529. [https://doi.org/10.1175/1520-0485\(2003\)033<0512:EPAHDI>2.0.CO;2](https://doi.org/10.1175/1520-0485(2003)033<0512:EPAHDI>2.0.CO;2)
- Valbuena, S. A., Bombardelli, F. A., Cortés, A., Largier, J. L., Roberts, D. C., Forrest, A. L., & Schladow S. G. (2022). 3D Flow Structures During Upwelling Events in Lakes of Moderate Size. *Water Resources Research*, **58**(3), 1–35. <https://doi.org/10.1029/2021WR030666>

# Differential cooling in lakes

D. Bouffard<sup>1,2\*</sup>, T. Doda<sup>1</sup>, C. Ramón<sup>3</sup> and H.N. Ulloa<sup>4</sup>

*1 Eawag, Swiss Federal Institute of Aquatic Science and Technology, Department of Surface Waters – Research and Management, Kastanienbaum, Switzerland*

*2. Institute of Earth Surface Dynamics, University of Lausanne, Lausanne, Switzerland*

*3 Department of Civil Engineering, University of Granada, Granada, Spain*

*4 Department of Earth and Environmental Science, University of Pennsylvania, Philadelphia, USA*

\*Corresponding author; e-mail [damien.bouffard@eawag.ch](mailto:damien.bouffard@eawag.ch)

## KEYWORDS

Lakes; differential cooling; convection; density current; internal waves.

## Introduction

We present here the results of a 4-year project that has aimed at making fundamental contributions in the area of transport and mixing induced by topography and surface heat fluxes. We have specifically focused on the flushing of littoral environments resulting from differential cooling in lakes (Bouffard & Wüest 2019). Briefly, shallower regions cool faster than deeper regions at night and thereby cause horizontal density gradients. The denser nearshore waters sink and flow downslope as a density current (also called thermal siphon, TS). This current can flush littoral regions within only a few hours. We asked the following questions:

- 1) What is the seasonality of this process?
- 2) Can we predict the intensity and occurrence of the TS?
- 3) Does wind modulate the intensity of the TS?
- 4) What are the dynamics of the TS?
- 5) What are the biochemical implications?

## Results and discussion

We investigated the TS, in the case of water temperatures  $T > 4^{\circ}\text{C}$ , by measuring the seasonal evolution of the process over a year in a small peri-alpine wind-sheltered lake (Rotsee, CH). We reported frequent cross-shore flows associated with the TS from summer to winter (Doda et al. 2022). We also showed that seasonal variability of the transport can be predicted by laboratory-based scaling formulae. We further observed that maximum flushing occurs synchronously with a weakening of the penetrative convection. By combining in-situ observations and large eddy simulations, we showed that penetrative convection can block the release of the density current (Ulloa et al. 2022, Doda et al. 2023). This interplay between density current and penetrative convection modifies our understanding of the lake's physical functioning and carries implications for ecosystem dynamics as well. The TS can indeed transport dissolved gases from littoral to pelagic regions of lakes (Doda et al., in review). However, specific, effective examples of this phenomenon have not yet been described in the literature. Here, we found that both branches of the circulation were capable of transporting gases laterally. The downslope current brought littoral gases to the base of the mixed layer in the stratified region whereas the surface flow transported gases towards the shore. We quantified this exchange for oxygen and methane. Yet, the specific question of the physical connectivity of cross-shore fluxes and flushing time scale is not limited to buoyancy-driven flows induced by differential cooling. We have further investigated the coupled effect of wind-induced and differential cooling-induced cross-shore transport dynamics (Ramón et al. 2022). Last, we have generalized our findings to other lakes (Doda et al., in prep). We identified TS events in six lakes and tested the same transport scaling formulae as in Rotsee. The results showed that the scaling relationships reproduced the spatial variability of TSs between lakes and we provided a procedure to predict the TS-induced transport from bathymetry, meteorological forcing

and vertical thermal structure. The main findings of the HYPOTHESIS project are summarized in Figure 1 with relevant published manuscripts.

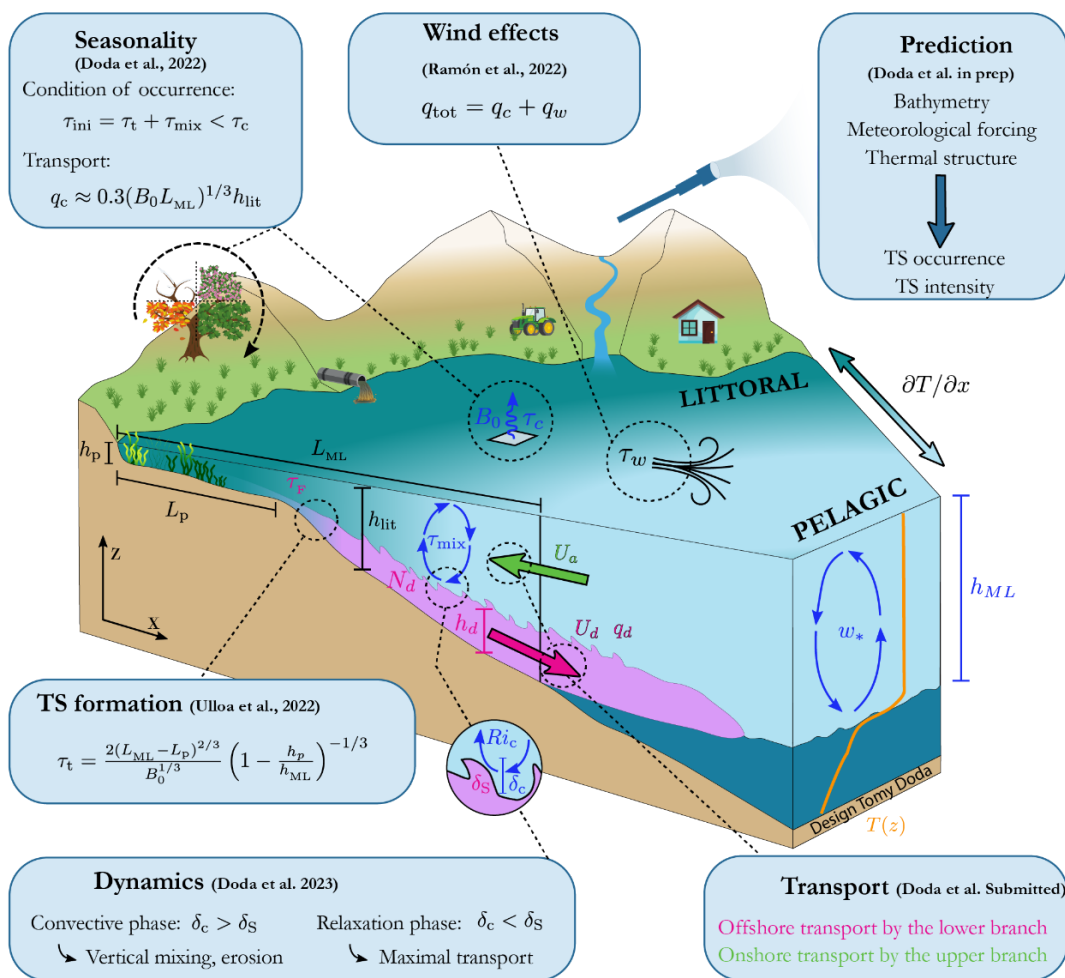


**Figure 1.** Schematic of cooling-driven thermal siphon, including the main quantities and findings of the HYPOTHESYS project.

## REFERENCES

- Bouffard, D.; Wüest, A. Convection in Lakes. *Annual Review of Fluid Mechanics* 2019, **51** (1), 189–215. <https://doi.org/10.1146/annurev-fluid-010518-040506>.
- Doda, T. ; Cruz, H. ; Runnalls, J. ; Ramón, C. L. ; Ulloa, H. N. ; Hédonin E. ; Plüss, M. ; Bouffard, D. Towards a prediction of cooling-driven lateral transport in lakes. **In preparation**
- Doda, T. ; Ramón, C. L. ; Ulloa H. N. ; Brennwald, M.S. ; Kipfer, R. ; Perga, M-E. ; Wüest, A. ; Schubert C. J.; Bouffard D. Lake surface cooling drives littoral-pelagic exchanges of dissolved gases. **Submitted (04.2023)**
- Doda, T.; Ulloa, H. N.; Ramón, C. L.; Wüest, A.; Bouffard, D. Penetrative Convection Modifies the Dynamics of Downslope Gravity Currents. *Geophysical Research Letters* 2023, **50** (2). <https://doi.org/10.1029/2022gl100633>.
- Doda, T.; Ramón, C. L.; Ulloa, H. N.; Wüest, A.; Bouffard, D. Seasonality of Density Currents Induced by Differential Cooling. *Hydrology and Earth System Sciences* 2022, **26** (2), 331–353. <https://doi.org/10.5194/hess-26-331-2022>.
- Ramón, C. L.; Ulloa, H. N.; Doda, T.; Bouffard, D. Flushing the Lake Littoral Region: The Interaction of Differential Cooling and Mild Winds. *Water Resources Research* 2022, **58** (3). <https://doi.org/10.1029/2021wr030943>.
- Ulloa, H. N.; Ramón, C. L.; Doda, T.; Wüest, A.; Bouffard, D. Development of Overturning Circulation in Sloping Waterbodies Due to Surface Cooling. *Journal of Fluid Mechanics* 2022, **930**. <https://doi.org/10.1017/jfm.2021.883>

# Stem stiffness behaviour in an oscillatory flow submerged canopy patch

A. Barcelona<sup>1</sup>, J. Colomer<sup>1</sup>, T. Serra<sup>1\*</sup>

<sup>1</sup>Department Physics, University of Girona, Girona, Spain

\*Corresponding author, e-mail [teresa.serra@udg.edu](mailto:teresa.serra@udg.edu)

## KEYWORDS

waves; coastal seagrasses; seagrass fragmentation; rigid vegetation; flexible vegetation.

## Introduction

Seagrasses are ecologically valuable coastal systems that shelter the seafloor from waves and currents (Gacia et al., 1999). They also improve water quality, provide habitat for aquatic life, sequester carbon, and stabilize sediment (Ricart et al., 2015). They are, however, placed in areas where anthropogenic activities such as anchoring, dredging, trawling, or sewage outflow are causing their decline. Seagrasses have declined by 30%-60% as a result of human pressure (Evans et al., 2018), having disappeared in some areas or changed from large continuous meadows to fragmented canopies, with a patchy distribution of plants dominating the seascape (Barcelona et al., 2021).

Therefore, fragmented landscape seagrasses are made up of patches of different sizes, changing the hydrodynamics compared to continuous meadows. In addition, vegetation produces a flow resistance that can differ depending on the plants' distinct structural characteristics like their flexibility (Zhang et al. 2015) and horizontal distribution (density, staggered or random). Stem stiffness and patch length add up to other structural parameters, such as canopy density and height, which all influence their overall functionality in modifying seafloor hydrodynamics in coastal areas. Understanding the relationship between all of the above-mentioned structural characteristics of the vegetation, along with the hydrodynamics, might offer clues as to what the optimal patch length scales, meadow densities or plant distributions can explain the resilience exhibited by some meadows.

In the present study, the behaviour of single patches of different sizes formed by a random distribution of rigid or flexible plants under oscillatory conditions has been investigated.

## Materials and methods

A series of laboratory experiments were carried out in an oscillatory flume with both rigid and flexible stems for different canopy densities, patch lengths, and wave frequencies to determine the interaction between hydrodynamics and the canopy structure.

For a full canopy, Zhang et al. (2015) found that the relationship between the *TKE*,  $U_w$  and the main canopy parameters followed:

$$\frac{TKE}{U_w^2} = \delta \left[ C_D \frac{l_t}{d} \frac{nd^2}{2(1-\phi)} \right]^{\frac{2}{3}} \quad (1)$$

Where  $\delta$  is a scale constant,  $C_D$  is the drag coefficient of the vegetation,  $l_t$  is the characteristic turbulent length scale of the eddies (Zhang et al., 2015),  $d$  is the stem diameter,  $n$  is the canopy density (in shoots  $m^{-2}$ ) and  $\phi = n \frac{\pi}{4} d^2$  is the canopy solid volume fraction. In the current study, the effect of the patch length has been included in the drag coefficient. In this case, the drag produced by the vegetation patch will change with the patch length, and equation (1) is modified and results to be:

$$\frac{TKE}{U_w^2} = \delta \left[ C_D \left( \frac{L_{patch}}{L_{canopy}} \right)^{\frac{1}{3}} \frac{l_t}{d} \frac{nd^2}{2(1-\Phi)} \right]^{\frac{2}{3}} \quad (2)$$

Zhang et al. (2015) considered  $l_t = d$  for  $S > 2d$  whereas  $l_t = S$  for  $S < 2d$ , where  $S$  is the plant to plant distance). In the present study,  $S > 2d$ ,  $l_t = d$ .

## Results and discussion

Plants that are flexible move with the flow in the upper canopy layer but have a more stiff structure in the inner canopy layer. Canopies of rigid plants, on the other hand, exert a significant drag on the flow along the entire length of their stem, resulting in a turbulent kinetic energy production. This distinction between the two canopy structures can help to explain their distribution in the environment, with rigid canopies being more common in more sheltered areas and flexible plants more common in more exposed areas with strong flow energy. In the inner canopy, rigid and flexible vegetation exhibits similar stem-like behaviour for  $\left[ C_{D-Patch} \frac{nd^2}{2(1-\Phi)} \right]^{\frac{2}{3}} U_w^2 > 2$  and  $\left[ C_{D-Patch} \frac{nd^2}{2(1-\Phi)} \right]^{\frac{2}{3}} U_w^2 > 4$ , respectively, whereas in the canopy top layer flexible plants move with the flow to cope with the hydrodynamics, presenting a blade-like behaviour. In contrast, neither rigid nor flexible plants for  $\left[ C_{D-Patch} \frac{nd^2}{2(1-\Phi)} \right]^{\frac{2}{3}} U_w^2 < 2$  or  $\left[ C_{D-Patch} \frac{nd^2}{2(1-\Phi)} \right]^{\frac{2}{3}} U_w^2 < 4$ , respectively, produce turbulent kinetic energy. Furthermore, for high wave frequencies, the behaviour of flexible plants may shift closer to that of rigid plants. Flexible plants, on the other hand, swing more when subjected to low oscillation frequencies.

## Acknowledgments

This work was supported by the “Ministerio de Economía y Competitividad” of the Spanish Government through the grant PID2021-123860OB-I00.

## REFERENCES

- Gacia, E., Granata, T.C., Duarte, C.M. (1999). An approach to measurement of particle flux and sediment retention within seagrass (*Posidonia oceanica*) meadows. *Aquatic botany*, **65**, 255-268.
- Ricart, A. M., York, P. H., Rasheed, M. A., Pérez, M., Romero, J., Bryant, C. V., Marcedie, P. I. (2015). Variability of sedimentary organic carbon in patchy seagrass landscapes. *Mar. Pollut. Bull.*, **100**, 476-482.
- Evans, S.M., Griffin, K.J., Blick, R.A.J., Poore, A.G.B. and Vergés, A. (2018). Seagrass on the brink: Decline of threatened seagrass *Posidonia australis* continues following protection. *PLOS ONE*, **14**(4): e0216107.
- Barcelona, A., Colomer, J., Soler, M., Gracias, N., Serra, T. (2021). Meadow fragmentation influences *Posidonia oceanica* density at the edge of nearby gaps. *Estuarine, Coastal and Shelf Science*, **249**, 107106.
- Zhang, Y., Tang, C., Nepf, H. (2018). Turbulent kinetic energy in submerged model canopies under oscillatory flow. *Wat. Resour. Res.*, **54**, 1734-1750.

# Thermal conditions and lake metabolism in the ice-covered North Aral Sea

G. Kirillin<sup>1\*</sup>, A. Izhitsky<sup>2</sup>, A. Kurbaniyazov<sup>3</sup>

<sup>1</sup>*Department of Ecohydrology and Biogeochemistry, Leibniz Institute of Freshwater Ecology and Inland Fisheries (IGB), Berlin, Germany*

<sup>2</sup>*Shirshov Institute of Oceanology, Moscow, Russia*

<sup>3</sup>*International University of Tourism and Hospitality, Turkestan, Kazakhstan*

\*Corresponding author, e-mail [georgiy.kirillin@igb-berlin.de](mailto:georgiy.kirillin@igb-berlin.de)

## KEYWORDS

Ice-covered lakes; basin-scale internal waves; dissolved oxygen; primary production; respiration.

## Introduction

Rapid desiccation of the Aral Sea, the former 4th largest lake worldwide, attracts continuous attention of researchers as an example of fast anthropogenically driven change of a large aquatic ecosystem on unprecedentedly large spatial scales. As a countermeasure preventing further desiccation, a dam was constructed in 2005 separating the northern part of the Aral Sea from the rest of the basin. The effort led to stabilization of the North Aral volume and salinity and was widely recognized as an exceptional success in large-scale water management and restoration. The study aims at investigation of the current hydrophysical state and annual thermal and oxygen regime of the North Aral Sea with regard to stabilization of its long-term dynamics, as well as the possible future projections in view of the global change effects on the regional hydrological regime. The study uses results from 1-year long monitoring of temperature and oxygen combined with outputs from several measurement campaigns, modeling, climate scenarios, and remote sensing.

## Materials and methods

We analyzed thermal stratification in terms of the Burger number; the internal wave speeds were estimated from the vertical stratification in the framework of the two-layer approximation (Lamb 1932, Csanady 1967). The measured values of the dissolved oxygen (DO) content were used for bulk estimations of the lake-wide metabolism, i.e., the balance between primary production and respiration as

$$\frac{d\text{DO}}{dt} = \frac{(Q_0 - Q_h)}{h_{\text{mix}}} + \overline{\text{GPP}} - \bar{R} \quad (\text{daytime}); \quad \frac{d\text{DO}}{dt} = \frac{(Q_0 - Q_h)}{h_{\text{mix}}} - \bar{R} \quad (\text{nighttime})$$

where  $d\text{DO}/dt$  is the local time derivative of DO,  $R$  is the respiration rate assumed to be the same for daytime and nighttime, and  $\text{GPP}$  is the gross primary production, all values averaged over the mixed layer with vertically homogeneous oxygen distribution.

## Results and discussion

The ice-covered period lasted from early December 2018 to 31 March 2019. First ice formed in shallow areas of the lake on 25-27 November 2018. The stratification had a two-layer structure with a thermally homogeneous mixed layer with temperature values of about  $-0.35^{\circ}\text{C}$  occupying the upper 10 meters of the water column, and a  $\approx 2^{\circ}\text{C}$  downward temperature increase down to the water depth of 12 m, where values of about  $2.5^{\circ}\text{C}$  were observed. The lower stratified part of the water column exhibited quasi-periodic oscillations with oscillations energy concentrated at significant spectral peaks with periods of 0.8 hours, 1.6 hours, 2.7 days and 9 days. The two shortest oscillation periods can be unambiguously related to the eigen oscillations (barotropic seiches) of the Shevchenko Bay, the semi-isolated part of North Aral, where the measurement station was installed.

Long-period oscillations can be ascribed to basin-scale rotation-affected internal waves developing at the density interface between the 10-m thick upper mixed layer and the 2-m thick warm layer beneath.

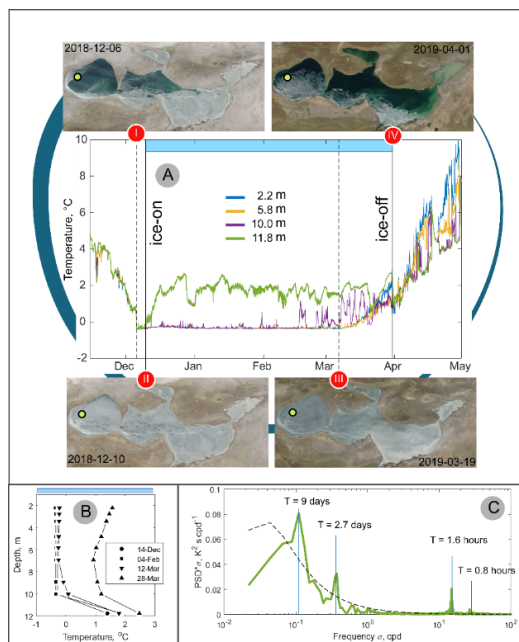


**Figure 1.** (A) Water temperature time series, (B) vertical temperature profiles, and (C) near-bottom temperature spectrum in winter 2018-2019. (A): temperature records between ice-on and ice-off at four selected water depths. The blue bar on top of the panel marks the ice cover duration. The four MODIS satellite images (NASA Worldview) with corresponding vertical lines across the temperature panel illustrate the ice conditions at the times of lake surface freezing [I-II], snow melt [III] and ice thaw [IV]. (B): vertical temperature profiles at different stages of the ice-covered period. (C): Spectral density of near-bottom (11.8 m depth) temperature oscillations. The dashed line corresponds to the lower confidence boundary for the spectral peaks defined as the upper 95% for the red noise signal (first order autoregressive process) containing the same variance as the observed time series \cite{gilman1963power}. Significant spectral peaks are marked with vertical lines.

Despite relatively low latitude ( $46^{\circ}\text{N}$ ), the cold arid climate of the North Aral Sea results in about 3 months of complete ice cover on the lake. Thanks to the high amount of solar radiation, primary production does not cease under ice: even in the mid-winter, the oxygen concentrations reveal a diurnal cycle, and the estimated gross primary production remains slightly higher than respiration. GPP sharply increases in spring before the ice break-up.

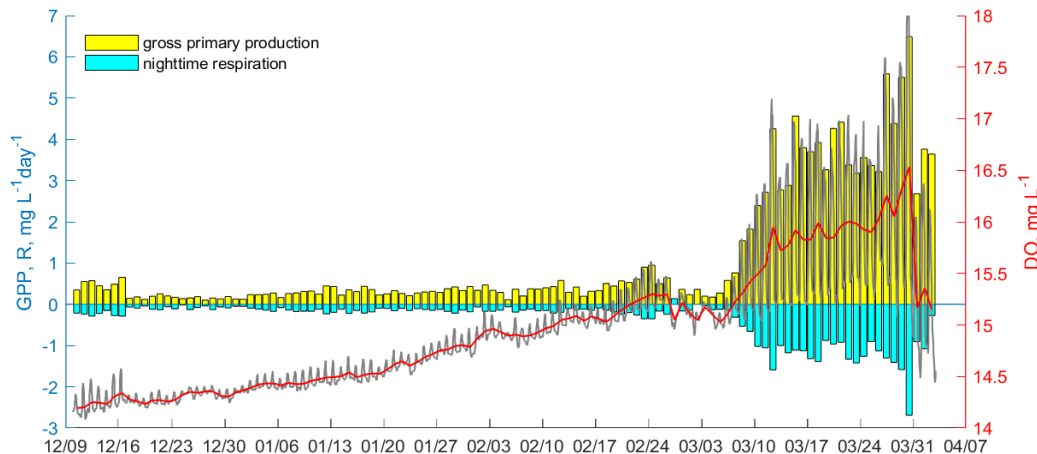


**Figure 2.** Dissolved oxygen concentrations and calculated components of lake metabolism in the ice-covered Aral Sea.

## REFERENCES

- Csanady, G. (1967) Large-scale motion in the Great Lakes. *Journal of Geophysical Research*, **72**, 4151–4162.  
 Lamb, H. (1932) Hydrodynamics, Cambridge University Press, Cambridge, UK

# Physical transport in a thermobarically stratified fjord-type lake

B. Laval<sup>1\*</sup>, L. Smith<sup>1</sup>, S. Vagle<sup>2</sup>, and E. Carmack<sup>2</sup>

<sup>1</sup> Department Civil, Environmental, University of British Columbia, Vancouver, BC, Canada

<sup>2</sup> Institute of Ocean Sciences, Fisheries and Oceans Canada, Sidney, BC, Canada

\*Corresponding author, e-mail [bernard.laval@ubc.ca](mailto:bernard.laval@ubc.ca)

## KEYWORDS

Lakes; deep water renewal; thermobaric; seasonal overturn.

## Introduction

Quesnel Lake lies in the watershed of the Fraser River, which drains a total of 217 000 km<sup>2</sup> of the interior of British Columbia (BC), Canada. This watershed is home to most of BC's anadromous sockeye salmon (*Oncorhynchus nerka*), which are the cornerstone of the BC's fishing industry. Although the Quesnel Lake watershed is only 5930 km<sup>2</sup> (Environment Canada, 2002), it has historically accounted for up to 30% of the Fraser River sockeye salmon run. Quesnel Lake also supports a resident population of Kokanee (land-locked *Oncorhynchus nerka*), the preferred prey food of Rainbow Trout (*Oncorhynchus mykiss*) that, in turn, are the basis of an economically important sport fishery. Typical of fjord-type lakes Quesnel Lake has complex geometry (Figure 1). It is narrow, long (>100 km total thalweg), dendritic (three arms of comparable size), and deep (maximum depth >500 m). The extreme depth complicates vertical exchange through thermobaric processes; however, the deep water of Quesnel Lake has near-saturation oxygen levels suggesting that it is well ventilated by oxygenated surface waters. By the same mechanism, nutrients from bottom waters are recycled to the surface where they then support primary production. A motivation for studying Quesnel Lake is thus to determine what mechanisms contribute to deepwater renewal, and how these mechanisms affect the lake's fisheries resources.

## Materials and methods

This research describes a 10-year mooring record at the deepest point in the lake, as well as field observations from winter 2006-2007, a winter with substantial spatial coverage of moored instruments in this topographically complex lake.

## Results and discussion

Results show a seasonal evolution of bottom water temperature with amplitude of ~0.2°C. Each year, bottom water warms continuously by ~0.1°C over 7 months (i.e. April through October), then more rapidly (~0.1-0.2°C over 1-2 months). Subsequently, bottom water cools rapidly (~0.1-0.2°C) in January, followed by slower cooling (~0.1°C) to reach an annual minimum in mid-April. The rapid cooling of bottom water in January occurs during cold wind-storms that drive cold surface water beyond the compensation depth at an apparent baroclinic seiche anti-node near the western region of the East Arm (Figure 2; M14) which induces thermobaric instability. Once reaching bottom, cold water flows laterally to the deepest regions. Later in the season bottom water is further cooled by a prolonged vernal turnover, during which seiche-induced benthic-mixing homogenizes bottom water (within 0.02°C) to a maximum height of ~400 m above the lake bottom. This thick benthic layer overlaps a surface mixed layer to allow a full-depth spring turnover. Our observations demonstrate wind forcing is an important driver of vertical mixing and transport even to 500 m depth in a thermobarically stratified fjord-type lake.

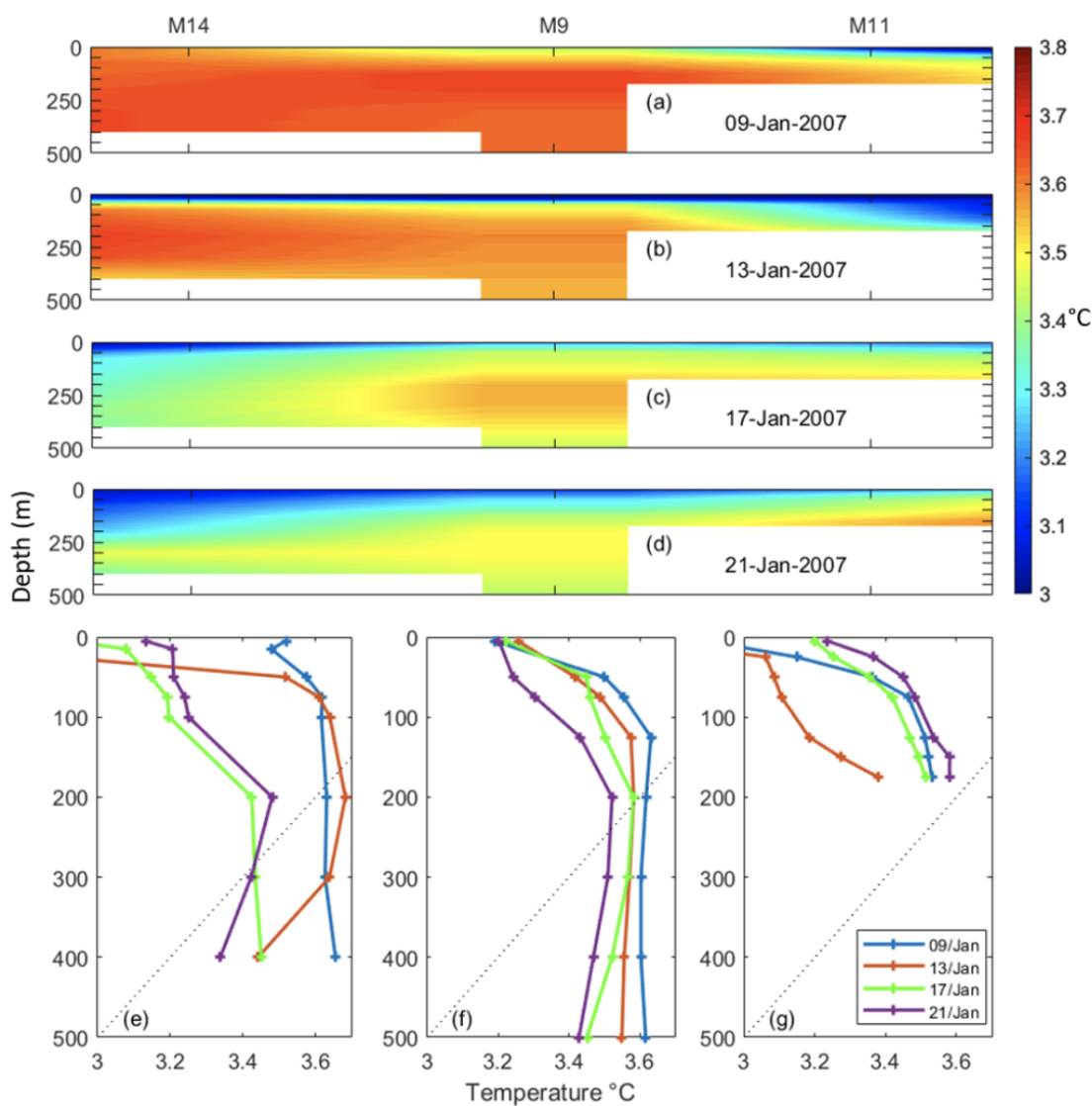


**Figure 1.** Snapshots of temperature contours in the East Arm of Quesnel Lake 9(a-d) at 4 times during and after a storm in January 2007 suggesting seiche anti-nodes in the vicinity of stations M14 and M11. Profiles of mooring temperature at the same time as the snapshots showing ventilation of bottom water by thermobaric instability.

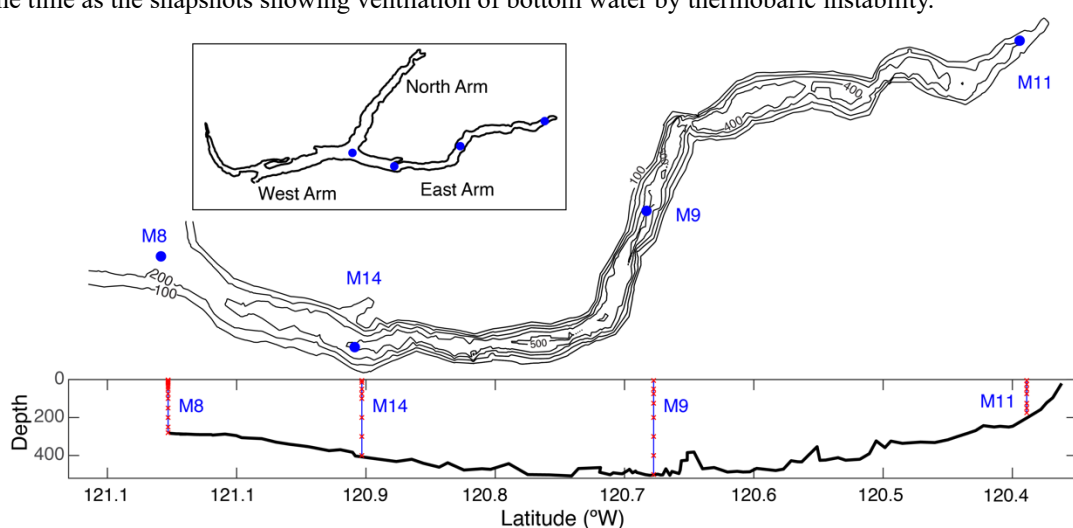


**Figure 2.** Map of Quesnel Lake with highlight on East Arm bathymetry and elevation view, showing mooring and thermistor locations.

# Identifying and quantifying deepwater-renewal processes during winter cooling in a large, deep lake (Lake Geneva)

N. Peng<sup>1\*</sup>, U. Lemmin<sup>1</sup>, F. Mettra<sup>1</sup>, R. S. Reiss<sup>1</sup>, D. A. Barry<sup>1</sup>

<sup>1</sup>*Ecological Engineering Laboratory (ECOL), Institute of Environmental Engineering (IIE), Faculty of Architecture, Civil and Environmental Engineering (ENAC), Ecole Polytechnique Fédérale de Lausanne (EPFL), 1015 Lausanne, Switzerland*

\*Corresponding author; e-mail: [naifu.peng@epfl.ch](mailto:naifu.peng@epfl.ch)

## KEYWORDS

Winter cooling; deepwater renewal; cold density currents; heat budget; deep Lake Geneva

## Introduction

Deepwater renewal during winter cooling is an important process that controls oxygen and nutrient exchange. Traditionally, winter cooling is considered to be solely driven by 1D vertical convection (e.g., Anneville et al., 2013) with complete overturning occurring when temperatures have become homogeneous over the full water depth. However, at the same time, differential cooling between shallow areas and deep waters (e.g., Fer et al., 2001; Ulloa et al., 2022) can produce density currents that flow from the shallow areas down into the deep layers of the basin, thus also contributing to deepwater renewal.

Lake Geneva is composed of two basins: the narrow *Petit Lac* (max. depth ~75 m) and the wide *Grand Lac* (max. depth ~309 m). Since the shallow *Petit Lac* basin cools faster than the deep *Grand Lac*, strong density currents can flow from the *Petit Lac* into the *Grand Lac* bottom layers during cold winters. Lake Geneva's last complete overturning reportedly took place during a severe cold spell (air temperatures down to -10°C) in February 2012 (Anneville et al., 2013). But is this true? To address this question, we will reanalyze this event by determining the contribution of vertical convection and density currents from the *Petit Lac* to the heat budget in Lake Geneva, and as a result, to deepwater renewal.

## Materials and methods

Field observations taken during early 2012 at five locations (*Petit Lac*, littoral and pelagic zones of the *Grand Lac*) are combined with a 3D hydrodynamic model (MITgcm, Marshall et al., 1997), calibrated for Lake Geneva (Cimatoribus et al., 2018). The model was forced by realistic meteorological data from MeteoSwiss COSMO-2 (Voudouri et al., 2017). In a novel approach, Lake Geneva's heat content variation  $\Delta H_C$  was decomposed to identify and quantify the contribution from vertical convection ( $F_{Surf}$ ), lateral cooling from the *Petit Lac* ( $F_{PL}$ ) and from the shallow littoral zone of the *Grand Lac* ( $F_{LZ}$ ):

$$\Delta H_C = F_{Surf} + F_{PL} + F_{LZ}, \quad (1)$$

## Results and discussion

Numerical modeling results, which were validated by the field measurements, showed that during this 2012 cooling event, in addition to convective cooling, a strong Lateral Cold Density Current (LCDC) (Figure 1) was initiated at the shallowest (southwest) end of the *Petit Lac* (Figure 1a). The LCDC grew in strength, “spilled over” into the *Grand Lac* and finally reached the deepest layers of the *Grand Lac* (Figure 1). Furthermore, weaker LCDCs discharged from the *Grand Lac* littoral zone also contributed to cooling the deepwater layers.

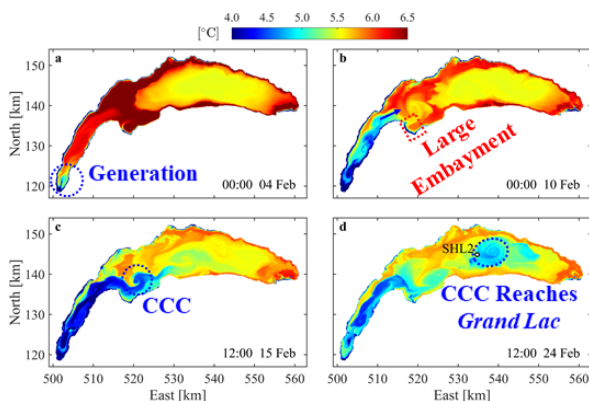


**Figure 1.** Evolution of bottom temperatures at different times during the strong cooling event in early 2012 obtained from numerical modeling results shows: (a) an LCDC is generated at the western end of the *Petit Lac*; (b) it extends further and overall lake bottom temperatures decrease due to cooling; (c) the LCDC fills the *Petit Lac* and “spills over” into the *Grand Lac*, forming a Cold Cyclonic Current (CCC); (d) the CCC finally reaches the bottom (309 m depth) of the *Grand Lac*. Dates and times are indicated in each panel and a temperature legend is given on top.

By applying the heat budget decomposition in equation (1), the contribution of each of the deepwater renewal processes was quantified. Results revealed that vertical convection ( $F_{Surf}$ ) only penetrated down to layers above ~200 m (the “overturbing depth”) during February 2012, thus indicating that complete overturning did not occur (Lemmin, 2020). On the other hand, the LCDC from the *Petit Lac* ( $F_{Surf}$ ) reached the deepest layers of the *Grand Lac* around late February, strongly cooling the layers from 200 m down to the lake bottom (309 m depth). At the same time, the waters of the LCDC transported oxygen and increased the dissolved oxygen levels in these lower layers to values observed at the lake surface. This highlights the importance of LCDCs to the lake’s ecosystem health.

These results demonstrate that deepwater cooling and renewal in Lake Geneva during the cold air spell in early 2012 were not the result of 1D vertical convective cooling as was previously reported, but were actually controlled by lateral advection, i.e., by LCDCs, mainly discharged from the *Petit Lac*, and also from the littoral areas of the *Grand Lac*. Since vertical convective cooling is expected to weaken in the future due to continued global warming, understanding the role and quantifying the contribution of each of these alternative 3D processes to deepwater renewal in winter in Lake Geneva and other deep lakes is essential and will become increasingly important in order to develop effective water management policies.

## REFERENCES

- Anneville, O. et al. (2013), L’empreinte du changement climatique sur le Léman. *Archives des Sciences*, **66**, 157–172. [http://jacquet.stephan.free.fr/Anneville\\_Arch-Sci\\_2013.pdf](http://jacquet.stephan.free.fr/Anneville_Arch-Sci_2013.pdf) (last access: 19.08.2022)
- Cimatoribus, A. A., Lemmin, U., Bouffard, D. and Barry, D. A., (2018), Nonlinear dynamics of the nearshore boundary layer of a large lake (Lake Geneva), *Journal of Geophysical Research: Oceans*, **123**, 1016–1031. <https://doi.org/10.1029/2017JC013531>
- Fer, I., Lemmin, U. and Thorpe, S. A. (2001), Cascading of water down the sloping sides of a deep lake in winter. *Geophysical Research Letters* **28**, 2093–2096, <https://doi.org/10.1029/2000GL012599>
- Lemmin, U., (2020), Insights into the dynamics of the deep hypolimnion of Lake Geneva as revealed by long-term temperature, oxygen, and current measurements, *Limnology and Oceanography*, **65**, 2092–2107. <https://doi.org/10.1002/limo.11441>
- Marshall, J. et al. (1997), A finite-volume, incompressible Navier Stokes model for studies of the ocean on parallel computers, *Journal of Geophysical Research: Oceans*, **102**, 5753–5766. <https://doi.org/10.1029/96JC02775>
- Ulloa, H. N. et al. (2022), Development of overturning circulation in sloping waterbodies due to surface cooling. *Journal of Fluid Mechanics*, **930**, A18. <https://doi.org/10.1017/jfm.2021.883>
- Voudouri, A., Avgoustoglou, E. and Kaufmann, P., (2017), Impacts of observational data assimilation on operational forecasts. In T. Karacostas, A. Bais, & P. Nastos (Eds.), *Perspectives on Atmospheric Sciences* (pp. 143–149). Cham: Springer. [https://doi.org/10.1007/978-3-319-35095-0\\_2](https://doi.org/10.1007/978-3-319-35095-0_2)

# Hunting for submesoscale temperature, salinity and current velocity signal from CTD and ADCP/RDCP profilers data in the Gulf of Finland, the Baltic Sea

M.J. Lilover<sup>1\*</sup>, U. Lips<sup>1</sup>, T. Liblik<sup>1</sup>, I. Suhhova<sup>1</sup>, and G. Väli<sup>1</sup>

<sup>1</sup>*Department of Marine Systems, Tallinn University of Technology, Tallinn, Estonia*

\*Corresponding author; e-mail [madis.lilover@taltech.ee](mailto:madis.lilover@taltech.ee)

## KEYWORDS

Baltic Sea; Gulf of Finland; CTD/ADCP profiles; upwelling/downwelling; submesoscale variability.

## Introduction

Variability of oceanographic fields at the spatial scales less than the mesoscale is well recognized based on recent remote sensing, modelling, and field studies in the oceans, particularly the Baltic Sea (BS). The sub-mesoscale currents are intermediate-scale flow structures that appear in density fronts and filaments, topographic wakes, and persistent coherent vortices at the surface and throughout the interior. They provide a dynamic conduit for energy transfer towards microscale dissipation and diapycnal mixing (McWilliams 2016). Horizontal scales 0.1-10 km and timescales from hours to days characterize the sub-mesoscale (SMS) motions. The preconditions for intensified SMS processes in regions are strong lateral buoyancy gradients, vorticity, and weak vertical stratification. In the BS, the freshwater input by rivers preserves the permanent lateral buoyancy gradients, which are continuously modified by wind mixing and currents. In the present paper, based on the high-frequency point measurements of the currents and thermohaline parameters, we characterize the SMS variability in the surface and sub-surface layer related to different forcing and background conditions, including upwelling/downwelling and their relaxations periods; we estimate the contribution of SMS processes in the development of the upper layer stratification.

## Materials and methods

Measurements of currents, water temperature and salinity were carried out at two locations in the Gulf of Finland (GoF) near Keri Island. Current profiles were measured at the deep KeN station (about 2 km North of Keri Island) by bottom-mounted ADCP for two months from 26.07.2018 to 30.09.2018. Simultaneously, the temperature and salinity profiles were measured by a bottom-mounted profiler (Flydog Marine) for three weeks from 26.07.2018 to 17.08.2018. At shallow station KeS (about 1.1 km East of the island), current profiles were measured by bottom-mounted RDCP for one month from 28.08.2018 to 02.10.2018. Simultaneously, temperature and salinity profiles were measured by a buoy-mounted profiler (Idronaut) for five weeks from 28.08.2018 to 05.10.2018. Though the distance between KeN and KeE stations was about 2.5 km, the station KeN was situated on the thalweg of the Gulf of Finland, and the station KeS was on the shallower area shadowed by Keri Island from the West. Current velocity energy spectra revealed in the upper layer the elevated kinetic energy values between timescales of 10 to 36 hours and from 36 to 168 hours; the latter can be interpreted as submesoscale processes uppermost timescale. Therefore, we decomposed the current velocities into three frequency bands: high frequency (HF) band (corresponding to timescales 2-36 h), medium frequency (MF) band (36-168 h) and low frequency (LF) band (>168 h). The temperature and salinity variability corresponding to the HF band was analysed at isopycnal surfaces to exclude the contribution of internal waves to the SMS signal.

## Results and discussion

At the 110 m deep station (KeN), observations comprised an upwelling event along the southern coast and the following downwelling period. When the westerly winds supporting downwelling

ceased, we observed the intensification of high-frequency temperature fluctuations in the thermocline (at depths 10-20 m) (Figure 1). These fluctuations coincided with changes in velocity and salinity. In the halocline, the cease of the wind resulted in increased velocity variability and local vertical mixing. The spectrum slope -2 of the temperature variance at isopycnal surfaces, characteristic for submesoscale processes, was observed in the entire water column for the time scales from 10 to 40 hours. At a shallow station (46 m deep, 2.5 km toward SE), observations covered a downwelling relaxation during two weeks of calm weather and a new downwelling with the duration of three weeks containing two subsequent stormy wind events. In the middle of downwelling relaxation, successive positive and negative temperature and salinity fluctuations were observed in a wide range of density isolines (1003.4 to 1005.2 kg/m<sup>3</sup>, approximately corresponding to a depth interval of 20-35 m) (Figure 1). As shown by earlier numerical model studies, those temperature and salinity fluctuations could be developed by the submesoscale vortices or spiral eddies during the relaxation phase of mesoscale fronts. At both measurement stations, the minimum and maximum temperature fluctuations at isopycnals caused by the submesoscale processes were remarkable, from -1.2 to 1.8 °C.

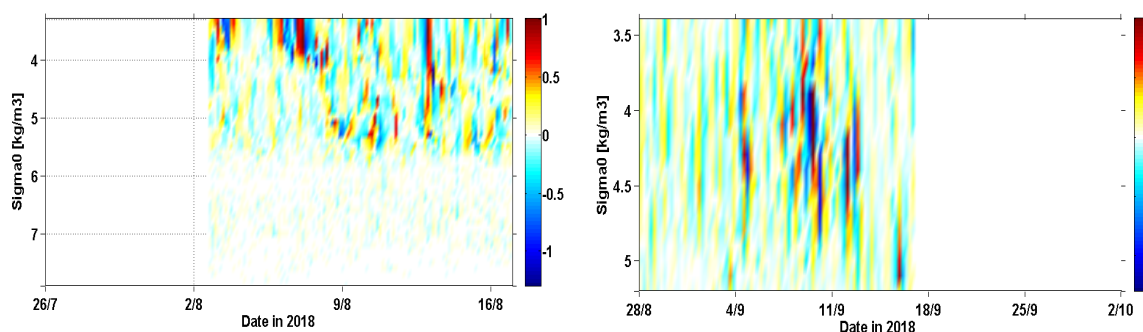


**Figure 1.** HF temperature fluctuations at isopycnal surfaces in deep station KeN (left panel) and shallow station KeS (right panel).

### Acknowledgements

This work was supported by the Estonian Research Council grant (PRG602).

### REFERENCES

- McWilliams, J.C. (2016), Submesoscale currents in the ocean, *Proc.R.Soc.*, A472: 20160117, <http://dx.doi.org/10.1098/rspa.2016.0117>.

# Analysis of spatiotemporal variability of remotely sensed variables to investigate thermal and morphological heterogeneity beneath the lakes surface

M. Amadori<sup>1\*</sup>, M. Bresciani<sup>1</sup>, C. Giardino<sup>1</sup>, H.A. Dijkstra<sup>2</sup>

<sup>1</sup>Institute for Electromagnetic Sensing of the Environment, National Research Council, Italy

<sup>2</sup>Institute for Marine and Atmospheric Research Utrecht, Utrecht University, the Netherlands

\*Corresponding author; e-mail [amadori.m@irea.cnr.it](mailto:amadori.m@irea.cnr.it)

## KEYWORDS

LSWT; Chlorophyll-a; Spatial patterns; Surface mixed layer; Empirical Orthogonal Functions.

## Introduction

When referring to remote sensing of inland waters, it is typically assumed that satellite-derived measurements only provide information on water surface features. Lake Surface Water Temperature (LSWT) is indeed mostly associated with a skin layer less than 1 mm thick, such that a direct comparison with *in-situ* data is often difficult. Recent applications have shown the potential of the spatiotemporal variability of LSWT for investigating subsurface dynamics e.g. regime shifts (Fichot et al, 2019). However, consolidated studies in the ocean (Frankignoul and Hasselmann 1977) largely demonstrated that Sea Surface Temperature (SST) carries information on the surface mixed layer, which reacts to atmospheric white noise by dampening high frequency forcing and leading to a red noise SST response.

In this contribution, we investigate the possibility to gather information on subsurface thermal complexity by analysing the spatiotemporal variability of remotely sensed products. Our case study is Lake Garda, the largest Italian lake characterised by deep clear waters, where a long time series of biophysical parameters from both satellite and *in-situ* measurements is available, as well as a consolidated knowledge of its main morphological features and thermal behaviour. After assessing the dominant spatiotemporal modes of variability for LSWT, chlorophyll-a (chl-a) and turbidity products, we interpret the obtained patterns using Hasselman's theory and estimate the thickness of the surface well-mixed layer as well as the thermal inertia of Lake Garda to atmospheric forcing.

## Materials and methods

Remote sensing biophysical products for Lake Garda are obtained from the ESA CCI ECV Lakes dataset (Cretaux, 2021) version 1. We use LSWT, chl-a and turbidity products from 1995 to 2018. For each quantity, a time series of gap-filled maps is obtained with uneven time spacing due to the different availability of products from different sensors. The approximately 20-year long time series are then pre-processed pixel by pixel by resampling every 10 days, linear detrending and removing the seasonal behaviour.

Empirical Orthogonal Functions (EOF) analysis is performed on LSWT, chl-a and turbidity time series to get the dominant modes explaining the spatiotemporal variability of these quantities. We then apply to LSWT Hasselman's theory on stochastic climate models, i.e. a first-order autoregressive model (AR1), for which the autocorrelation function  $\varrho_k$  between observations  $k$  periods apart can be described as:

$$\varrho_k = \alpha_k \quad (1)$$

where  $\alpha = e^{-\gamma \Delta t}$  is a constant coefficient depending on the damping time scale  $\gamma$  and the sampling time  $\Delta t$  of the signal. Hence, we fit the autocorrelation of the time series of detrended and de-seasonalized LSWT in each pixel of the map with eq. (1) and compute  $\gamma$ , from which we estimate the mixed layer depth (*MLD*) following 3.7 in Frankignoul and Hasselmann (1977).

## Results and discussion

Results in Figure 1 show that for a) LSWT and b) chl-a the first dominant mode (EOF1) has a dipole pattern between the northern and southern basins of Lake Garda, suggesting that these two areas are anti-correlated one-another. EOF1 of turbidity (c) shows a different pattern, with the two anti-correlated basins longitudinally displaying an east-west gradient. We argue that the pattern observed in Figure 1 a) and b) is due to different thermal behaviour of the two sub- basins and can be interpreted as mixed layer depth variability, which affects the surface temperature as well as chl-a dynamics, while not having significant effects on turbidity in Lake Garda.

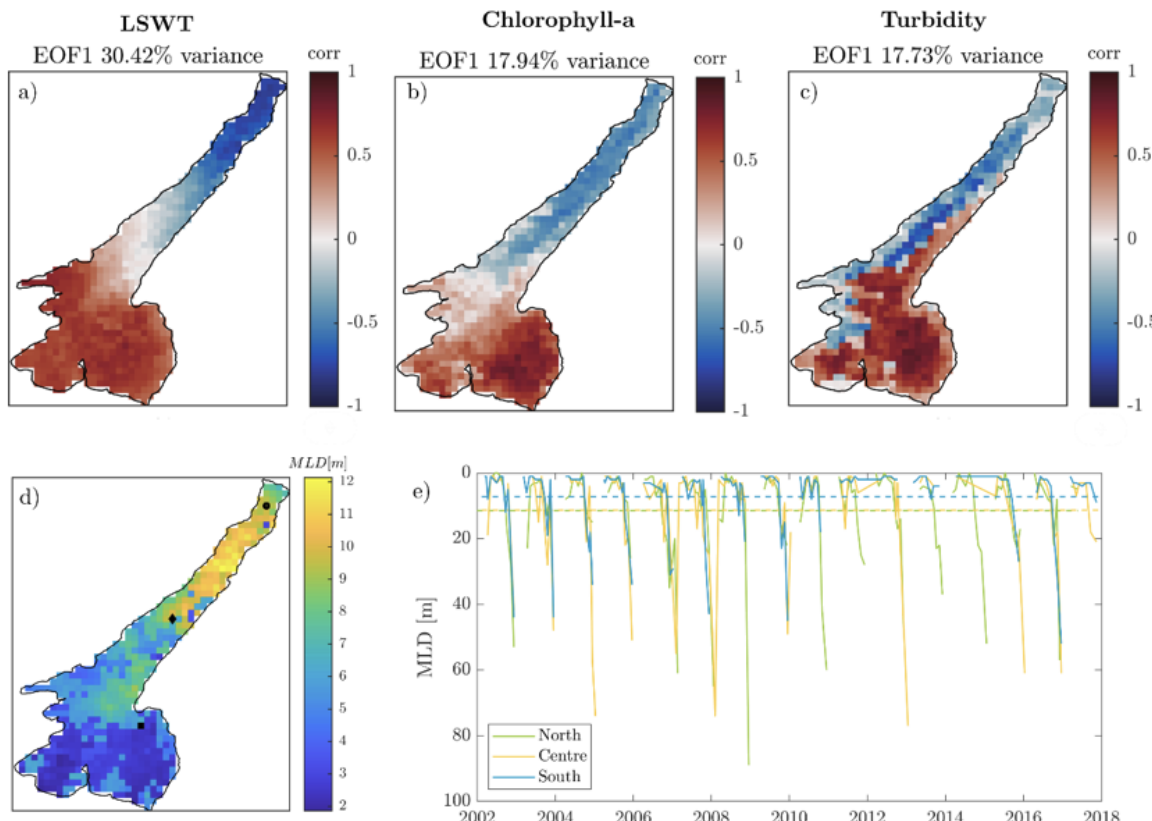


**Figure 1** EOF1 from LSWT (a), chl-a (b) and turbidity (c) analysis; (d) map of MLD estimated with Hasselman's theory; (e) MLD from three in-situ observations (black dots in (d) map).

By applying Hasselman's theory to LSWT anomalies we obtain an estimate of mixed layer depth (Figure 1d) whose spatial pattern is consistent with LSWT and chl-a dominant modes of variability. The time series of mixed layer depth computed from *in-situ* thermal profiles in three observation points (Figure 1e) confirm that such variability exists in the lake. These results open new opportunities for further investigation on surface mixed layer dynamics in lakes from remotely sensed quantities.

## REFERENCES

- Creteaux et al. (2021) ESA Lakes Climate Change Initiative (Lakes\_cci): Lake products, Version 1.1. NERC EDS Centre for Environmental Data Analysis. doi:10.5285/ef1627f523764eae8bbb6b81bf1f7a0a.
- Fichot et al, (2019), Assessing change in the overturning behavior of the Laurentian Great Lakes using remotely sensed lake surface water temperatures, *Remote Sensing of Environment*, doi: 10.1016/j.rse.2019.111427.
- Frankignoul and Hasselmann, (1977). Stochastic climate models, Part II Application to sea-surface temperature anomalies and thermocline variability, *Tellus*, 29:4, 289-305, DOI: 10.3402/tellusa.v29i4.11362.

# Satellite Earth observation to monitor lake mixing anomalies worldwide

E. Calamita<sup>1\*</sup>, M. Brechbühler<sup>1</sup>, I. Woolway<sup>2</sup>, C. Albergel<sup>3</sup>, D. Odermatt<sup>1</sup>

<sup>1</sup>*Eawag, Swiss Federal Institute of Aquatic Science and Technology, 8600 Dübendorf, Switzerland.* <sup>2</sup>*School of Ocean Sciences, Bangor University, Menai Bridge, Anglesey, Wales.*

<sup>3</sup>*European Space Agency Climate Office, ECSAT, Harwell Campus, OX11 0FD Didcot, Oxfordshire, United Kingdom.*

\*Corresponding author; e-mail [elisa.calamita@eawag.ch](mailto:elisa.calamita@eawag.ch)

## KEYWORDS

Lakes; mixing regime; mixing anomalies; climate change; regime shift.

## Introduction

Lake mixing regime is key because it regulates the entire phenology of lake ecosystems. The temporal progression of lake stratification and mixing regulates the transport of oxygen (Livingstone 2003; Woolway and Merchant 2019) as well as the nutrients and energy in lakes with important consequences for the lake biota.

Climate change can strongly affect lake mixing and can also push lakes towards a lake mixing regime shift. Dimictic lakes are those lakes that mix from top to bottom (overturn) twice in a year and they are particularly susceptible to changes in mixing. It is well recognized that climate change is shortening the duration of lake winter ice phenology (Stefanidis et al. 2022), thus the duration of winter inverse stratification (Woolway et al. 2022). Recent modelling studies show that warming over the next century will shift many temperate dimictic lakes towards a predominantly monomictic regime (Shatwell et al. 2019; Woolway and Merchant 2019).

Despite the importance of lake mixing regime shifts, we lack a systematic overview of their occurrence in lakes worldwide. The study of lake mixing regime shifts require indeed long term observations to observe such shifts and to identify the drivers (Mesman et al. 2021). However, Earth Observations (EO) allow monitoring consistently and systematically many lakes globally distributed. Moreover, modelling studies found that most lakes that are projected to alter their mixing regimes in the future are currently undergoing anomalies in mixing behavior relative to their dominant mixing classification (Woolway and Merchant 2019). Thus, identifying mixing anomalies occurring nowadays in lakes can be helpful to identify those lakes that are more prone to have a future mixing regime shift.

In this study, we use the spatial component of remotely sensed lake surface water temperature to reveal information about lake mixing and mixing anomalies.

## Materials and methods

The spatially distributed lake surface water temperature (LSWT) used in this study is from the European Space Agency's Climate Change Initiative (CCI) Lakes project (CCI Lakes; <http://cci.esa.int/lakes>), which contains daily observations from 2024 lakes worldwide (v2.0.1; Carrea et al. 2022). We apply a thermal front tracking method to identify mixing anomalies in dimictic lakes worldwide to spot lake mixing anomalies in dimictic lakes worldwide. In dimictic lakes, the thermals bar forms in spring and autumn during the mixing phase of the lake. Finally, we calculated the unitless measure of lake susceptibility to experience an incomplete turnover during fall, meaning that the lake would not be able to fully inversely stratify during the winter, following the procedure of Fichot et al. (2019).

## Results and discussion

By tracking the thermal bar we found that 59.1 % of the LakeCCI lakes (1197 lakes) experience on average two overturning per year. However, only 35.0 % of the LakeCCI lakes can be classified as dimictic because when discarding lakes that are too small, too shallow and lakes that are saline, for

which the classification approach cannot be accurate, we remain with 709 dimictic lakes (Fig. 1). Results show that 16 of the above classified dimictic lakes in the LakeCCI dataset experienced at least one anomaly during the last two decades, meaning that they did not experience inverse winter stratification at least ones. Moreover, these 16 lakes experienced from 1 to 6 anomalies during the last two decades. Results also show that none of the analyzed dimictic lakes had a clear shift from dimictic to monomictic regime during the last two decades, meaning that we did not find anomalies occurring consistently for all winters after a specific year.

We found that lakes experiencing more anomalies today are more prone to undergo a mixing regime shift in the future, as showed by the positive correlation between the number of anomalies and the susceptibility index. This result demonstrates that although EO cannot produce scenarios and thus predict mixing regime shifts in the future; they can help to spot very susceptible cases that would require a more-in-depth analysis, also through modelling.



**Figure 1.** Geographical distribution of the 709 dimictic lakes analysed in this study.

## REFERENCES

- Carrea, L. et al. (2022). ESA Lakes Climate Change Initiative (Lakes\_cci): Lake products, Version 2.0.1.
- Fichot, C. G., K. Matsumoto, B. Holt, M. M. Gierach, and K. S. Tokos. (2019). Assessing change in the overturning behavior of the Laurentian Great Lakes using remotely sensed lake surface water temperatures. *Remote Sens. Environ.* **235**: 111427. doi:10.1016/j.rse.2019.111427
- Livingstone, D. M. (2003). Impact of Secular Climate Change on the Thermal Structure of a Large Temperate Central European Lake. *Clim. Change* **57**: 205–225. doi:10.1023/A:1022119503144
- Mesman, J. P., J. A. A. Stelzer, V. Dakos, S. Goyette, I. D. Jones, J. Kasparian, D. F. McGinnis, and B. W. Ibelings. (2021). The role of internal feedbacks in shifting deep lake mixing regimes under a warming climate. *Freshw. Biol.* **66**: 1021–1035. doi:10.1111/fwb.13704
- Shatwell, T., W. Thiery, and G. Kirillin. (2019). Future projections of temperature and mixing regime of European temperate lakes. *Hydrol. Earth Syst. Sci.* **23**: 1533–1551. doi:10.5194/hess-23-1533-2019
- Stefanidis, K., G. Varlas, G. Papaioannou, A. Papadopoulos, and E. Dimitriou. (2022). Trends of lake temperature, mixing depth and ice cover thickness of European lakes during the last four decades. *Sci. Total Environ.* **830**: 154709. doi:10.1016/j.scitotenv.2022.154709
- Woolway, R. I., B. Denfeld, Z. Tan, J. Jansen, G. A. Weyhenmeyer, and S. La Fuente. (2022). Winter inverse lake stratification under historic and future climate change. *Limnol. Oceanogr. Lett.* **7**: 302–311. doi:10.1002/lo2.10231
- Woolway, R. I., and C. J. Merchant. (2019). Worldwide alteration of lake mixing regimes in response to climate change. *Nat. Geosci.* **12**: 271–276. doi:10.1038/s41561-019-0322-x

# The Lakes\_cci project: presenting the satellite-derived lakes variables for climate studies

M. Pinardi<sup>1\*</sup>, M. Bresciani<sup>1</sup>, R. Caroni<sup>1</sup>, G. Tellina<sup>1</sup>, J.F Crétaux<sup>2</sup>, S. Simis<sup>3</sup>, C. Duguay<sup>4,5</sup>, C.J. Merchant<sup>6,7</sup>, Laura Carrea<sup>6</sup>, H. Yesou<sup>8</sup>, A. Andral<sup>9</sup>, C. Giardino<sup>1</sup>

<sup>1</sup> Institute for Electromagnetic Sensing of the Environment, National Research Council, Milan, Italy

<sup>2</sup> LEGOS (CNES/CNRS/IRD/UPS), Université de Toulouse, Toulouse, France.

<sup>3</sup> Plymouth Marine Laboratory, Plymouth, United Kingdom.

<sup>4</sup> Department of Geography and Environmental Management, University of Waterloo, Waterloo, Ontario, Canada.

<sup>5</sup> H2O Geomatics Inc., Waterloo, Ontario, Canada.

<sup>6</sup> University of Reading, Meteorology Department, Reading, United Kingdom.

<sup>7</sup> National Centre for Earth Observation, Reading, United Kingdom.

<sup>8</sup> ICUBE-SERTIT, Université de Strasbourg, Strasbourg, France.

<sup>9</sup> Collecte Localisation Satellite, Toulouse, France.

\*Corresponding author, e-mail [pinardi.m@irea.cnr.it](mailto:pinardi.m@irea.cnr.it)

## KEYWORDS

Lakes Essential Climate Variables; global; chlorophyll-a; lake ice cover; heatwave.

## Introduction

Lakes are a vital resource for freshwater supply, and key sentinels for global environmental change. They are responding rapidly to climate change and in coming decades it is projected that global warming will have a more persistent and stronger effects on hydrology, nutrient cycling, and biodiversity (Carpenter et al. 2011). Factors driving lake condition vary widely across space and time, and lakes, in turn, play an important role in local and global climate regulation, with positive and negative feedback depending on the catchment (Adrian et al. 2009). Understanding the complex behaviour of lakes is essential to effective water resource management and mitigation of climate change effects and, in such a context, remote sensing allows unique insights by providing both synoptic and relatively high frequency observations (e.g., Neil et al. 2019).

## Methods

The ESA Lakes\_cci project has the main objective to use satellite data to create the largest and longest possible consistent, global record of lake essential climate variables: Water Level (LWL), Water Extent (LWE), Surface Water Temperature (LSWT), Ice Cover (LIC) and Water-Leaving Reflectance (LWLR, with turbidity and chlorophyll-a products). Recently, also lake Ice Thickness (LIT) and Storage Change (LSC) were added. The data span combined satellite observations from 1992 to 2020 inclusive and quantifies over 2000 relatively large lakes (Carrea et al. 2023). Selected use cases are presented to demonstrate the scientific contribution of the project in understanding the response of phytoplankton in European lakes to the 2019 heatwave events (Free et al. 2022), and in supporting a long-term lake ice phenology data record of the Northern Hemisphere (Cai et al. 2022a).

## Heatwave and storm events impact on lakes

Satellite-derived chlorophyll-a (Chl-a) products for 36 European lakes (Lakes\_cci dataset v1.1) during a widespread double heatwave event in the summer of 2019 were examined, evaluating how the response varies depending on latitude, nutrients and the lake average depth. The results show that the timing and magnitude of the response to the heatwaves depends on lake depth and nutrients (Fig. 1). Deep and medium depth lakes at higher latitudes displayed a synchronous Chl-a increase with temperature, possibly as the result of an improved light climate resulting from increased stratification, but with the response strength dependent on nutrient status (e.g., in the deep peri-Alpine Maggiore and Geneva lakes). Warmer, southern shallow lakes had the most asynchronous response. Chlorophyll-a peaks typically occurred five days after the peak of the

heatwave for shallow lakes. In several nutrient-rich lakes the response to the heatwave was dwarfed by large algal blooms occurring later during the typical cyanobacterial bloom period in early autumn (e.g., in the shallow turbid Razim and Balaton lakes in Eastern Europe).

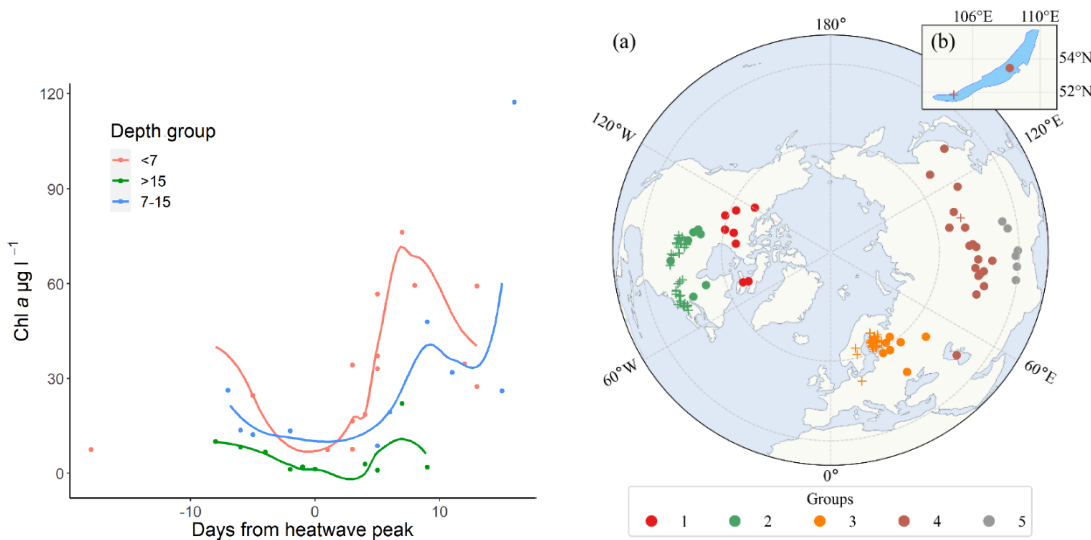


**Figure 1.** On the left, timing and concentration of peak chlorophyll-a with respect to the second 2019 heatwave. Lakes coloured and lowess smoother applied by mean depth group (source: Free et al. 2022). On the right, 46 study lakes divided into five groups (coloured circles) and 89 sites with in situ observations (+ symbols with colours corresponding to those of groups) (a). Example of in situ and remote sensing data for Lake Baikal (b). Northern North America (Group 1), southern North America (Group 2), northwestern Eurasia (Group 3), northern Eurasia (Group 4), and southern Eurasia (or the Tibetan Plateau, Group 5).

### Long-term lake ice phenology data record of the Northern Hemisphere

Of the 2024 lakes included in the Lakes\_cci dataset, 1391 lakes have been identified as forming an ice cover. The LIC variable is derived from MODIS Aqua/Terra satellite observations and covers the 2000-2020 period. The data is currently being processed to extract dates associated with lake ice phenology (IP) (freeze-up, break-up and ice duration) for climate analysis. It will supplement in situ observations and the IP dataset of Cai et al. (2022b) produced using passive microwave data that covers only 56 of the largest lakes of the Northern Hemisphere (1989-2021). Analysis of the passive microwave derived IP for 46 lakes (best quality records; Fig. 1a,b) has revealed overall trends toward later freeze-up, earlier break-up and shorter ice durations, with the most significant and dramatic changes occurring in the freeze-up dates of lakes in northwestern Eurasia (average change rates of 0.83 and 0.79 d/yr for freeze-up start and freeze-up end or ca. 27 days over the 33-year period). These results will soon be compared to those obtained from the Lakes\_cci dataset in an effort to provide consistent global records of lake IP for climate change studies.

### REFERENCES

- Cai et al. (2022a). A 41-year (1979–2019), Passive-microwave-derived lake ice phenology data record of the Northern Hemisphere. *Earth System Science Data*, 14(7), 3329-3347.
- Cai et al. (2022b), Lake ice phenology in the Northern Hemisphere extracted from SMMR, SSM/I and SSMIS data from 1979 to 2021. PANGAEA, <https://doi.org/10.1594/PANGAEA.946231>
- Carrea et al. (2023), Satellite-derived multivariate world-wide lake physical variable timeseries for climate studies. *Scientific Data* 10 (1), 30.
- Free et al. (2022), Investigating lake chlorophyll-a responses to the 2019 European double heatwave using satellite remote sensing. *Ecological Indicators*, 142, 109217.

# Mobile eddy covariance measurements as a key to improve estimates of momentum, mass and energy fluxes between atmosphere and inland waters

U. Spank<sup>1,\*</sup>, M. Mauder<sup>1</sup>, J. Matschullat<sup>2</sup>, G. Licht<sup>3</sup> and M. Koschorreck<sup>4</sup>

<sup>1</sup> Chair of Meteorology, Faculty of Environmental Sciences, Technische Universität Dresden, Tharandt, Germany

<sup>2</sup> Chair for Geochemistry and Geoecology, Faculty of Geosciences, Geoengineering and Mining, Technische Universität Bergakademie Freiberg, Germany

<sup>3</sup> Chair for Software Technology and Robotics, Faculty of Mathematics and Computer Science, Technische Universität Bergakademie Freiberg, Germany

<sup>4</sup> Department Lake Research, Helmholtz Centre for Environmental Research – UFZ, Magdeburg, Germany

\*Corresponding author, e-mail [uwe.spank@tu-dresden.de](mailto:uwe.spank@tu-dresden.de)

## KEYWORDS

Atmosphere-water-interaction; Autonomous mobile measurements; Mass, energy and momentum fluxes; Micrometeorological observation; Spatial variability of meteorological and limnological driver variables.

## Introduction

The correct estimation of mass and energy exchange between inland waters and the atmosphere is important both for answering scientific questions and for solving practical problems in the management of water quantity and quality. Direct measurements are possible, but difficult and costly. Thus such measurements can usually only be carried out in the context of special projects and experiments. Therefore, momentum, mass and energy fluxes are usually determined indirectly via the specific gradient and the associated transfer coefficient. However, the accuracy and precision of the fluxes determined in this way depend significantly on the representativeness of the meteorological and limnological data used and, above all, on the parameterization of the transfer coefficients. Numerous studies have shown that the parameterization of the transfer coefficients must not only be based on local meteorological conditions, but that micro-scale site effects must also be taken into account. This means that reliable data from a water body must be collected at least for defined periods of time. This makes it possible to transfer standard meteorological measurements, e.g. from nearby weather stations, to the water and to determine local properties of the transfer coefficients. The installation of a floating eddy covariance (EC) measuring station would be a good way to achieve these goals. However, this is usually not possible for financial and other reasons. The installation of a permanently anchored measuring station is out of the question, especially if this conflicts with other demands on the use of the water body. Here, we introduce our prototype of a mobile EC measurement system (Fig. 1). An autonomously navigating robotic boat serves as a carrier for an open-path EC measurement system. The fluxes were determined using spatio-temporal covariances instead of temporal covariances, which by default are the basis of flux determinations by EC. Three measurement campaigns were carried out at the Bautzen reservoir in Lusatia (Germany, Fig. 2), testing the robotic boat and the methodology to determine mass and energy fluxes under different weather conditions. The comparison of fluxes, determined in this way, with data from the stationary EC sites showed promising results. The mobile setup enabled to explore the mass and energy exchange at the water surface and make it possible to detect the spatial variability of the water body in relation to the turbulence structure of the atmospheric boundary layer. Mobile EC measurements are therefore an excellent alternative when it is not possible to install a fixed floating EC measurement station as well as they provide a method to extend the capabilities of stationary EC sites to better address spatial variations.



**Fig. 1** Autonomously navigating robotic boat with mobile eddy covariance system (foreground) and fully equipped floating outdoor laboratory (background) on the Bautzen reservoir (Germany, June 2022).

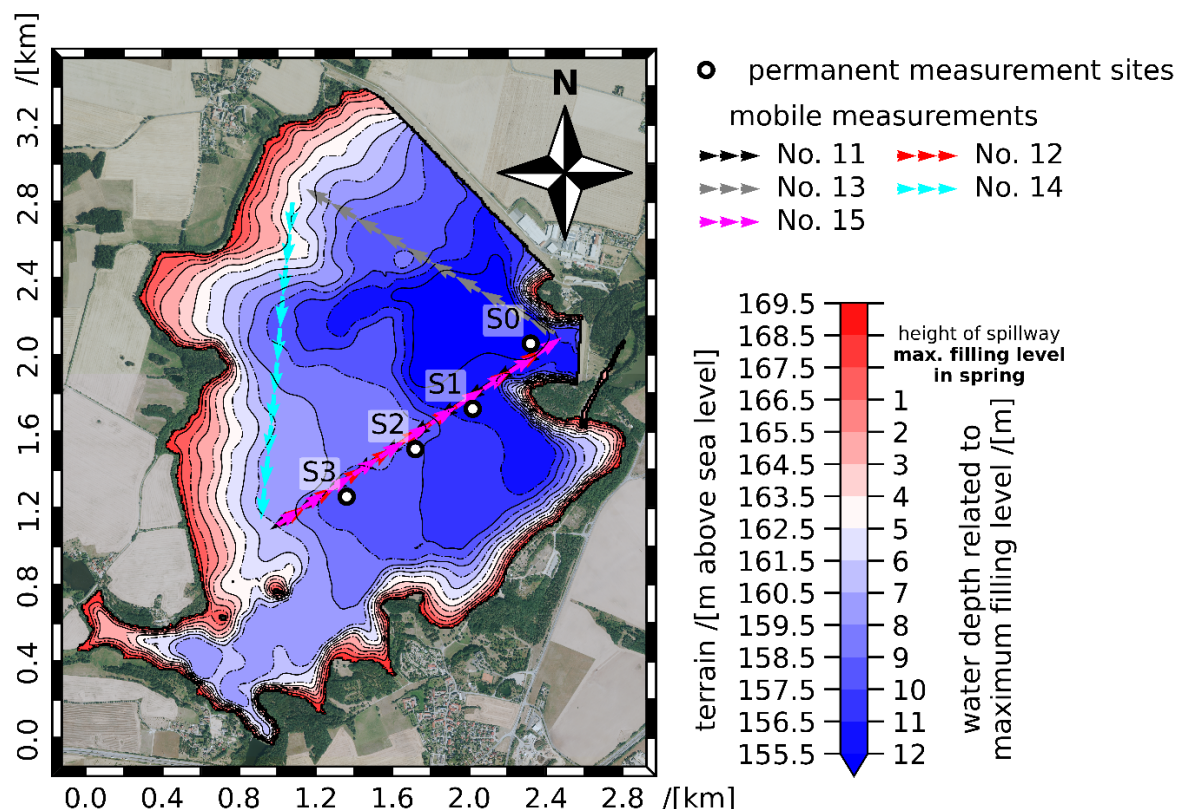


**Fig. 2** Bathymetry of the Bautzen reservoir, position of the permanent stationary EC measurement sites and mobile EC measurements from 16 June 2023 carried out with the robot boat.

# In-situ observations of the acoustic scattering characteristics from a suspension of flocculated particles

J.C. Mullarney<sup>1\*</sup>, I.T. MacDonald<sup>2</sup>, C.A. Eager<sup>2,3</sup>

<sup>1</sup> Coastal Marine Group, School of Science, University of Waikato, Hamilton, New Zealand

<sup>2</sup> National Institute of Water & Atmospheric Research (NIWA), Hamilton, New Zealand <sup>3</sup> Waikato Regional Council, Hamilton, New Zealand

\*Corresponding author, e-mail [julia.mullarney@waikato.ac.nz](mailto:julia.mullarney@waikato.ac.nz)

## KEYWORDS

Sediment transport; acoustic backscatter; flocculation; form function; scattering characteristics

## Introduction

Studies of sediment transport in aquatic environments rely on accurate measurements of suspended sediment concentrations and particle sizes. Such data is essential to elucidate key physico-chemical processes associated with particle flocculation, and for validation and improvement of numerical models. For non-cohesive sand particles, profiles of concentrations can be estimated from backscatter data from acoustic instruments coupled with in-situ water samples (Thorne and Hurther, 2014). However, for cohesive particles, measurements are complicated by flocculation (aggregation) of individual particles, phytoplankton, bacteria, and detrital organic material, which changes both physical properties (e.g. settling velocities) and the acoustic backscatter signal. Theoretical expressions for the scattering characteristics are absent and must be derived empirically (Thorne et al. 1995).

## Materials and methods

We report field observations from the muddy and tidally influenced Kaipara River in the North Island of New Zealand. Measurements over the ebb phase of two tidal cycles included horizontal profiles of acoustic backscatter over 4 frequencies (1, 2, 4, and 5 MHz) close to the water surface, in addition to physico-chemical properties, aggregated particle characteristics from floc cameras, and suspended sediment concentrations from optical backscatter sensors calibrated against in-situ water samples.

A laboratory calibration following the method of Wilson and Hay (2017) was undertaken to obtain the system constant  $K_{TR}$ , and effective radii for the ABS transducers. Using the field data, estimates of the two key parameters that describe the scattering characteristics of the suspended particles, namely the ensemble backscatter form function and the ensemble total scattering cross section, were derived.

## Results and discussion

Figure 1 shows observations of suspended sediment concentrations (panels a,b), a measure of fit quality (panels c,d), and the particle scattering characteristics (panels e-h). For the first tide, the form function and scattering cross section increased with concentration as expected. At the lower frequencies in particular, little attenuation of sound due to particles was observed. However, for the second tide, the form function remained relatively uniform even during the increase in concentrations. Values of the form function varied by around a factor of two between tides, despite similar observed mass concentrations. These differences are likely owing to a dependence on other variables, which will be explored further, noting that estimates were obtained by using the radius of the primary, and not the flocculated, particles in the relevant equations. We further investigate results of the inversion algorithm which converts the acoustic backscattered signal into estimates of suspended sediment concentration.

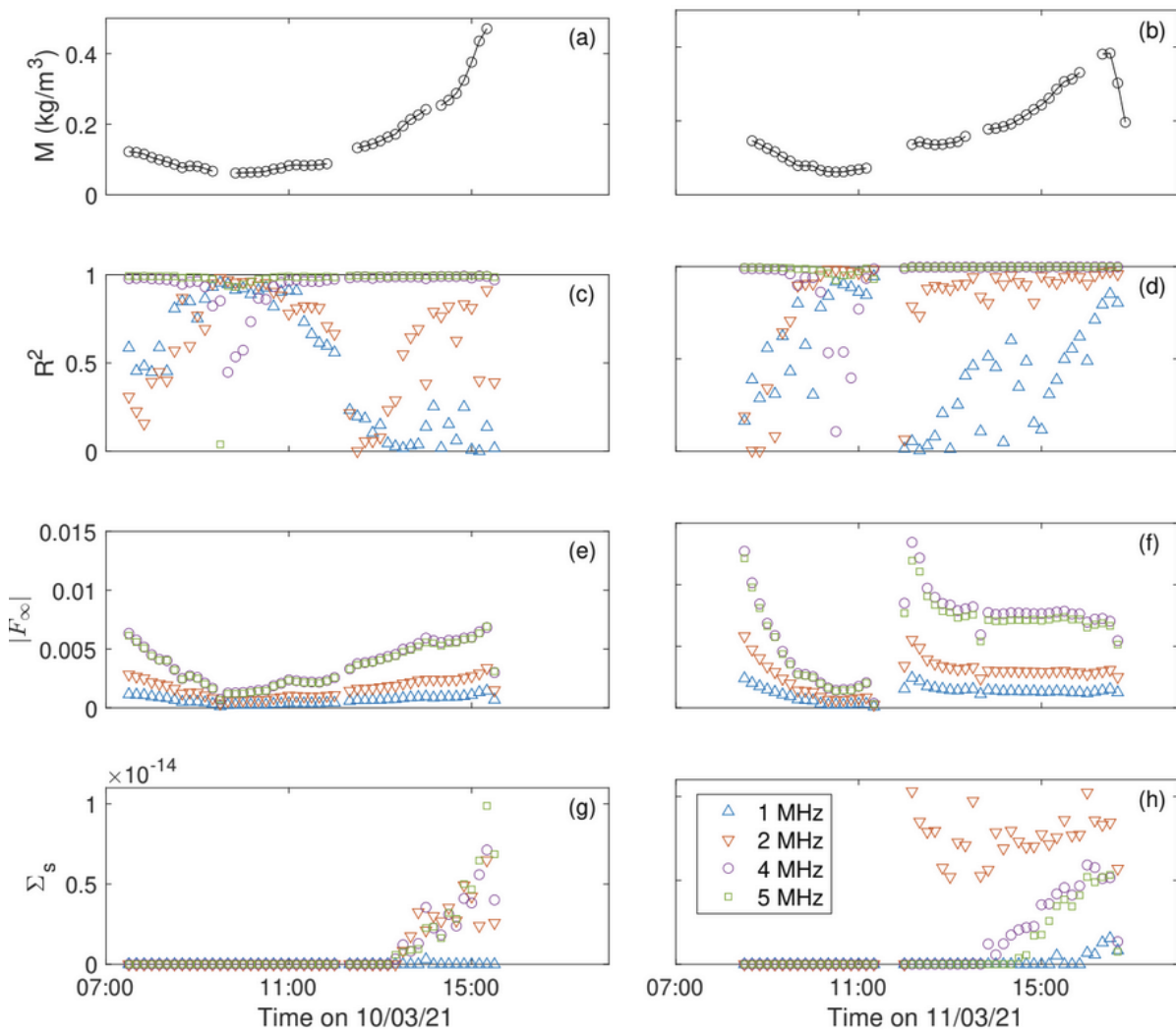


**Figure 1.** Results of inversion process for different frequencies across two different ebb tides (left and right columns). (a,b) Mass concentration from calibrated OBS sensor; (c,d) Quality of fit of empirical expressions to data; (e,f) ensemble form function and (g, h) ensemble total scattering cross section.

## REFERENCES

- Thorne, P.D., Waters, K.R., and Brudner, T.J. (1995), Acoustic measurements of scattering by objects of irregular shape, *J. Acoust. Soc. Am.*, **97**, 242–251.
- Thorne, P.D., and Hurther, D. (2014). An overview on the use of backscattered sound for measuring suspended particle size and concentration profiles in non-cohesive inorganic sediment transport studies. *Cont. Shelf Res.*, **73**, 97-118.
- Wilson, G.W., and Hay, A.E (2017), Short-pulse method for acoustic backscatter amplitude calibration at MHz frequencies, *J. Acoust. Soc. Am.*, **142**, 1655–1662.

# Turbid inflow into a drinking water reservoir

R. Pieters<sup>1\*</sup>, L. Gu<sup>2</sup> and G. Lawrence<sup>3</sup>

<sup>1</sup>*Earth, Ocean and Atmospheric Sciences, University of British Columbia, Vancouver, Canada*

<sup>2</sup>*Environmental Management and Quality Control, Metro Vancouver, Burnaby, Canada*

<sup>3</sup>*Civil Engineering, University of British Columbia, Vancouver, Canada*

\*Corresponding author, e-mail [rpieters@eoas.ubc.ca](mailto:rpieters@eoas.ubc.ca)

## KEYWORDS

Turbidity; Inflow; Stratification; Reservoir; Drinking Water.

## Introduction

Coquitlam Reservoir is the largest drinking water supply for Metro Vancouver, British Columbia, Canada, and is expected to meet the projected increase in drinking water demand for the region. While the reservoir is generally very clear (turbidity < 1 NTU), tributary inflows to the reservoir can occasionally be highly turbid. Turbid inflows are most likely to occur during fall and winter rain storms, when glacial fines enter the tributaries by bank erosion or landslides. In the reservoir, these fines are slow to settle. Water leaves Coquitlam Reservoir at the dam to provide residual flow in Coquitlam River below the dam, at the existing drinking water intake near the dam, and at the BC Hydro tunnel for hydroelectric generation. We summarize extensive survey and mooring data, trace the fate of turbid inflows through the reservoir, examine the likelihood of turbid events, and discuss the implications for siting of a second intake.

## Study site and methods

Coquitlam Reservoir, located in the coastal mountains north of Metro Vancouver, Canada ( $49^{\circ} 21' N$ ,  $122^{\circ} 46' W$ ), is a long (13 km), narrow (1 km) fjord lake with steep sides (Fig. 1). The 30 m dam at the south end of the reservoir raised the water level of the original lake resulting in a mean depth of 65 m and a maximum depth of 180 m. A granitic drainage ( $190 \text{ km}^2$ ) and high rainfall (yield  $3.7 \text{ m/yr}$ ), result in a phosphorus limited, oligotrophic system.

Surveys of the reservoir were conducted using a Seabird SBE19 or SBE25 profiler with a Wetlabs CStar transmissometer (660 nm) and/or a Seapoint optical backscatter sensor. Bottle samples were collected and analyzed within 24 hours using a Hach Model 2100A turbidity meter. A potential intake site in the main basin, COQA, has steep bathymetry with cliff faces suitable for tunnel intakes. A mooring at COQA included WETlabs ECO NTUSB self-contained turbidity recorders at 9, 34 and 63 m from a reference water level of 145 mASL. These sensors have proven stable and accurate, allowing the collection of a reliable record of low turbidity data. Also included were Seabird SBE56 and RBR SoloT temperature recorders at both COQA and COQ4s.

## Results and discussion

Profiler surveys suggested that the central basin of Coquitlam Reservoir had lower turbidity, being away from Cedar Creek and other sources of turbidity at the south end of the reservoir, and relatively far from the north basin where turbidity is dominated by Coquitlam River. To further assess the main basin, moorings were installed at COQA in December 2007 to allow continuous measurement of turbidity. The lowest turbidity of the three depths is shown in Fig 2.

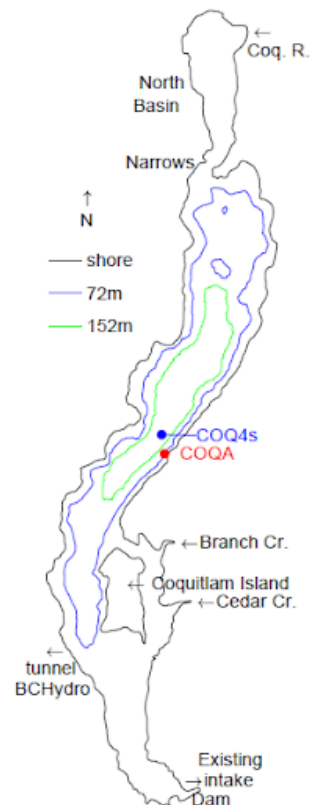


Figure 1. Map of Coquitlam Reservoir

The minimum turbidity at COQA was generally well below 1 NTU (average 0.3 NTU). In the eighteen-year record, there were only two occasions when the turbidity rose above 1 NTU (January 2005 and November 2006, max 1.21 NTU); during these events, the turbidity exceeded 1 NTU for a total of approximately 100 days.

The turbidity shows a distinct seasonal cycle with turbidity declining in spring and summer, and peaking in fall and early winter. For comparison, the seasonal cycle of flow and stratification is summarized in Fig. 3. Inflow in 2006 had a broad peak from April to June due to spring freshet, and on top of this were short duration peaks due to rain storms (blue, Fig. 3a). Over 10 years, the average monthly flow peaks in November (black, Fig. 3a). The duration of high flows also peaks in November (black, Fig. 3b). After a maximum in summer, the stratification begins to decline in fall, but it declines slowly because of the time required to cool the large volume of the reservoir (blue, Fig. 3b). As a result, the temperature stratification was often sufficient to isolate turbid inflows in the epilimnion and thermocline during late fall at the time of peak inflow.

In fall, as the epilimnion deepens, turbidity is diluted by mixing with less turbid water from below, and diluted with tributary inflow that is less turbid after an erosion event has subsided. In winter, when stratification is weak, turbid inflows often plunge to a variety of depths, including to the deepest part of the reservoir (180 m).

For a second intake, the main basin is furthest from sources of turbidity. A multi-depth withdrawal would avoid lenses of turbidity isolated in the thermocline. In addition, the deep part of the reservoir can receive turbid inflow during turbidity events. Finally, the existing intake at the south end of the reservoir could be retained as an alternate.

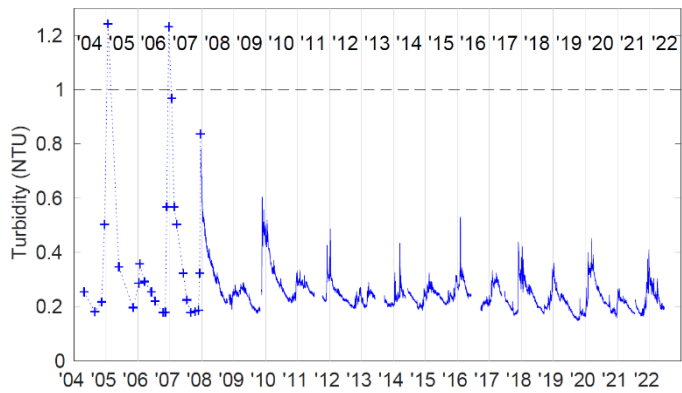


**Figure 2.** The minimum turbidity of the three depths at COQA, from profiler surveys (estimate, dashed line 2004-2007), and mooring data (solid line 2007-2022).

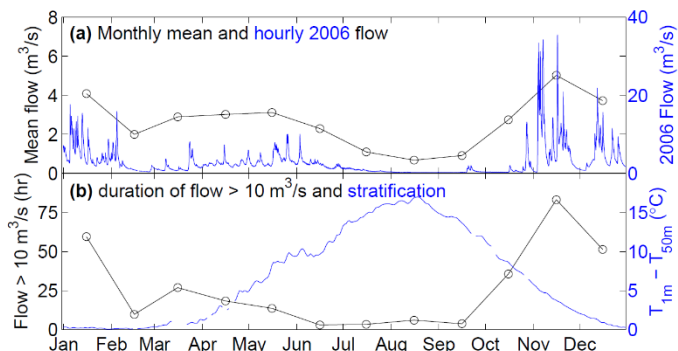


**Figure 3.** (a) Mean monthly flow, Cedar Cr., 2001-2010 (black); hourly flow, Cedar Cr., 2006 (blue). (b) Average monthly duration of hourly flow  $> 10 \text{ m}^3/\text{s}$ , Cedar Cr., 2001-2010 (black); and daily average difference in temperature between 1 and 50 m, Coquitlam Reservoir, 2004-2008 (blue).

# Turbulent Schmidt number measurements in a density current flowing over surface roughness

A. Di Bernardino<sup>1</sup>, P. Monti<sup>2\*</sup>, G. Leuzzi<sup>2</sup>, and G. Querzoli<sup>3</sup>

<sup>1</sup> Department of Physics, Sapienza University of Rome, Rome, Italy

<sup>2</sup> Department of Civil Constructional and Environmental Engineering, Sapienza University of Rome, Rome, Italy

<sup>3</sup> Department of Environmental Civil Engineering and Architecture, University of Cagliari, Cagliari, Italy

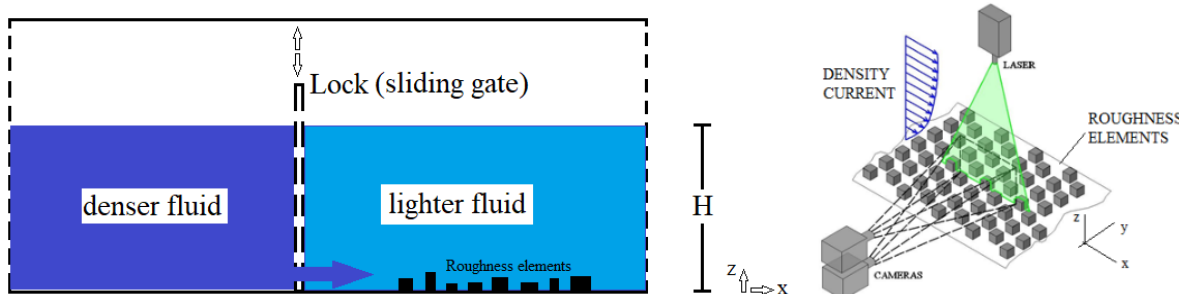
\*Corresponding author; e-mail [pao.lo.monti@uniroma1.it](mailto:pao.lo.monti@uniroma1.it)

## KEYWORDS

Stably stratified flows; Vertical Mixing; Lock exchange; Turbulent Schmidt number; Mixing efficiency.

## Introduction

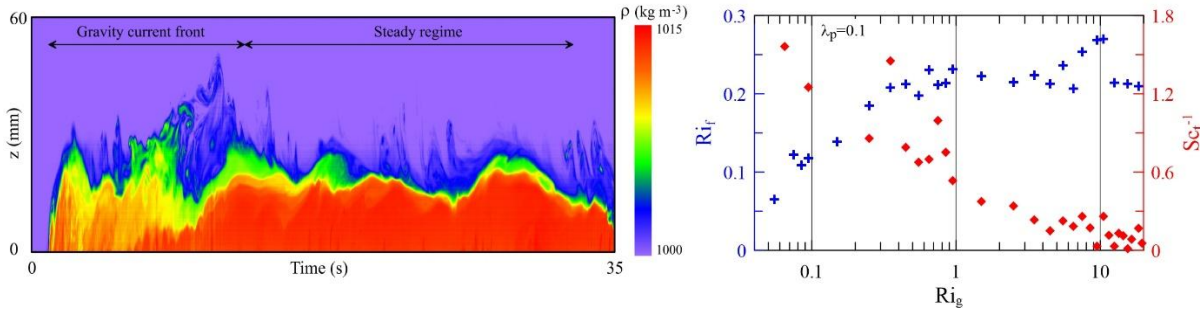
Vertical turbulent mixing can be strongly attenuated by density stratification due to negative (downward) buoyancy force. In environmental flows, this is generally associated with vertical variations in temperature, as occurs in lakes or in the atmosphere, or in temperature and salt concentration, as in oceans. In common practice, vertical exchanges of momentum and scalars are modelled by means of empirical laws that are included in turbulence closures. Unfortunately, their estimate is not an easy task and there is still a lack of knowledge regarding their values. The present work fits in this field of studies and focuses on the determination of some variables of interest for stably stratified flows obtained by means of experimental data collected in the water channel of the Hydraulic Laboratory of the Department of Civil, Constructional and Environmental Engineering (Sapienza University of Rome). The figure below shows a sketch of the water channel (left picture) and the measurement setup (right).



The channel has a length of 740 cm and a rectangular section 35 cm high and 25 cm wide. The channel is subdivided into two separate sections by means of a movable gate. The left part is filled with a mixture of fresh water and salt (denser fluid), whose density ( $\rho_d$ ) is higher than that of the fresh water (lighter fluid,  $\rho_l$ ) contained in the right section. The water depth in the two volumes is  $H$ . The denser fluid is premixed with a fluorescent dye (Rhodamine-WT). The experiment starts by removing the gate, which allows the denser fluid to flow from left to right beneath the lighter fluid. The density differences set in all the experiments ( $\Delta\rho = \rho_d - \rho_l$ ) are small enough to avoid any significant distortions in the path of the laser light rays used for the measurements. The roughness elements are 1.5 cm tall. Three plan area indices, i.e.,  $\lambda_p = A_p/A_T = 0.1, 0.25$ , and  $0.4$ , have been considered in the experiments, where  $A_p$  is the plan area occupied by the roughness elements and  $A_T$  is the total plan area. The acquisition

facility consists of a green laser (5 W, wavelength 532 nm) emitting a light sheet illuminating the acquisition plane (2 mm thick) and of two synchronized cameras, acquiring 100 frames per second at 1024x1280 pixels in resolution. The two cameras are aligned horizontally to optimize the framing of the area of interest (~8.5 cm wide (x-axis) and ~6.9 cm high (z-axis)) and to reduce the

unavoidable image distortion as much as possible. The first camera acquires the positions of non-buoyant particles premixed in both the fluids and allows us the evaluation of the instantaneous velocity fields by means of a feature-tracking algorithm. A Gaussian interpolation algorithm is applied at each time instant to the scattered velocity samples on the x-z plane to obtain the instantaneous velocity field on a regular 102x128 array ( $\sim 0.067\text{-cm}$  spatial resolution). The fluid density is acquired via planar laser-induced fluorescence (PLIF), a technique often employed to investigate tracer dispersion in water. The second camera is equipped with a band-pass filter tuned on 587 nm (Rhodamine-WT excited by green light at 532 nm, emits red light at 587 nm) to sense only the fluorescent light emission. The images are calibrated so that the dye concentration (directly related to the fractional volume of the dyed fluid) at a given pixel is proportional to the luminosity measured, which, in turn, is proportional to the salt concentration (i.e., fluid density). The instantaneous concentration field is mapped onto the instantaneous velocity field using an affine transformation accounting for the different points of view of the two cameras. During each experiment, about 8,000 instantaneous velocity and density fields are collected. The figure below (left) shows an example of time history of the density acquired along a vertical profile passing through the center of the framed area. After the passage of the gravity current front, a quasi-steady regime lasting several tens of seconds takes place, during which the statistics of the variables are determined.



The mean density,  $\bar{\rho}$ , is calculated for each of the 102x128 nodes of the array by applying the canonical Reynolds-averaging method. Similarly, the mean velocity components,  $\bar{u}$  and  $\bar{w}$ , the vertical fluxes of momentum,  $\bar{u}'\bar{w}'$ , and mass,  $\bar{w}'\bar{\rho}'$ , are determined for the same array (here,  $u$  and  $w$  are the streamwise and vertical velocity components, respectively; the prime denotes the fluctuation around the mean). Therefore, it is possible to determine the fields of the turbulent diffusivities of mass,  $K_\rho = -\bar{w}'\bar{\rho}'/\bar{d\rho}/dz$ , and momentum,  $K_m = -\bar{u}'\bar{w}'/\bar{du}/dz$ , based on the gradient-transport hypothesis – as well as the turbulent Schmidt number ( $Sc_t = K_m/K_\rho$ ) – and to analyze their dependence on the gradient Richardson number,  $Ri_g = -(g/\rho_{ref})(\bar{d\rho}/dz)/(\bar{du}/dz)^2$ , where  $\rho_{ref}$  is the reference density and  $g$  the gravity acceleration. The flux Richardson number,  $Ri_f = B/(B + \epsilon)$ , also known as to the mixing efficiency (here,  $B = (g/\bar{\rho}_{ref})\bar{w}'\bar{\rho}'$  is the buoyancy flux and  $\epsilon$  is the dissipation rate of turbulent kinetic energy) has also been determined. The figure above (right) shows  $Ri_f$  (blue symbols) and  $Sc_t^{-1} = K_\rho/K_m$  (red symbols) against  $Ri_g$  ( $\lambda_p = 0.1$ ;  $H=15$  cm; reduced gravity,  $g' = g\Delta\rho/\rho_{ref} = 14.6 \text{ cm s}^{-2}$ ; buoyancy velocity,  $U = \sqrt{g'H} = 14.8 \text{ cm s}^{-1}$ ; Reynolds number,  $Re = UH/v = 22,200$ ; Froude number,  $Fr = U_f/U = 0.35$ ;  $U_f$  is the front velocity and  $v$  is water viscosity). Although the results are preliminary and referring to a single  $\lambda_p$ , they seem encouraging as the two curves are similar to those obtained via direct numerical simulations and field campaigns reported in previous published papers.

# Three-dimensional modelling of gravity currents in an idealized stratified ice-covered lake

F.S. Sharifi<sup>1,2\*</sup>, R. Hinkelmann<sup>2</sup>, T. Hattermann<sup>3</sup>, and G. Kirillin<sup>1</sup>

<sup>1</sup> Department of Ecohydrology and Biogeochemistry, Leibniz Institute of Freshwater Ecology and Inland Fisheries (IGB), Berlin, Germany

<sup>2</sup> Technische Universität Berlin, Chair of Water Resources Management and Modeling of Hydrosystems, Institute of Civil Engineering, Faculty VI Planning Building Environment, Berlin, Germany

<sup>3</sup> Department of Physics and Technology, UiT The Arctic University of Norway, Norway

\*Corresponding author; e-mail [fatemeh.sharifi@igb-berlin.de](mailto:fatemeh.sharifi@igb-berlin.de)

## KEYWORDS

Ice-covered lakes; diffusion-driven flows; upward boundary currents; gravity currents modelling; heat redistribution.

## Introduction

Circulation in ice-covered lakes is characterized by the absence of wind shear, closed boundaries, a constant temperature at the ice surface, and thermal stratification below its temperature of maximum density  $T_{md}$ . In polar regions, if no heat enters the lake body from sediment, inflows or solar radiation, the lake can remain in a quasi-steady thermally stratified state without buoyancy production. Water temperatures increase nearly linearly from the freezing point at the ice-water boundary to values close to  $T_{md}$ . In this case, the diffusion-driven boundary flow described by Phillips (1970) and Wunsch (1970) may play a significant role in renewing deep waters and heating the ice cover. In a linearly stratified fluid with sloped lateral boundaries, an upward flow along the boundaries develops due to adjustment of neutral buoyancy surface to the slope. The resulting basin-scale circulation in enclosed lakes remains currently unknown, and is potentially affected by the shape and size of the lake basin, strength of stratification, and the earth rotation. Our study analyses the complicated thermal dynamics of ice-covered lakes and how external influences and diffusion-driven flow regulate them.

We analyse main features of the diffusion-density driven circulation in a thermally stratified lake of an idealized shape by using the Regional Ocean Modeling System (ROMS), aiming at

- 1) exploring the role played by lake size, bottom slope angle, and earth rotation affect boundary flow and residual lake-wide circulation.
- 2) estimating the effects of the heat release from sediment as an additional driver of circulation.

## Materials and methods

The initial surface temperature was set to 0°C, and the initial bottom temperature was set to 4°C. The maximum depth of the modeled lake varied in the range 15 - 150 m, and the lake length varied between 0.4 and 45 km, with corresponding variations of the baroclinic Rossby radius 500- 4800 m. To investigate the effect of heat input and output from the bottom values 3 W m<sup>-2</sup> and 5 W m<sup>-2</sup> were utilized in our model runs as constant bottom heat fluxes.

## Results and discussion

The hydrostatic Bussinesq model was capable to qualitatively reproduce major features of the diffusion-driven flows with upward boundary currents and downward current in the lake interior (Figure 1a), but the mixing rates and current magnitudes could be overestimated due to numerical model restrictions. Diffusion-gravity flow created complex circulation patterns with anticyclonic or cyclonic lake-wide gyres affected by Coriolis acceleration. Gyres alternate with vertical circulation cells in the vertical plane but rotate in opposite directions in the horizontal plane (Figure 1b and 1c). The numerical results revealed vertical and horizontal current velocities in the range of 10<sup>-6</sup> and 10<sup>-3</sup> ms<sup>-1</sup>, respectively.

Addition of bottom heat flux changed horizontal and vertical circulation to downward boundary currents and upward flow in the center of the lake because heat stored in sediment warmed shallow areas faster than the lake interior and started to sink. The numerical findings showed that the horizontal current velocities were in the range of  $10^{-3} \text{ ms}^{-1}$ , while the vertical velocity order increased to  $10^{-5} \text{ ms}^{-1}$ .

The effect of surface heat fluxes and salinity gradients on circulation are among other factors affecting the circulation and are subject to further study.

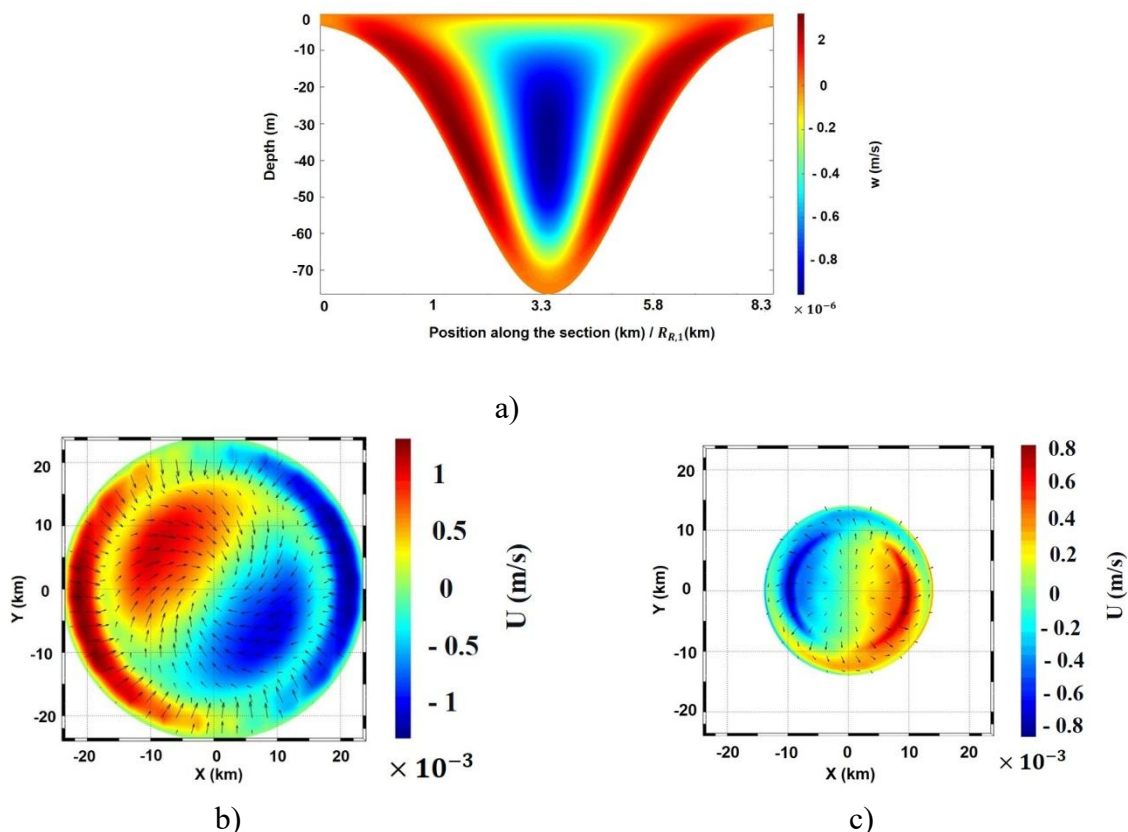


**Figure 1.** a) A vertical velocity field demonstrates upward boundary currents and interior return downwelling (positive values indicate upwelling and negative values indicate downwelling.). As the equilibrium between pressure gradient and Coriolis acceleration, b) the horizontal velocity cross section depicts clockwise rotation near the surface (lake depth=2m), and c) a horizontal velocity cross section illustrating counterclockwise rotation near the bottom (lake depth=40m).

## REFERENCES

- Phillips OM. (1970) On flows induced by diffusion in a stably stratified fluid. *Deep Sea Research and Oceanographic Abstracts*. 17, 3. 435–443.  
 Wunsch Carl. (1970) On oceanic boundary mixing. *Deep Sea Research and Oceanographic Abstracts* 17, 2. 293–301.

# Entrainment and mixing in gravity currents over complex boundaries

C. Adduce<sup>1\*</sup>

<sup>1</sup> Department Civil, Computer Science and Aeronautical Technologies Engineering  
Roma Tre University, Roma, Italy

\*Corresponding author; e-mail [claudia.adduce@uniroma3.it](mailto:claudia.adduce@uniroma3.it)

## KEYWORDS

Gravity Currents; Entrainment; Mixing; Laboratory experiments; Large Eddy Simulations.

Gravity currents, caused by a density difference between two fluids, are density-driven flows developing mainly in the horizontal direction. The density difference can be due to temperature and salinity gradients or sediment concentration. Gravity currents can occur in the oceans and lakes as dense currents and turbidity currents or in the atmosphere as avalanches and sand storms (Hopfinger, 1983; Simpson, 1997; Meiburg and Kneller). In addition, gravity currents can be due to anthropic activities as accidental oil spills in marine areas or pollutant's release in rivers with a significant impact on marine and fluvial ecosystems. These currents develop generally over complex boundaries and the interaction with the topography can deeply affect the dynamics of these flows, the associated mixing and modify the final properties of water masses.

A simple technique employed to produce gravity currents in the laboratory is the lock-release. It consists in filling a tank with two fluids at different density separated by an impermeable sliding gate. When the gate is removed the two fluids interact and produce a dense current which propagates along the bottom of the tank and entrains ambient fluid. Several laboratory experiments and numerical simulations have been performed to study the dynamics of lock release gravity currents flowing over a horizontal boundary (Ooi et al. 2009; Adduce et al., 2012; Ottolenghi et al., 2016; Inghilesi et al. 2018). While most of the previous investigations focused on the study of gravity currents flowing over a horizontal boundary, gravity currents propagating over a complex topography often occur in geophysical and engineering applications. As an example, a barrier could be built to stop turbidity currents occurring in lakes or reservoirs, or at least to weaken it, or divert the current (De Cesare et al. 2001).

In this lecture, the dynamics of gravity currents flowing over complex boundaries are presented. Gravity currents flowing over small and steep slopes, single triangular obstacle and an array of obstacles, are analysed by both laboratory experiments and Large Eddy Simulations. In the laboratory, gravity currents are produced by a lock release and an image analysis technique is applied to measure instantaneous density fields. Relevant dimensionless parameters, as Reynolds and Froude numbers and depth ratios, are varied and their effect on the gravity currents dynamics and the associated entrainment are discussed for each boundary considered. The results show that the dynamics of the current is deeply affected by the presence of a complex boundary, which has an effect on both entrainment and mixing. In addition, the mixing and dilution occurring within the gravity currents become more complex when these flows develop over topographies. Then a detailed evaluation of the density structure within the mixed fluid is of central importance for the evaluation of the entrainment.

## REFERENCES

- Adduce, C., Sciortino, G. and Proietti, S., (2012), Gravity currents produced by lock exchanges: experiments and simulations with a two-layer shallow-water model with entrainment, *J. Hydraul. Eng.*, **138**(2), 111-121.
- De Cesare, G., Schleiss, A. and Hermann, F., (2001), Impact of turbidity currents on reservoir sedimentation, *J. Hydraul. Eng.* **127**, 6–16 .

- Hopfinger, E., (1983), Snow avalanche motion and related phenomena, *Annu. Rev. Fluid Mech.* **15**, 47–76.
- Inghilesi R., Adduce C., Lombardi V., Roman F. and Armenio V., (2018), Axisymmetric three-dimensional gravity currents generated by lock-exchange, *J. Fluid. Mech.*, **851**, 507–544
- Meiburg, E. and Kneller, B., (2010), Turbidity currents and their deposits, *Annu. Rev. Fluid Mech.*, **42**, 135-156.
- Ooi S.K., Constantinescu S.G. and Weber L., (2009), Numerical simulations of lock exchange compositional gravity currents, *J. Fluid. Mech.*, **635**, 361–388
- Ottolenghi, L., Adduce, C., Inghilesi, R., Armenio, V. and Roman, F., (2016), Entrainment and mixing in unsteady gravity currents, *J. Hydraul. Res.*, **54(5)**, 541-557.
- Simpson, J.E., (1997), Gravity Currents: in the Environment and the Laboratory, *Cambridge University Press*.

# A simple model for predicting ice timing and thickness in lakes

M. Fregona<sup>1,2</sup>, M. Leppäranta<sup>2</sup>, I. Mammarella<sup>2</sup> and S. Piccolroaz<sup>1\*</sup>

<sup>1</sup> Department Civil, Environmental and Mechanical Engineering, University of Trento, Trento, Italy

<sup>2</sup> Institute for Atmospheric and Earth System Research, University of Helsinki, Helsinki, Finland

\*Corresponding author; e-mail [s.piccolroaz@unitn.it](mailto:s.piccolroaz@unitn.it)

## KEYWORDS

Winter limnology; modelling; ice cover; water temperature; *air2water*.

## Introduction

In lakes that freeze in winter, the ice cover plays an important role for human activities and lake ecology and can be used as an informative indicator of climate change. Being able to accurately predict ice-on and ice-off dates and ice thickness is therefore a relevant task, which becomes particularly intriguing when simple ice models can be used with relatively good predictive capabilities. Here we present an ice module that complements the existing *air2water* model (Piccolroaz et al., 2013), a hybrid physically-based/statistical model originally developed to predict Lake Surface Water Temperature (LSWT) and epilimnion depth considering air temperature as the only input variable, with the ability to simulate ice cover growth and decay.

## Materials and methods

Consistent with the rationale of the original *air2water* model, the new ice module is developed preserving: i) its simplicity (air temperature being the only forcing variable), ii) its parsimony (from 8 to 10 model's parameters), and iii) the physically based derivation of the equations, one for ice growth, based on Stefan's Law with atmosphere coupling, and the other for ice melting, based on heat exchanges between the layers of the system (Leppäranta, 1993). The extended version of the *air2water* model is tested using long time series of observed LSWT and ice thickness (1960-2021) for 29 Finnish lakes with different climate and lake type conditions. The model's parameters are calibrated using an automatic optimization algorithm and considering a multi-objective performance metric given by the combination between LSWT and ice-thickness Root Mean Square Errors (RMSEs). Two-thirds of the available data set is used for calibration, the remaining one-third is kept for validation.

## Results and discussion

When the model is calibrated equally weighting LSWT and ice thickness RMSEs, the model performance in validation across the 29 lakes is as follows: RMSE for daily LSWT equal to  $1.37 \pm 0.35$  °C and for ice thickness equal to  $10 \pm 3$  cm, the mean error (bias) for ice-on and ice-off dates is  $-9 \pm 7$  and  $-3 \pm 4$  days, respectively (Figure 1). Similar performances are obtained when calibrating the model using only LSWT observations, thus allowing for the application of the model to lakes without ice thickness observations. In this case, the RMSE for LSWT ( $1.17 \pm 0.29$  °C) is lower compared with that obtained for the original *air2water* model without the ice module ( $1.21 \pm 0.29$  °C), meaning that the ice module, besides providing a reliable quantification of the ice thickness and timing, improves the simulation of LSWT.

Overall, the results suggest that the proposed model is competitive compared to more complex lake ice models available in the literature, e.g., *Simstrat* (Goudsmit et al., 2002) and *FLake* (Mironov, 2008), in terms of performance in predicting LSWT, ice thickness, and ice cover timing. This is particularly interesting considering the parsimony of the *air2water* model in terms of input variables (only air temperature) compared to other models. A further extension of the ice module by incorporating various ice types and layers is currently being undertaken.

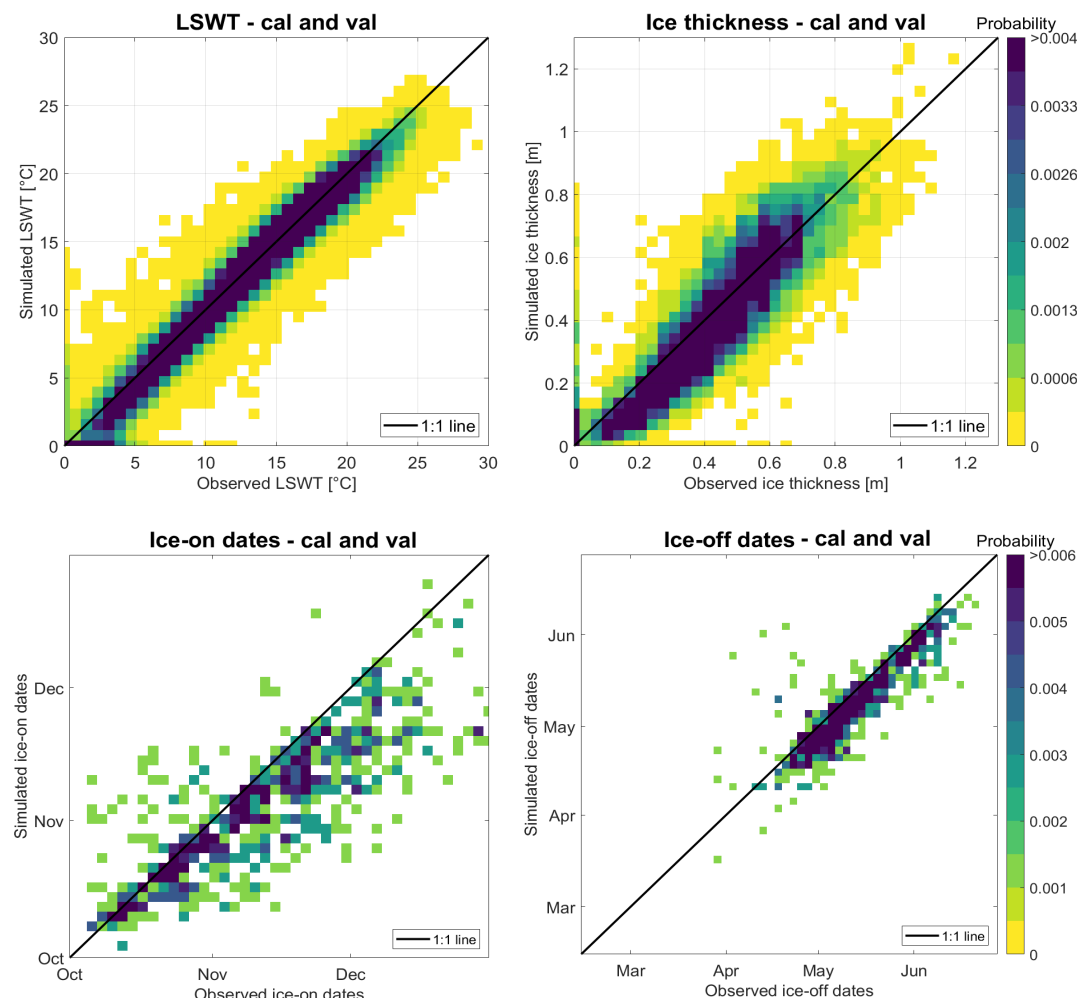


**Figure 1.** Heat map-scatter plots between observed and simulated LSWT and ice thickness values, and ice-on and ice-off dates in calibration and validation periods considering 29 Finnish lakes. The results refer to the performance obtained calibrating the model equally weighting LSWT and ice thickness RMSEs. The colour indicates the probability density (i.e., number of points falling in each cell, divided by the total number of points). The black line is the 1:1 line.

## REFERENCES

- Piccolroaz, S., Toffolon, M., and Majone, B. (2013), A simple lumped model to convert air temperature into surface water temperature in lakes, *Hydrology and Earth System Sciences*, **17**, 3323–3338, <https://doi.org/10.5194/hess-17-3323-2013>.
- Leppäranta, M. (1993), A review of analytical models of sea-ice growth. *Atmosphere-Ocean*, **31**(1), 123–138, <https://doi.org/10.1080/07055900.1993.9649465>.
- Goudsmit, G.-H., Burchard, H., Peeters, F., and Wüest, A. (2002), Application of k- $\epsilon$  turbulence models to enclosed basins: The role of internal seiches, *Journal of geophysical research Oceans*, **107**(C12), 23–1–23–13, <https://doi.org/10.1029/2001JC000954>.
- Mironov, D. (2008), Parameterization of lakes in numerical weather prediction. description of a lake model. *COSMO Technical Report, Deutscher Wetterdienst*, **11**, 41 pp., 2008

# Modeling two-way ice-wave interactions in the Great Lakes using a fully-coupled FVCOM\_ice+wave model

J. Wang<sup>1\*</sup>, D. Cannon<sup>2</sup>, A. Fujisaki-Manome<sup>2,3</sup>, D. Beletsky<sup>2</sup>, S. Constant<sup>1</sup>, S. Ruberg<sup>1</sup>, S. Orendorf<sup>2</sup>

<sup>1</sup>Great Lakes Environmental Research Laboratory, NOAA, Ann Arbor, Michigan, USA

<sup>2</sup>Cooperative Institute for Great Lakes Research, University of Michigan, Ann Arbor, Michigan, USA

<sup>3</sup>Dept. of Climate and Space Sciences and Engineering, University of Michigan, Ann Arbor, Michigan USA

\*Corresponding author; email: [jia.wang@noaa.gov](mailto:jia.wang@noaa.gov)

## KEYWORDS

Great Lakes, wave dynamics, ice-induced wave attenuation, FVCOM–SWAVE–CICE, two-way ice-wave interactions

## Introduction

A two-way fully coupled wave-ice model is being developed with the ability to resolve ice-induced attenuation of waves and ice breaking by waves. Wave and ice interactive dynamics in the Laurentian Great Lakes were simulated using the Finite-Volume Community Ocean Model (FVCOM) framework. Seven simple, flexible, and efficient parameterization schemes originating from the WAVEWATCH III® IC4 were used to quantify the wave energy loss during wave propagation under ice. Ice-induced reductions of wind energy input and wave energy dissipation via whitecapping and breaking were also implemented (i.e., blocking effect). The model showed satisfactory performance in both wave and ice modeling, as validated using buoy-observed significant wave height during the ice-free season and satellite-retrieved ice concentration, respectively. Simulations were run over the basin-scale, and the five-lake computational grid provided spatial distribution of ice-induced wave attenuation in the heavy-ice year 2014. Results suggest that, with the exception of Lake Ontario and central Lake Michigan, lake ice almost completely inhibited waves in the Great Lakes under heavy-ice conditions. A practical application of the model in February 2011 revealed that simulations could accurately reproduce the ice-attenuated waves when validated by wave observations from bottom-moored AWAC. However, the AWAC wave data showed quick responses between waves and ice, while the model with one-way coupling was unable to simulate the quick response of ice melting. We are further developing a module in which wave-induced ice breakage reduces the floe size, thus increasing the lateral ice area and leading to enhanced lateral melting. This module is being applied to the five-lake model to complete the two-way coupling between ice and waves. Further validation using in-situ measurements is being conducted.

## Materials and methods: FVCOM–SWAVE–CICE

We used FVCOM (Chen et al. 2003). FVCOM-SWAVE is a finite-volume unstructured-grid third-generation wave model evolved from the Simulating WAves Nearshore (SWAN), which models the wave generation, propagation, dissipation, refraction, and nonlinear. The FVCOM includes an internally-coupled ice model, which was employed in this study to simulate the lake ice dynamics (Bai et al. 2020). The CICE is an unstructured-grid, finite-volume version of the Los Alamos Community Ice Code that was implemented into the FVCOM framework, and it employs the same governing equations as the CICE and has been widely applied to many cold regions including the Great Lakes.

## Results and discussion

We conducted two simulations. Case 1 is one-way coupling that includes only the dampening of waves by ice cover (Bai et al. 2020). Case 2 includes two-way coupling that also incorporates how waves break big ice floes to small ones, which increases the lateral areas and thus enhances the lateral melting, in addition to original bottom and surface melting.

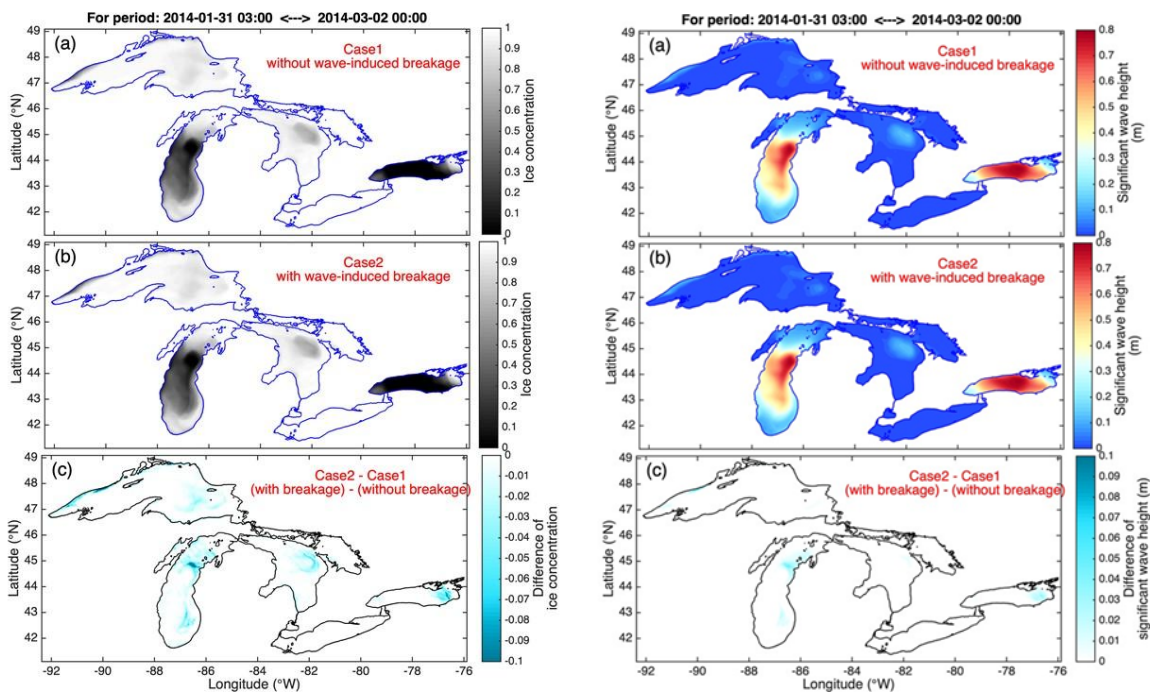


**Figure 1.** Simulated ice concentration (left) and significant wave height (right) in 2014 Ice Season: 2-way vs. 1-way interaction. Averaged ice concentration (left) and significance wave height (right) in the Great Lakes during period 20140131 03:00–20140302 00:00 based on results of Case1 (a) and Case2 (b), and their difference is shown in (c) (Case2–Case1), which indicates where waves break ice cover to small floes.

Figure 1 shows that 1) ice cover dampens the significant wave height, and 2) waves break ice from big floes to small floes mainly in the marginal ice zone (MIZ), where waves loss energy to breaking the ice cover. The wind-wave mechanical breakage is ubiquitous near the MIZ because local wind and remote wind can produce short waves and swells, respectively. The wave breakage of ice cover will be validated using in situ moored data with SWIP and AWAC profilers.

## REFERENCES

- Bai, P., J. Wang, P. Chu, N. Hawley, A. Fujisaki-Manome, J. Kessler, B.M. Lofgren, D. Beletsky, E.J. Anderson, and Y. Li, (2020). Modeling the ice-attenuated waves in the Great Lakes, *Ocean Dynamics*, **70**: 991–1003, <https://doi.org/10.1007/s10236-020-01379-z>
- Bai, X., Wang, J., Schwab, D. J., Yang, Y., Luo, L., Leshkevich, G. A., Liu, S. (2013). Modeling 1993–2008 climatology of seasonal general circulation and thermal structure in the Great Lakes using FVCOM. *Ocean Modelling*, **65**, 40-63.
- Chen, C., Liu, H., Beardsley, R. C. (2003). An unstructured grid, finite-volume, three-dimensional, primitive equations ocean model: application to coastal ocean and estuaries. *Journal of atmospheric and oceanic technology*, **20**(1), 159-186

# Energy considerations to understand the impact of cooling and wind on freeze-up in lakes

M. Toffolon<sup>1\*</sup>, L. Cortese<sup>1,2,3</sup>, and D. Bouffard<sup>2</sup>

<sup>1</sup> Department Civil, Environmental and Mechanical Engineering, University of Trento, Trento, Italy

<sup>2</sup> Department of Surface Waters Research & Management, Swiss Federal Institute of Aquatic Sciences, Kastanienbaum, Switzerland

<sup>3</sup>Boston University, Boston, USA

\*Corresponding author; e-mail [marco.toffolon@unitn.it](mailto:marco.toffolon@unitn.it)

## KEYWORDS

Ice cover; Energy budget; Heat loss; Inverse stratification; Wind mixing.

## Introduction

The freezing time in lakes is controlled primarily by atmospheric cooling, but other factors may play a role, such as wind forcing. In most cases, predicting the ice-on date is achieved by means of complex mechanistic models or by simplified statistical regressions considering integral quantities like negative degree days. By exploiting a minimal model built on sound physical grounds, we focus on the pre-freezing period that goes from mixed conditions (lake temperature at 4°C) to the formation of ice (0°C at the surface) in dimictic lakes.

## Materials and methods

The SELF model is based on a simplified energy balance that considers the cooling of water due to heat loss and the wind-driven mixing of the surface layer (see details in Toffolon et al., 2021). These two factors govern the inverse stratification dynamics by playing opposite roles in determining the time required for ice formation, as qualitatively described in Figure 1. Their interaction contributes to the large interannual variability observed in ice phenology: more intense cooling does indeed accelerate the rate of decrease of lake surface water temperature (LSWT), while stronger wind deepens the surface layer, increasing the heat capacity and thus reducing the rate of decrease of LSWT.

The SELF model was applied to five Swiss lakes (Toffolon et al., 2021), and the results were compared with simulations from the one-dimensional model Simstrat (Gaudard et al., 2019).

## Results and discussion

An example of model's results is shown in Figure 2, where the contrasting effects of wind and cooling appear clearly. The model can also be interpreted through an approximate analytical solution, which elucidate the general tendency of the system and suggests a power law dependence of the pre-freezing duration on the thermal and mechanical energy fluxes.

A single parameter is included in the SELF model, the efficiency of the wind energy transfer to the change of potential energy in the lake, and its calibrated value may be interpreted to understand the mechanical energy balance that controls the development of inverse stratification in lakes. The simplicity of the model, the reduced number of inputs, and its physical grounds, make SELF suitable to be used for the analysis of the effects of changing climatological conditions in long-term scenarios of freeze-up in lakes.

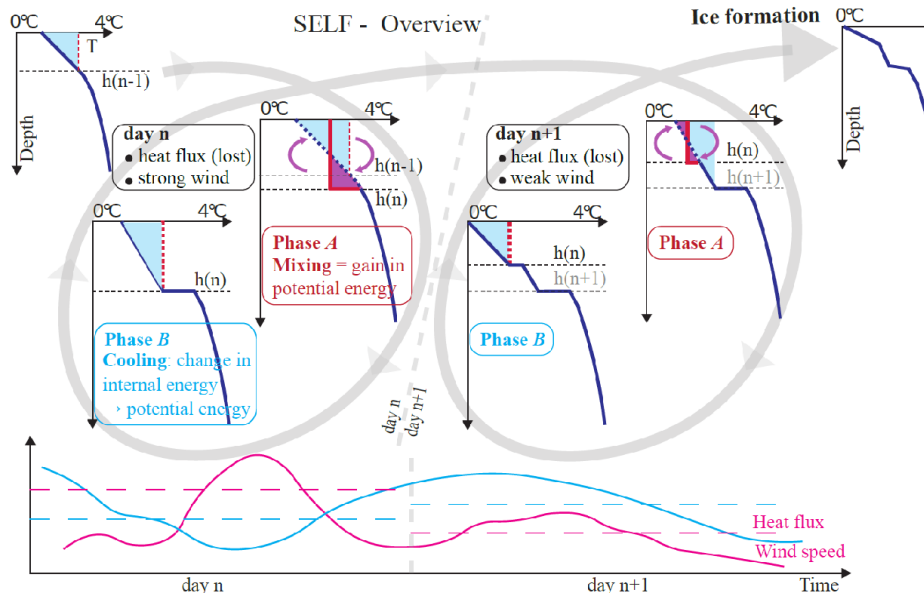


**Figure 1.** Conceptual sketch of the minimal model describing the main processes in the pre-freezing period (after Toffolon et al., 2021). Starting from stratified initial conditions (temperature  $T$  profile on the top left) at day  $n$ , part of the wind energy is used to mix the surface layer (phase A). This step sets the thickness of the surface layer, which stratifies due to the heat loss (phase B). The two phases are repeated for day  $n+1$  until the wind stress becomes low enough (reducing the thickness of the surface layer) and the cooling strong enough that the temperature at the surface may drop below  $0^{\circ}\text{C}$ , thus forming an ice sheet.

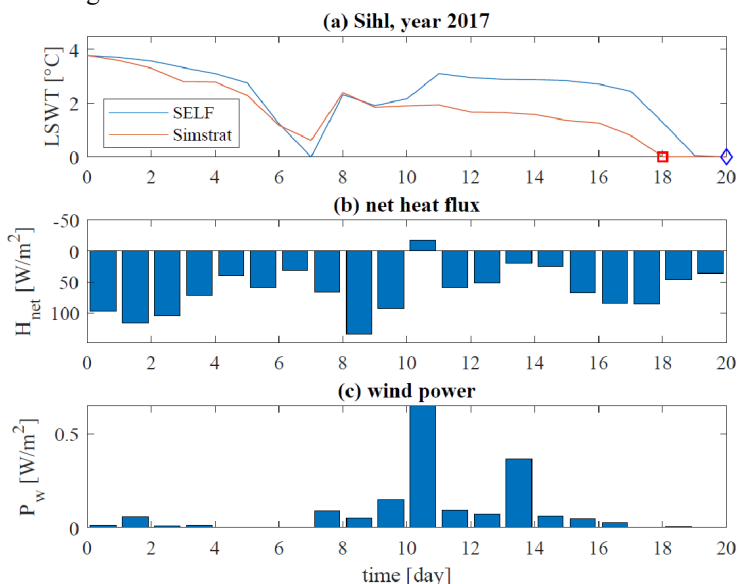


**Figure 2.** Example of the dynamics in the pre-freezing period for winter 2017/18 in Lake Sihl: (a) comparison of the results of Simstrat and SELF with symbols representing the ice-on day, (b) daily averaged net heat flux (positive values for cooling), and (c) daily averaged wind power.

## REFERENCES

- Gaudard, A., Råman Vinnå, L., Bärenbold, F., Schmid, M., and Bouffard, D. (2019), Toward an open access to high-frequency lake modeling and statistics data for scientists and practitioners – the case of Swiss lakes using Simstrat v2.1, *Geosci. Model Dev.*, **12**, 3955–3974, doi:10.5194/gmd-12-3955-2019, 2019.
- Toffolon, M., Cortese, L., and Bouffard, D. (2021), SELF v1.0: a minimal physical model for predicting time of freeze-up in lakes, *Geosci. Model Dev.*, **14**, 7527-7543, doi:10.5194/gmd-14-7527-2021.

# Simulation of short-term effects of pumped-storage hydropower on stratification and ice cover in two Norwegian reservoirs

G. Donini<sup>1,2\*</sup>, A. Adeva Bustos<sup>2</sup>, and M. Toffolon<sup>1</sup>

<sup>1</sup> Department Civil, Environmental and Mechanical Engineering, University of Trento, Trento, Italy

<sup>2</sup> SINTEF Energy Research, 7034 Trondheim, Norway

\*Corresponding author; e-mail [gaia.donini@unitn.it](mailto:gaia.donini@unitn.it)

## KEYWORDS

Pumped-storage; CE-QUAL-W2; Ice cover; Stratification; Short-term effects.

## Introduction

Pumped-storage systems are expected to be used more frequently in the future to provide a balancing system for energy obtained from intermittent renewable sources (e.g., wind, solar). For this purpose, traditional hydropower plants already in operation may be converted into pumped-storage systems, potentially altering the thermal equilibrium of the reservoirs by means of the two-way connection due to pumping operations. Although effects on stratification and ice cover in similar systems have already been observed (e.g., Bermúdez et al., 2018, Kobler et al., 2019), isolating the impact on short time scales deserves further investigation.

## Materials and methods

The expected impacts caused by the implementation of pumped-storage operations are analysed considering a study site located in southern Norway, the Rosskrepp hydropower system (Figure 1), where an upgrade to a pumped-storage system is under discussion. The results of an optimal price-based scheduling model (Alic, 2022) are used to generate the discharges exchanged between the upper (Rosskreppfjorden) and lower (Oyarvatn) reservoir as a function of natural inflows and energy prices, in order to compare the two management configurations (pumped-storage vs conventional hydropower). The hydrodynamic response is simulated using CE-QUAL-W2 (Wells, 2021), a two-dimensional laterally averaged model, which provides temperature and velocities generated by the different operations in the two reservoirs. In order to test the short-term effects of pumping, we analyse the effects of varying the discharges exchanged in various configurations (different magnitude, duration, and timing) while keeping the same net volume exchanged in a single day. The impact of such operations is quantified by comparing the extent of modifications to the thermal stratification and the recovery time by analysing the behaviour in the following days (assuming no further disturbances). Different periods of the year are considered to test the importance of seasonality.

## Results and discussion

Preliminary analyses focused on the winter period show that the greater the amount of water pumped, the more severe are the effects on the two reservoirs compared to conventional hydropower. As expected, the impacts are more noticeable in the area closest to the inlet/outlet (shown in Figure 2). Especially in the lower (and smaller) reservoir, stratification tends to be heavily affected at the end of the day of operation, and the effects persist also after ten days. These effects also depend on the way in which operations are modulated, even if the net amount of water exchanged in a day does not change. Conversely, the upper (and larger) reservoir is less impacted, and the effects disappear completely after ten days. The analysis of short-term operations may allow for understanding how pumping operations can be modulated to improve of the strategy that best tackle the reduction of environmental impacts and ice cover alteration.

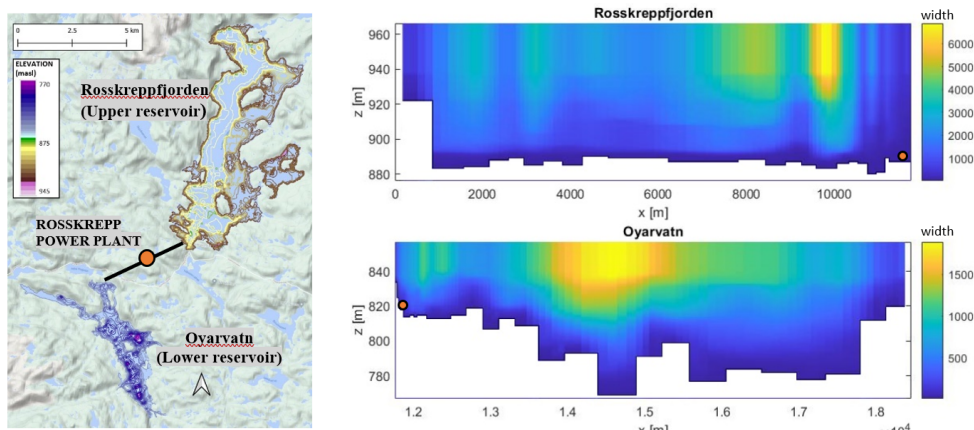


**Figure 1.** Map of the case study (left) and (right) the CE-QUAL-W2 2D bathymetry of the two reservoirs, with the indication of the inlet/outlet structures; the direction of the natural flow is from left to right.

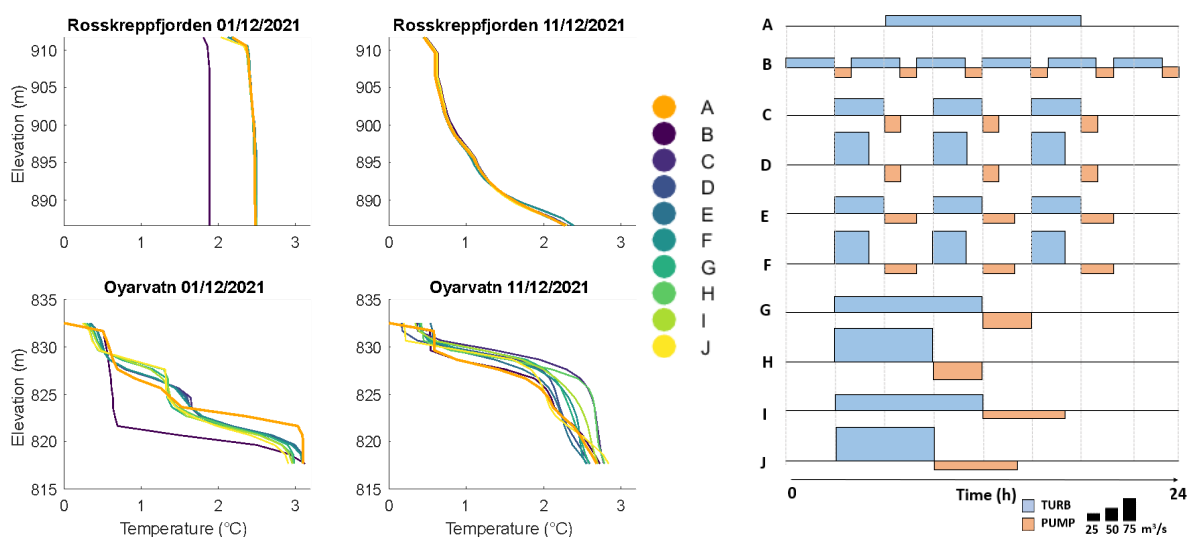


**Figure 2.** Water temperature profiles at the inlet/outlet at the end of single-day operations and after ten days of inactivity (left), considering different scenarios (A-J, right): A refers to conventional hydropower, and B-J simulate different options to modulate the pumping while keeping the same net daily exchange of water volume.

## REFERENCES

- Alic, A., (2022), Optimal price-based scheduling of a pumped-storage hydropower plant considering environmental constraints, Master thesis, University of Trento, Italy.
- Bermúdez, M., Cea, L., Puertas, J., Rodríguez and N., Baztán, J., (2018), Numerical Modeling of the Impact of a Pumped-Storage Hydroelectric Power Plant on the Reservoirs' Thermal Stratification Structure: a Case Study in NW Spain, *Environ Model Assess* **23**, <https://doi.org/10.1007/s10666-017-9557-3>.
- Kobler, U.G., Wüest, A. and Schmid, M., (2019), Combined effects of pumped-storage operation and climate change on thermal structure and water quality, *Climatic Change* **152**, 413–429, <https://doi.org/10.1007/s10584-018-2340-x>.
- Wells, S.A., (2021), *CE-QUAL-W2: A two-dimensional, laterally averaged, hydrodynamic and water quality model, version 4.5. User manual*, State University.

# Unexpected inflow behaviour complicates assessment of heat usage potential for an ice-covered lake

M. Schmid<sup>1\*</sup>, T. Lorimer<sup>1</sup>

<sup>1</sup> Eawag, Swiss Federal Institute of Aquatic Science and Technology, Surface Waters - Research and Management, Kastanienbaum, Switzerland

\*Corresponding author, e-mail [martin.schmid@eawag.ch](mailto:martin.schmid@eawag.ch)

## KEYWORDS

ice-covered lakes, heat usage, numerical modelling, ectogenic meromixis.

## Introduction

Lake St Moritz is a medium-sized Swiss alpine lake (area 0.78 km<sup>2</sup>, max. depth 44 m, 1768 m a.s.l.) that is currently used for heat extraction to heat a few local buildings. The goal is to increase this heat extraction, while avoiding ecologically relevant changes to lake temperature and winter ice cover. Two special properties of the lake complicate the environmental impact assessment of a heat extraction increase: 1) a strongly seasonally varying and short residence time (mean 40 days) driven by the River Inn; and 2) density stratification induced by a small tributary, the Ovel dal Mulin, draining a gypsum-rich catchment (Schmid and Dorji, 2006). We conducted a modelling study to assist the impact assessment, using several winters of continuous temperature monitoring data during heat extraction, and the one-dimensional Simstrat lake model.

## Materials and methods

Measurements of water temperature were provided by the project "Integrated monitoring of ice in selected Swiss lakes" (Tom et al., 2019). Data was collected from 2016 to 2020 with Vemco Minilog-II temperature sensors attached to a mooring installed in the eastern part of the lake. Data regarding the inflow Ovel dal Mulin and its contribution to the density stratification in Lake St. Moritz were available from a previous study (Schmid and Dorji, 2008). Simulations of different scenarios for heat usage were run with the one-dimensional lake model Simstrat (Gaudard et al., 2019). The scenarios simulated included a scenario without heat extraction from the lake, a scenario for the presently installed heat extraction as well as several scenarios for upscaling the present installations. All scenarios were run with and without the inflow of the Ovel dal Mulin.

## Results and discussion

The combined analysis of the observations and the simulation results revealed unexpected features with implications for heat usage, the first two of which are exemplified in Figure 1:

i) the temperature dynamics under the ice could only be explained by an inflow of water to the hypolimnion that exceeds the observed discharge of the "small" tributary by approximately a factor of 40; ii) the main inflow to the lake, the River Inn, flows through the lake at very shallow depths of less than 1 m under the ice in winter, whereas in summer it flushes the top 10 to 15 m of the lake; and iii) the redistribution of water from shallower to deeper layers in the lake by the heat extraction system can potentially have a larger effect on hypolimnion temperatures in summer than in winter, even though the volume flows through the system are much smaller in summer. The simulated impacts of an upscaling of heat usage on under-ice temperatures in the lake significantly depended on the model assumptions regarding the behaviour of the inflow Ovel dal Mulin. As a consequence, it was recommended to proceed with a stepwise upscaling including a monitoring of the resulting impacts. This case study highlights the importance of considering individual lake properties, including major and minor (often unknown) inflows and the seasonal stratification dynamics, when assessing the potential of heat extraction from a lake.

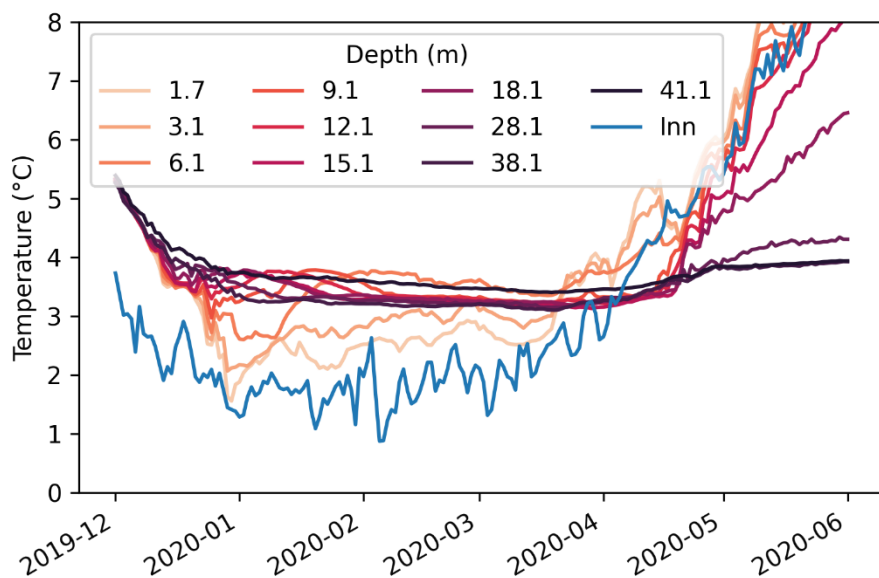


**Figure 1.** Observed temperatures in Lake St. Moritz and its main inflow, the River Inn, from December 2019 to May 2020. Two particular features of the observations are i) a signal of slightly elevated temperature moving upward through the water column from 18 to 6 m depth in January 2020, and ii) the temperature at 1.1 m depth remaining warmer than that of the River Inn throughout the winter, indicating that the River water is flowing through the lake above this depth.

## REFERENCES

- Gaudard, A., Råman Vinnå, L., Bärenbold, F., Schmid, M., Bouffard, D., (2019), Toward an open access to high-frequency lake modeling and statistics data for scientists and practitioners – the case of Swiss lakes using Simstrat v2.1, *Geoscientific Model Development*, **12**, 3955-3974, <https://doi.org/10.5194/gmd-12-3955-2019>
- Schmid, M., Dorji, P., (2006), Permanent lake stratification caused by a small tributary - the unusual case of Lej da San Murezzan. *Journal of Limnology*, **67**, 35-43, <https://dx.doi.org/10.4081/jlimnol.2008.35>
- Tom, M., Suetterlin, M., Bouffard, D., Rothermel, M., Wunderle, S., Baltsavias, E., (2019), Integrated monitoring of ice in selected Swiss lakes. Final project report. ETH Zürich, University of Bern, Eawag, <https://doi.org/10.48550/arXiv.2008.00512>

# Mixing properties of steady gravity currents flowing over sloping terrain

M.R. Maggi<sup>1\*</sup>, M.E. Negretti<sup>2</sup>, E.J. Hopfinger<sup>2</sup> and C. Adduce<sup>3</sup>

<sup>1</sup> Institute of Marine Sciences, National Research Council, Rome, Italy

<sup>2</sup> Univ. Grenoble Alpes, CNRS, Grenoble INP, LEGI, 38000 Grenoble, France

<sup>3</sup> Department of Engineering, Roma Tre University, Via Vito Volterra 62, 00146 Rome, Italy

\*Corresponding author, e-mail [mariarita.maggi@uniroma3.it](mailto:mariarita.maggi@uniroma3.it)

## KEYWORDS

Gravity currents; Laboratory investigations; Entrainment; Turbulence processes; Mixing.

## Introduction

Gravity currents are buoyancy driven flows with the differences being, in general, caused by salinity, temperature or suspended particles (Simpson, 1997). A significant number of river-reservoir systems have large diurnal variations in atmospheric heating rates and develop gravity currents in the downstream river/ reservoir due to colder denser flow releases from an upstream reservoir. Moreover, in lakes, downslope gravity currents contribute to the littoral- pelagic exchange of heat, dissolved compounds and particulate matter.

Gravity currents involve a large variety of different processes, e.g. flow instabilities, boundary layers, vortices and internal waves, which occur in very localized regions. Most of the previous studies dealing with gravity currents considered these flows developing over horizontal or constant slope boundaries (Maggi et al., 2023). However, in nature slope changes are frequent and generally linked with an increase of turbulence intensity and mixing. In this study, we explore, by means laboratory investigation using high-resolution velocity and density measurements, the mean flow, the turbulence characteristics and mixing properties, of constant upstream buoyancy supply gravity currents flowing from a horizontal boundary onto a tangent hyperbolic shaped slope.

## Experimental details and results

The laboratory experiments are performed at the LEGI facilities in 6m long Perspex tank, described in detail elsewhere (Negretti et al., 2017). At the end of the horizontal portion a curved slope with a hyperbolic tangent profile and total length of 87cm is placed. A sketch of the experimental apparatus is shown in Fig.1. The buoyancy driven flow has been generated using saline solutions injected in the left side at the bottom of the channel with constant flow rate  $Q$  through a pump.

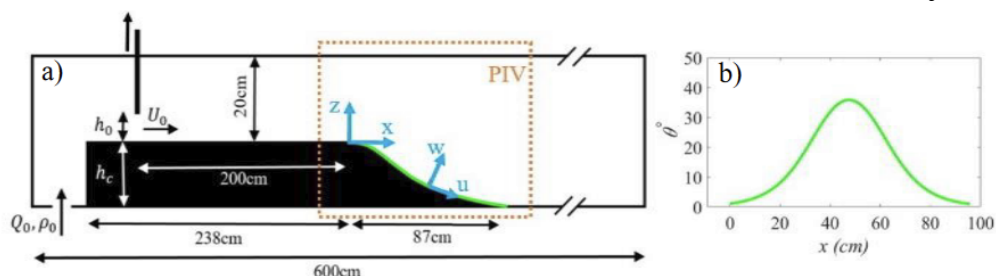


**Figure 1.** a) Schematic side-view of the tank used to perform laboratory experiments. b) Slope angle evolution along the x direction

A total of 12 experiments were performed. The volumetric inflow rate  $Q$  (per unit width) at the top of the slope and the reduced gravity  $g'$  of the inflow are the two parameters varied. Each experiment was recorded with an acquisition frequency of 23.23Hz. For temporal average, 2000 frames have been taken into account, considering only the steady flow regime, i.e., after the current head has passed.

In this study we focus our analysis on the steepest portion of the slope where  $\theta = 31^\circ$  using a 20cm window for space averages. Our choice was dictated by the observed dynamic complexity, indeed in this portion of the slope the current accelerates until Kelvin–Helmholtz instabilities develop, which causes the slowdown of the dense flow followed by a nearby maximum constant velocity. On the other hand, downstream the slope, on the horizontal boundary, the maximum velocity remains nearly unchanged because both the gravitational force and entrainment are drastically reduced.

Fig.2 shows time-averaged along-slope velocity  $\langle u \rangle$  (a), slope normal velocity  $\langle w \rangle$  (b) and scaled Reynolds shear stresses (c) for the experiments  $Q2g5$ ,  $Q2g15$ , and  $Q3g15$ , that are representative of all the experiments conducted. All the experiments show velocity profiles

$\langle u \rangle$  similar to those of a plane turbulent wall jet (fig.2a). The height where maximum velocity occurs,  $\langle u_m \rangle$ , appears conditioned by interfacial drag and moves closer to the bottom. Fig.2b shows the time-averaged vertical velocity  $\langle w \rangle$  and even in this case all the experiments show a similar trend with  $\langle w \rangle$  that tends to zero from the slope bottom up to the shear layer and is negative in the outer part of the current and in the ambient fluid. The large negative values of  $\langle w \rangle$  in the shear zone indicate large entrainment. Key quantities for describing turbulence processes are the Reynolds stresses expressing turbulent transport of momentum. Fig.2c shows scaled Reynolds shear stress profiles. In the steepest portion of the slope there are the highest values of the shear stresses observed along the stream-wise direction due to the acceleration phase and rapid onset of the shear instabilities which spread over the full current depth. In  $Q2g15$  and  $Q3g15$  where  $g'$  is larger, higher acceleration due to the larger gravitational force, gives rise to a wider region of nearly constant shear.

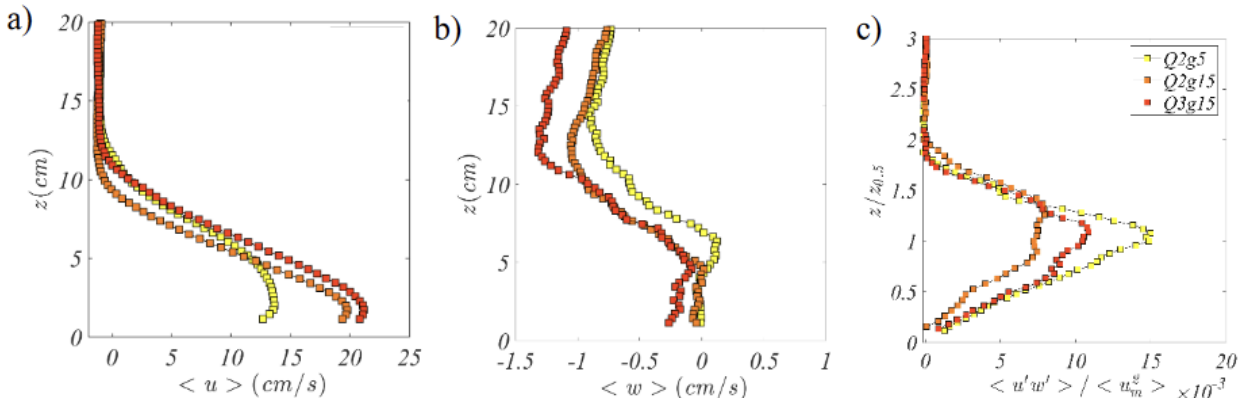


**Figure 2.** Time-averaged streamwise velocity profiles  $\langle u \rangle$  (a), vertical velocity  $\langle w \rangle$  (b) and profiles of scaled Reynolds shear stresses (c) for experiments Q2g5, Q2g15, and Q3g15.

## REFERENCES

- Simpson, J.E. (1997). Gravity Currents: In the Environment and the Laboratory, Cambridge University Press.
- Maggi, M., Adduce, C., and Lane-Serff, G. (2023). Gravity currents interacting with slopes and overhangs, *Adv. Water Resour.* **171**, 104339.
- Negretti, N., Flor, J. and Hopfinger, E. (2017). Development of gravity currents on rapidly changing slopes,” *J. Fluid Mech.* **833**, 70–97.

# Science communication and teaching in secondary schools through limnology

M. Pilotti<sup>1\*</sup> and G. Valerio<sup>1</sup>

<sup>1</sup> Department of Civil, Environmental, Architectural Engineering and Mathematics, Università degli Studi di Brescia, Italy

\*Corresponding author, e-mail [marco.pilotti@unibs.it](mailto:marco.pilotti@unibs.it)

## KEYWORDS

Lakes; physical models; mass and energy balance; stratification; secondary schools.

## Introduction

According to recent statistics, in Italy, there is a deficiency in graduated people in scientific matters and the Ministry of Education is making an effort to increase this type of competence at the secondary school level. Whereas the standard (and ex-post counterproductive) approach to this problem is that of increasing the burden of the scientific curricula during the last three years of Licei Scientifici (corresponding to the 11th, 12th and 13th year of High School), we believe that a more effective way is that of communicating the interest of science and research, by showing its application to some real problem of the local community.

We believe that for communities living around a lake, devising a set of seminars on limnology is an excellent way to get this goal. A large lake is a complex ecosystem in which fluid dynamic, hydrological, ecological and chemical aspects are closely interconnected. In addition, the lake, as an integrator of flows from the upstream watershed, is a natural gauge of environmental sustainability. Moreover, typically lakes become focal points that define the character and identity of the surrounding area. Accordingly, limnology is a comprehensive matter that covers many scientific subjects and is a good way to show the practical relevance of several topics studied in the classrooms under the assumption that the relevance of the problem could be the driver to trigger interest in a University curriculum in the scientific area.

In doing this, it is very important not to duplicate the often ineffective style of some curricular courses: we believe that involvement is more important than completeness and exactness and the seminars must be based on hands-on experiments, alternating some sessions with data manipulation through spreadsheets and simple programming. As a collateral fallout of this teaching effort, increasing scientific competence and awareness of people on lakes will also foster an appreciation for the relevance of research and can trigger cooperation through, e.g., citizen science in the community. Here we present our past experience in this field.

## Implementation

During the 2015-2016 and 2017-2018 school years we undertook an experimental activity to disseminate scientific aspects related to deep lakes in the province of Brescia. The activities involved 4 classes attending the fourth year of Liceo Scientifico in the area of Lake Iseo and Brescia. We prepared a set of 8 seminars + 1 field monitoring campaign briefly described in the following table. Each seminar presents a topic that is then explored by the class.

## Some results

The activities took place over a 6-month period, with a series of seminars at 20-day intervals one from the next. Interspersed with these seminars was a research task assigned to the students, who carried it out by dividing into working groups. Some examples of topics are presented at the web page <https://aslantonietti1718.altervista.org/chi-siamo/> created by the students as a specific assignment. We eventually asked students to prepare a final report and to set up a presentation, involving the acquired skills.

	<i>Title of seminar</i>	<i>Leading Idea</i>	<i>Methods</i>	<i>Curricular competence</i>
1	Why should we care about water and lakes ?	Importance of water resources and of lakes	Quantification of personal domestic consumption of drinking water	Natural sciences, statistics
2	How long does it take to empty a sink ?	Physical laws have a predictive power	Experiments of mass conservation with a simple tank. Use of a spreadsheet.	Physics, math
3	How long does water stay in a lake ?	Simple models must be refined to get the right answer...	Experiment of pollutant dilution with time in a Completely Stirred Tank Reactor	Physics, math
4	The role of density in lake dynamics	When thermal stratification is at play, the model must be further refined...	Simplified physical model of a stratified lake, with visualization of overflow, intrusion and plunging (see Figure 1). Generation of internal waves by wind	Physics, math
5	Introduction to scientific programming	Sometimes a spreadsheet is not the easiest way to deal with the problem...	Introduction to the implementation of simple algorithms with a free PASCAL compiler	Algorithmic thinking, math, computer science
6	Why lake Endine freezes in winter and Lake Iseo does not ?	The implications of the energetic balance of a lake	Hands on working on the data measured by our floating station in Lake Iseo. Computation of energy balance with a spreadsheet and with a simple code	Physics, math, computer science
7	The role of earth rotation on the dynamics of a large lake	Sometimes earth rotation has a role to play...	Visit to the laboratory of the University. Physical experiment exploring the role of Coriolis'force on the lake inflow Physical experiments on Taylor's columns	A glance on the world of University and of research
8	Some chemical and ecological dynamics of a lake	Physics, chemistry and ecology are deeply interconnected in a lake	The chemistry of photosynthesis The prey-predator model A simple code to solve the the Lotka Volterra system of equations	Chemistry, ecology Physics , math, computer science
9	Field trip and measurement campaign on lake Iseo	Is it only theory ?	Lake trip to the LDS. Use of an oceanographic probe, of a Van Dorne bottle and of Secchi disk. Evaluation of P and N concentration in deep and epilimnetic waters	Experimental skills in the field, group working.

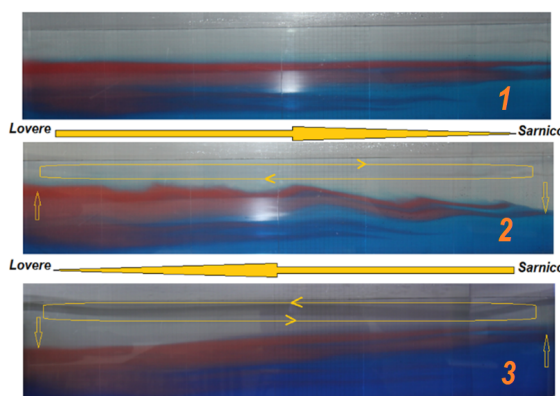


**Figure 1.** A simple class experiment for the qualitative reproduction of thermocline tilting in Lake Iseo under the effect of alternating northward and southward daily winds aligned with the lake axis, triggering an H1 mode.

# Weakening of inverse stratification in northern lakes

J. Jansen<sup>1\*</sup>, R. I. Woolway<sup>2</sup>, Z. Tan<sup>3</sup>

<sup>1</sup> Department of Ecology and Genetics – Limnology, Uppsala University, Uppsala, Sweden

<sup>2</sup> School of Ocean Sciences, Bangor University, Bangor, UK

<sup>3</sup> Pacific Northwest National Laboratory, Richland, Washington, US

\*Corresponding author, e-mail [joachim.jansen@ebc.uu.se](mailto:joachim.jansen@ebc.uu.se)

## KEYWORDS

Lakes, inverse stratification; ice; climate change.

## Introduction

Inverse stratification is a defining feature of northern lakes in winter. This thermal state is broadly defined by a 0-4 °C vertical temperature profile, and enables the development of chemical gradients and ecological niches that shape winter food webs. Importantly, the strength of the density gradient modulates the extent and velocity of density-driven currents under ice, including downslope flows and radiatively driven convection. Recent studies have shown that the duration of the inverse stratification period is rapidly declining as a result of warmer winters (Woolway et al., 2021). This pattern may be part of a broader shift in lacustrine winter heat budgets, effectuated by changes in radiative transfer through thinning ice, earlier snowmelt and a rise in rain-on-snow events. Increased sediment heat storage (summer) and release (winter) may also affect winter water temperatures. In this work, we compiled the largest synthesis dataset of under-ice temperature profile measurements to date (11868 lakes, 1960-2022) in order to identify and explain climate-driven trends in winter thermal structure.

## Materials and methods

A synthesis dataset of water temperature, ice thickness, snow depth and specific conductance of seasonally frozen lakes was constructed from governmental and institutional data repositories in Scandinavia and North America. For each lake we also obtained morphometric information. We computed water density from temperature, depth and salinity (Chen & Millero, 1977), and estimated vertical density gradients between the top 1 m below the ice, and the bottom  $0.7 \cdot z_{\max}$ . Long-term trends were assessed with the Theil-Sen estimator in a subset of 668 lakes with  $\geq 15$  years of winter temperature profiles available.

We combined stochastic and process-based approaches to understand spatiotemporal patterns in the data. We identified key drivers of the under-ice density gradient and its trend via random forest analysis, and applied hierarchical GAMs (Pedersen et al., 2019) to visualize dependencies on individual predictor variables, such as latitude or time of year, and assess the role of drivers with known spatiotemporal gradients. We further estimated seasonal under-ice warming rates for different snow depths to test the hypothesis that thinner snow cover allows for faster warming. Finally, to evaluate our understanding of processes behind observed trends and enable prediction of future trajectories we fitted the Arctic Lake Biogeochemistry Model (Tan et al., 2015) to observations from a subset of lakes with long-term records.

We find that the vertical density gradient has weakened significantly in the last 60 years and that this is caused primarily by warming of surface waters below the ice (Figure 1).

## Results and discussion

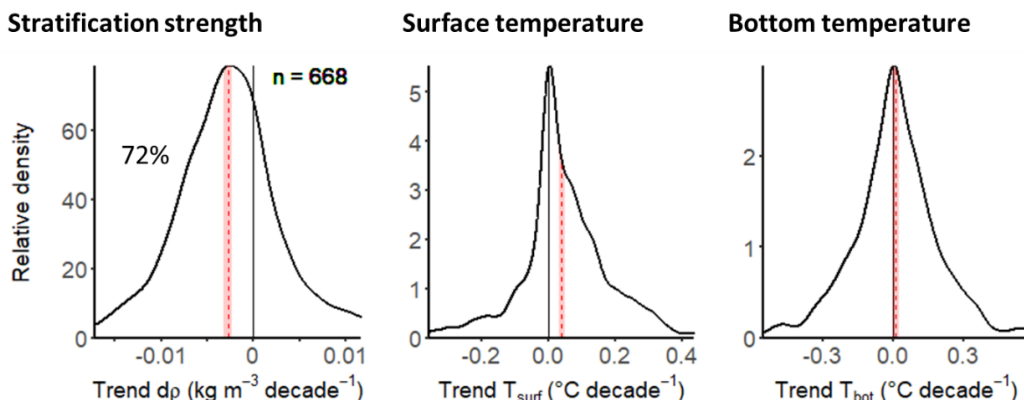


**Figure 1.** Probability density curves of long-term ( $\geq 15$  year) trends in the under-ice water density gradient, surface- and bottom temperatures. 72% of lakes in the dataset has experienced a weakening inverse stratification.

Random forest analysis reveals that the positive under-ice surface temperature trend is primarily associated with negative trends in ice thickness and snow depth (ERA5 single-level reanalysis product). Conversely, the HGAM shows that the strongest long-term warming trend occurs near the end of the ice-cover season, suggesting that storage and release of summer heat in lake sediments, which would be most intense at winter's start, plays a minor role.

Snow affects the transfer of shortwave radiation via albedo and scatter, which are in turn governed by snow depth, coverage, age and water content (Leppäranta, 2015). We find that thinner snow is associated with stronger seasonal heating, and that snow depths  $> 0.2$  m effectively prevent warming of water under ice (Figure 2, left). Thicker ice is associated with stronger warming (Figure 2, right), likely because ice thickness peaks toward the end of the season when insolation rapidly increases. Our analysis suggests that ubiquitous weakening under-ice stratification is primarily associated with changes in snow cover phenology.

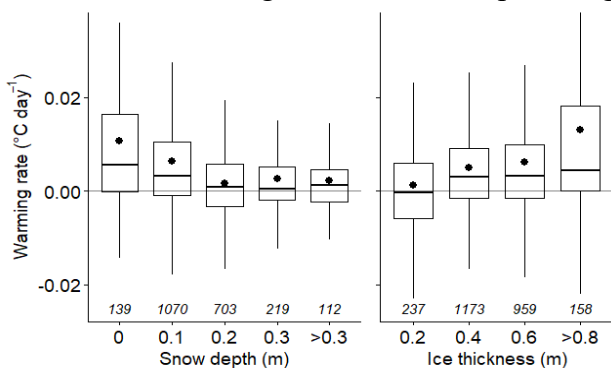


**Figure 2.** Under-ice warming (or cooling) rates of the layer 1m below the ice-water interface, binned by snow depth (left) and ice thickness (right). Daily rates are Theil-Sen estimators for each lake-year with  $\geq 3$  observations, and *italic labels* denote the number of lake-years. Category labels represent upper bounds of the bins.

## REFERENCES

- Chen, C.T. and Millero, F. (1977). The use and misuse of pure water PVT properties for lake waters. *Nature* **266**, 707–708. doi:10.1038/266707a0
- Leppäranta, M. (2015). Freezing of Lakes and the Evolution of their Ice Cover, Springer-Verlag, Berlin, Germany
- Pedersen E.J., Miller D.L., Simpson G.L. and Ross N. (2019). Hierarchical generalized additive models in ecology: an introduction with mgcv. *PeerJ* **7**:e6876. doi:10.7717/peerj.6876
- Tan, Z., Zhuang, Q., and W. Anthony, K. (2015), Modeling methane emissions from arctic lakes: Model development and site-level study, *J. Adv. Model. Earth Syst.*, **7**, 459– 483, doi:10.1002/2014MS000344.
- Woolway, R.I., Denfeld, B., Tan, Z., Jansen, J., Weyhenmeyer, G.A. and La Fuente, S. (2021). Winter inverse lake stratification under historic and future climate change. *Limnol. Oceanogr. Lett.* doi:10.1002/lo2.10231

# Role of aquatic vegetation and meteorological forcing on the hydrodynamics of Mantua Lakes: insights from a bathymetric survey and hydraulic modelling

M. De Vincenzi<sup>1\*</sup>, M. Amadori<sup>2</sup>, L. Adami<sup>1</sup>, M. Tubino<sup>1</sup>

<sup>1</sup>Department of Civil, Environmental and Mechanical Engineering, University of Trento, Italy

<sup>2</sup>Institute for Electromagnetic Sensing of the Environment, National Research Council, Milan, Italy

\*Corresponding author; e-mail [matteo.devincenzi@unitn.it](mailto:matteo.devincenzi@unitn.it)

## KEYWORDS

Shallow fluvial lakes; aquatic vegetation; eutrophication; numerical modelling; water management.

## Introduction

Shallow fluvial lakes are dynamic ecosystems where water circulation is governed by wind and through-flowing discharge. In these lakes the aquatic vegetation both shapes and is shaped by water circulation, as a strong interaction exists between biological and physical processes. Hence, the understanding of lakes hydrodynamics is essential to plan effective safeguard and remediation measures in such environments. An interesting case study for this topic is the Mantua Lake system, where all the above-cited features are present.

In this contribution we present the preliminary results of a modelling study on lake hydrodynamics and vegetation management in the Superior Lake of Mantua.

## Materials and methods

Mantua Lakes are a shallow fluvial lake system located in Northern Italy which was created in the 12<sup>th</sup> century by the damming of the Mincio River. The river drains a watershed that is intensively exploited by agriculture. This resulted in a high nutrient input load that since the 1970s has caused the lakes' eutrophication, eventually worsened by summer low discharges due to water diversion for irrigation purposes. In addition, macrophytes of the species *Nelumbo nucifera* (lotus flower) were introduced in 1921 as a food source and now represent a problem for their high invasiveness which requires massive cutting efforts. Until now, restoration strategies have been missing due to the deficit of hydrodynamic studies. The first (and unique) modelling study by Fenocchi (2015) emphasized the lack of information about the lake's topography and the absence of field data for validation.

Hence, we started our investigation from a bathymetric survey of the Superior Lake of Mantua (Fig. 1a, area 4 km<sup>2</sup>, mean depth 3.3 m). We produced a detailed bathymetric map consisting of 200 lake transects, 25 m spaced by testing a “DeeperSonar CHIRP+” sonar, a low-cost instrument conceived for fishing that was proved to be also suitable for scientific purposes. The lake showed a bifurcated morphology, with a main channel of 6.5 m maximum depth in the northern part and a less deep one located further south (Fig. 1b).

Based on the acquired bathymetry, we set up a three-dimensional hydrodynamic model (Delft3D FLOW, Lesser et al., 2004) with horizontal resolution 25 m, vertical resolution 0.2 m, where the presence of aquatic macrophytes was simulated through the “(Rigid) 3D vegetation model” implemented in Delft3D. The model was calibrated with in-situ temperature profiles acquired with a multiparameter probe and water velocity data measured with an ADCP along lake transects. We simulated different scenarios to assess the impact of variables such as discharge, wind, and vegetation on lake hydrodynamics.

## Results and future developments

Preliminary results obtained by numerical simulations showed the establishment of an area with speeds of the order of a few millimeters per second inside the main patch of emergent vegetation, which can potentially lead to sediment deposition and oxygen depletion as confirmed by available D.O. profiles (Telò et al., 2007). Simulations proved that the removal of vegetation can reduce water stagnation, enhancing velocity up to 1.5 cm/s (Fig. 1c).

Further investigations are planned to better understand the interactions between aquatic vegetation and hydro-thermodynamic processes in this lake. In particular, numerical experiments with particle tracking and field campaigns will be conducted to study water residence time and the small-scale hydrodynamics triggered by temperature gradients inside and outside the vegetation patches. From a more operational perspective, the developed model will be adopted in support of local management strategies. In this regard, collaboration with the lake's management agency has already started for e.g. evaluating the effects of water diversion from agricultural canals to the lake, as well as defining optimal vegetation shaping for limiting water stagnation.

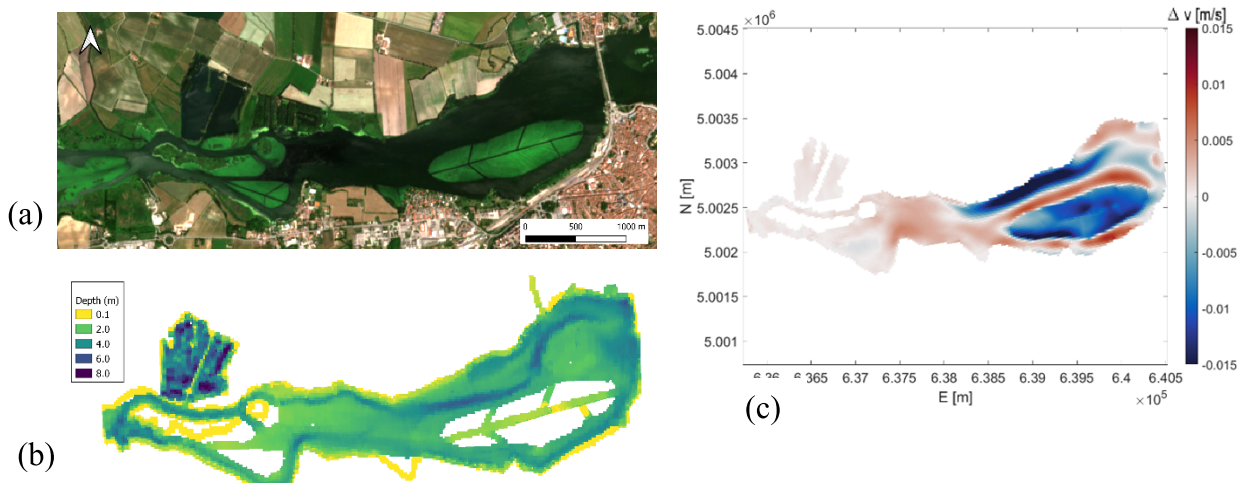


**Figure 1.** (a) Satellite image of the Superior Lake of Mantua; (b) Bathymetric map acquired during the field campaign in 2022; (c) Effect of the main lotus flower patch on the surface water speed.

## REFERENCES

- Fenocchi, A. (2015), Circulation dynamics in a shallow fluvial lake. The case of the Superior Lake of Mantua. Ph.D. Thesis.
- Lesser, G.R., Roelvink, J.A., Van Kester, J.A.T.M., Stelling, G.S. (2004), Development and validation of a three-dimensional morphological model. *Coast. Eng.*, **51**, 883-915, doi:10.1016/j.coastaleng.2004.07.014.
- Telò, R., Pinardi, M., Bartoli, M., Bodini, A., Viaroli, P., Racchetti, E., Cuiuzzi, D., Vannuccini, M., Previdi, L. (2007), Caratterizzazione dello stato ambientale del fiume Mincio e analisi della strategia di riqualificazione integrata e partecipata. Final report.

# Inter-basin exchange in a multi-basin polymictic lake

A. Cortés<sup>1,2\*</sup>, S.A. Valbuena<sup>1,2</sup>, A.L. Forrest<sup>1,2</sup>, and S.G. Schladow<sup>1,2</sup>

<sup>1</sup> Department of Civil and Environmental Engineering, University of California Davis, California, USA

<sup>2</sup> Tahoe Environmental Research Center, University of California Davis, California, USA

\*Corresponding author; e-mail [alicortes@ucdavis.edu](mailto:alicortes@ucdavis.edu)

## KEYWORDS

Inter-basin exchange; Multi-basin lake; polymictic; baroclinic pumping; hypereutrophic.

## Introduction

Understanding the transport and horizontal water exchanges occurring in lakes is essential to predict biogeochemical changes in them. Most of our knowledge of lake hydrodynamics and mixing comes from lakes with simple bathymetries (Umlauf & Lemmin, 2005). However, many lakes around the world show more complicated morphometry, such as Fjord-type lakes or multi-basin lakes (Lawrence et al., 1997; Rueda et al., 2005). In multi-basin lakes, the hydrodynamic connection between basins is limited by one or several physical constraints. Thus, each basin could be subjected to different hydraulic and meteorological forcing, which further challenges our understanding of how connected a given basin is to the rest of the lake and how this connection varies across daily to seasonal scales. Most of the literature has focused on inter-basin exchanges due to wind-driven oscillations of the thermocline (i.e., baroclinic oscillations, Imam et al., 2019). Ekman transport (the interaction of wind, Coriolis and drag forces) has also been proven to be a key process leading to inter-basin exchange in large lakes (Jabbari et al., 2021). The main aim of our study is to gain a better understanding of the role of complex bathymetry on the transport and horizontal water exchange in multi-basin lakes across daily to seasonal scales. We combine field observations and numerical 3D model results to provide an understanding of the physical relationship between the basins of our study lake.

## Materials and methods

Clear Lake, in the coastal range of California, is a moderate-sized ( $176 \text{ km}^2$ ) multi-basin natural lake located at an elevation of  $404 \text{ m}$ . a.s.l. ( $39^\circ 00' \text{ N}$ ,  $122^\circ 45' \text{ W}$ ). The lake is warm, shallow (mean depth  $\approx 8 \text{ m}$ , maximum depth  $\approx 15 \text{ m}$ ), and each basin mixes multiple times annually (polymictic). The lake is divided into three distinct basins or arms: the Upper Arm, the Lower Arm, and the Oaks Arm (Rueda & Schladow, 2003). Upper Arm is the largest and shallowest basin, while Lower and Oaks Arms are smaller and deeper basins. The basins are all interconnected by a passage referred to as the Narrows. The overall lake residence time is 4.5 years, and advective flow through the lake is not considered to be a major factor in water movement. Clear Lake is hypereutrophic, contaminated with mercury, prone to intensive harmful algal blooms, and subject to episodic hypoxia. The lake has been the site of intensive limnological monitoring for the last 5 years, coupled with the development of a three-dimensional (3D), time-varying hydrodynamic and water quality model. The 3D numerical model Si3D has been extensively used in lakes and reservoirs to study underlying physical and biological interactions (Rueda & Schladow, 2003; Valbuena et al., 2022). The model can represent important physical processes including diel and seasonal stratification, mixing, internal waves, and Coriolis forcing; it is computationally efficient both because of its solver and parallel architecture; it is available in the public domain.

## Results and discussion

The model results show that large-scale circulation in each basin of the lake is controlled by the interactions between the diurnal winds, weak stratification, and rotational effects (i.e., baroclinic

pumping), and the complex topography at the confluence of the three basins. The two basins that are aligned with the predominant northwesterly winds display baroclinic pumping, which comprises a cycle of (1) a setup phase when winds are strong (afternoon and evening) generating horizontal density gradients across the longitudinal axis of the lake basins aligned with the wind direction; and (2) a relaxation phase when winds die down (night and morning) and the baroclinic pressure gradients become the dominant forcing mechanism in the system, driving currents greater than  $20 \text{ cm s}^{-1}$  towards the east at the surface and the west near the bottom. Rotational effects create a residual cyclonic circulation in each basin and the formation of strong alongshore currents which are likely to enhance mixing.

We evaluated the effect of the topographic scale on transport and inter-basin exchange by artificially varying the basin length scale between  $5 \text{ km}$  and  $25 \text{ km}$  (real length) in our simulations. When the lake fetch is  $5 \text{ km}$  or lower the lake tends to remain more quiescent, warmer, and with a shallower thermocline. Small differences are observed when the lake fetch ranges between  $10 \text{ km}$  and  $25 \text{ km}$ . We also used model results to quantify how connected is each basin to the rest of the lake by isolating and modeling individual basins. Results show that the general stratification patterns are similar in the whole lake and individual basin runs. Nonetheless, the average temperature, stability, and thermocline depth and its deepening decrease when simulating individual basins (Fig 1). This suggests a significant connectivity between basins, that enhances mixing.

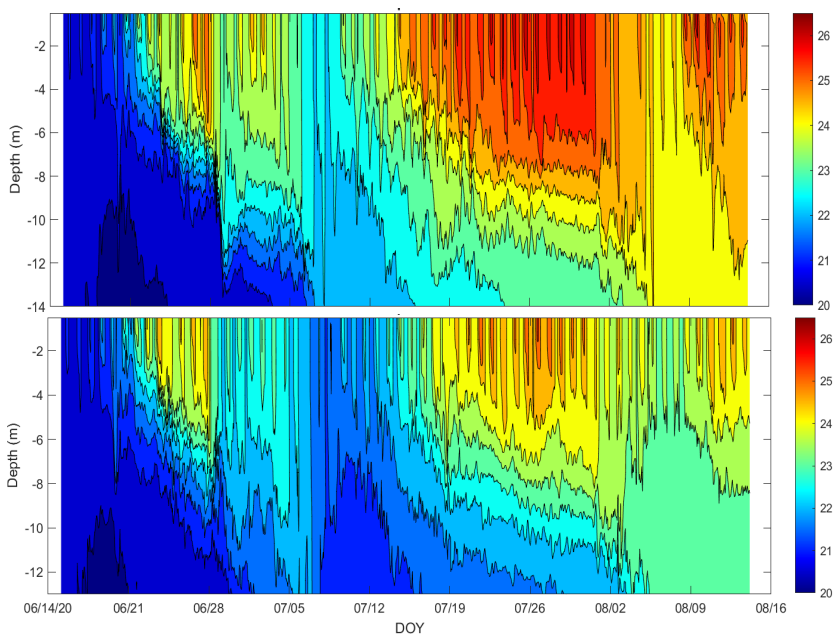


**Figure 1.** Model lake temperature time series in the Lower Arm basin during summer (June-August) 2020, using the bathymetry of the whole lake (top) and the individual basin (bottom)

## REFERENCES

- Umlauf, L. & Lemmin, U., (2005), Interbasin exchange and mixing in the hypolimnion of a large lake: The role of long internal waves. *Limnol. Oceanogr.* **50**, 1601–1611, <https://doi.org/10.4319/lo.2005.50.5.1601>
- Lawrence, G. A., Burke, J. M., Murphy, T. P. and Prepas, E. E., (1997), Exchange of water and oxygen between the two basins of Amisk Lake. *Can. J. Fish. Aquat. Sci.* **54**, 2121–2132, <https://doi.org/10.1139/f97-235>
- Rueda, F. J., Schladow, S. G., Monismith, S. G. and Stacey, M. T., (2005), On the effects of topography on wind and the generation of currents in a large multi-basin lake. *Hydrobiologia* **532**, 139–151, <https://doi.org/10.1007/s10750-004-9522>
- Imam, Y. E., Laval, B., Pieters, R. and Lawrence, G., (2019), The baroclinic response to wind in a multiarm multi-basin reservoir. *Limnol. Oceanogr.*, 11328, <https://doi.org/10.1002/lno.11328>
- Jabbari, A., Ackerman, J.D., Boegman, L. et al., (2021), Increases in Great Lake winds and extreme events facilitate inter-basin coupling and reduce water quality in Lake Erie. *Sci Rep* **11**, 5733, <https://doi.org/10.1038/s41598-021-84961-9>
- Rueda, F. J. & Schladow, S. G., (2003), Dynamics of a large polymictic lake. II: Numerical simulations. *J. Hydraul. Eng.* **129**, 92–101, [https://doi.org/10.1061/\(ASCE\)0733-9429\(2003\)129:2\(92\)](https://doi.org/10.1061/(ASCE)0733-9429(2003)129:2(92))
- Valbuena, S. A., Bombardelli, F. A., Cortés, A., Largier, J. L., Roberts, D. C., Forrest, A. L., and Schladow, S.G., (2022), 3D flow structures during upwelling events in lakes of moderate size. *Water Resources Research*, **58**. <https://doi.org/10.1029/2021WR030666>

# Under-ice cyclonic gyre formation in a narrow, elongated lake

K. Hughes<sup>1,2</sup>, A.L. Forrest<sup>1,2\*</sup>, A. Cortés<sup>1,2</sup>, H.J. Oldroyd<sup>1,2</sup>, F. Bombardelli<sup>1,2</sup>

<sup>1</sup> Department of Civil and Environmental Engineering, University of California Davis, California, USA

<sup>2</sup> Tahoe Environmental Research Center, University of California Davis, California, USA

\*Corresponding author; e-mail [aforrest@ucdavis.edu](mailto:aforrest@ucdavis.edu)

## KEYWORDS

Rotational forcing; cyclonic gyres; ice-cover; Coriolis; dimictic turnover

## Introduction

Limnologists typically ignore Coriolis as a forcing mechanism for lakes with length scales smaller than the internal Rossby radius of deformation ( $L_{ri}$ ). Depending on latitude,  $L_{ri}$  can vary from 2-5 km under normal summer stratification conditions; however, when lakes cool below the temperature of maximum density during ice-covered conditions, density differences can decrease significantly, and  $L_{ri}$  will typically range from 400-800 m. In lakes where both the length and width exceed this value, the formation of basin-scale gyres has been observed (Forrest et al., 2013, Kouraev et al. 2019). We hypothesized that gyres could potentially form on smaller ice-covered lakes and could potentially drive mixing under-ice.

## Materials and methods

To test this hypothesis, we selected Lake Massawippi, QC, Canada (14 km long x 1.6 km max. width) as a study site (45.25° N, 71° W). This lake is ice-covered for 3-4 months of the year with up to 50 cm of ice. We measured continuous water temperature and specific conductance time-series at multiple depths in the water column at two locations in the northern end of the lake (~750 m width) during almost a full year in 2019 (Fig. 1). The deeper thermistor chain (M1) was in ~45 m water depth and was positioned on the western side of the observation transect. The shallower thermistor (M2) chain was in ~25 m of water. We complemented the time-series data with profiling data and ice thicknesses across a selected transect, and continuous measurements of meteorological conditions (Fig. 1 – star) near the lake. Finally, we measured water velocities at the center of the basin with an Acoustic Doppler Current Profiler (ADCP) located between the two thermistor chains (M3).

## Results and discussion

The conductivity signal that slowly increased through the winter begins dropping around Day 96 (Fig. 2a) indicating an increased ice-melt rate at the surface. In the days leading up to ice-off (Days 104 – 116; ice-off at 114 – black line), there is a point when the water column becomes well mixed down to a depth of roughly 15 m (M1 – Fig. 2b) and 20 m (M2- Fig. 2c) at ~2.3 °C (Days 107 and 109 respectively). Following this, colder water (~2.0 °C) is shown to remain in place with warmer water (up to 2.4 °C) both above and below. The fact that this water is vertically unstable for 4-5 days suggests that the lateral pressure gradients are being balanced by rotation in this system through the potential presence of a gyre.

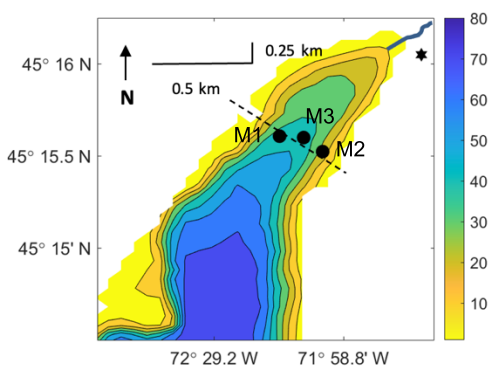


**Figure 1.** Lake Massawippi bathymetry map of northern basin with location of measurements, circles – mooring locations, star – meteorological station. Black dashed line is the transect line for CTD casts. The Tomifobia River outlet is at the northern end of the lake.

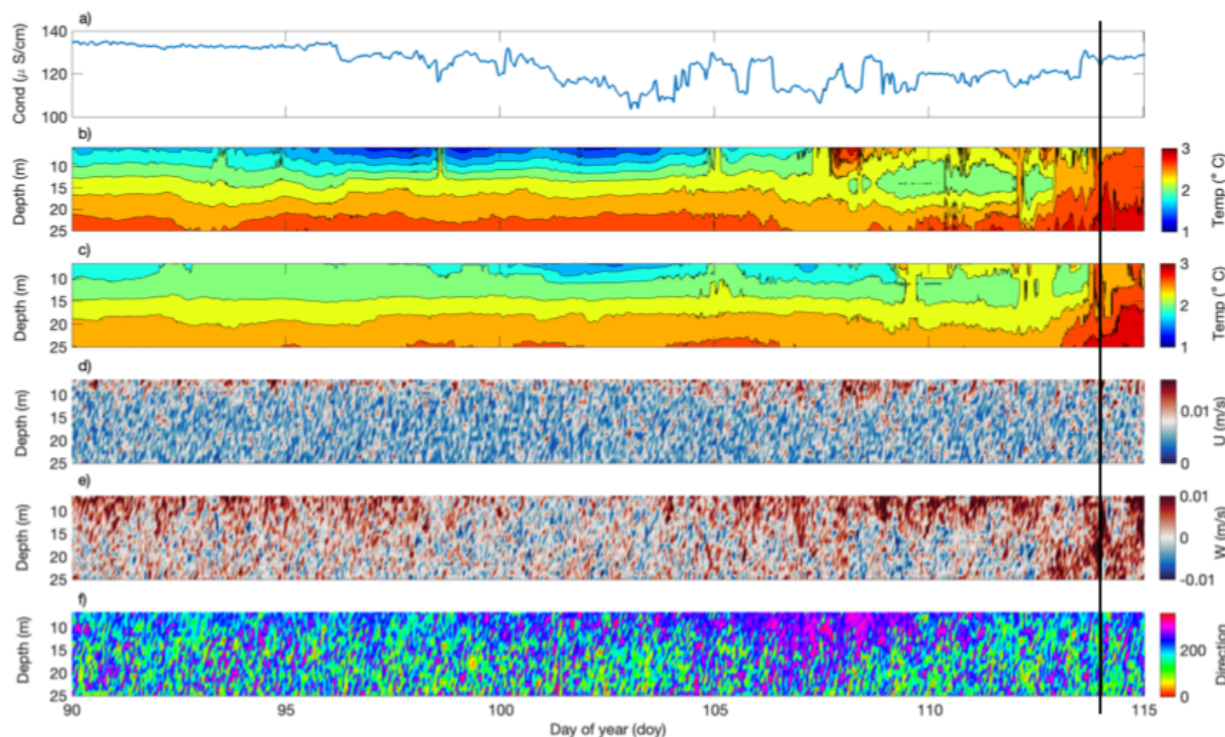


**Figure 2.** a) Water conductivity ( $\mu\text{S}/\text{cm}$ ) measured at 5.5 m water depth. b) Water temperature ( $^{\circ}\text{C}$ ) contours averaged at 10 minutes from a) M1 and b) M2. Hourly measurements from the ADCP including c) horizontal magnitudes, d) vertical velocities, and e) direction of flow from Day 90 to 115. Ice-off occurred on Day 114, denoted by thick black line.

Observations of velocity at M3 show that on Day 108, there is an increase in velocity magnitude up to 15 mm/s (Fig. 2d) moving towards the NW where the outlet is located (Fig. 2e). From Day 109-112, there is also a strong upwards vertical velocity signature (8-10 mm/s). Combining these observations of both temperature and velocity indicates a possible divergent flow with upwelling at the middle of basin. This gives rise to the conceptual model that a gyre has formed (Fig. 3) driving upwelling in the middle of the lake. Narrow lakes such as Lake Massawippi have the potential of supporting many such gyres if the forcing conditions are right that will potentially interact with both other gyres as well as the boundaries. Understanding the dynamics of these gyres in smaller ice-covered lakes is essential as they can drive deepwater ventilation, across- and along-slope transport. All of these processes will have implications for primary productivity of the lake during the summer months.

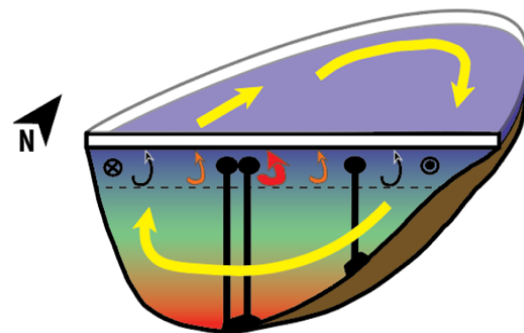


**Figure 3.** Conceptual model of formed cyclonic gyre in Lake Massawippi under-ice.

## REFERENCES

- Forrest, A. L., Laval, B. E., Pieters, R., & SS Lim, D. (2013). A cyclonic gyre in an ice-covered lake. *Limnology and Oceanography*, **58**(1), 363-375.
- Kouraev, A. V., et al. (2019). Giant ice rings on lakes and field observations of lens-like eddies in the Middle Baikal (2016–2017). *Limnology and Oceanography*, **64**(6), 2738-2754.

# Role of lake water balance on the intensity of surface cyanobacterial bloom

F. Hinegk<sup>1\*</sup>, S. Piccolroaz<sup>1</sup>, S. Speltoni<sup>1,2</sup>, M. Amadori<sup>1,3</sup>, S. Pozzi<sup>4</sup>, and M. Toffolon<sup>1</sup>

<sup>1</sup> Department Civil, Environmental and Mechanical Engineering, University of Trento, Trento, Italy

<sup>2</sup> Laboratory of Hydraulics, Hydrology and Glaciology (VAW), ETH Zurich, Zurich, Switzerland

<sup>3</sup> Institute for Electromagnetic Sensing of the Environment, National Research Council of Italy

<sup>4</sup> Agenzia Provinciale per la Protezione dell'Ambiente, Trento, Italy

\*Corresponding author, e-mail [francesca.hinegk@unitn.it](mailto:francesca.hinegk@unitn.it)

## KEYWORDS

Algal blooms; cyanobacteria; eutrophic lakes; hypolimnetic withdrawal.

## Introduction

Cyanobacterial blooms are a severe environmental issue in inland water bodies, due to their detrimental effects on water quality and to the potential harmfulness associated to the release of toxins by some species. Analyzing the relationships between the abundance of cyanobacteria and the environmental forcings is key for a better understanding of cyanobacterial dynamics and can provide useful tools for predicting and managing bloom events. In this study, we use statistical analysis and numerical modelling for investigating such relationships in Lake Serraia (Trentino, Italy).

## Materials and methods

Lake Serraia is a small and shallow eutrophic peri-alpine lake, which has undergone several anthropogenic modifications in the past decades. Its thermal stratification is heavily influenced by a hypolimnetic oxygenation system installed in 2006 (Toffolon et al., 2013) and its water balance is altered by a withdrawal that transfers the lake deep waters to an upstream lake for hydropower use, thus limiting the natural outflow. The lake is periodically affected by cyanobacterial blooms usually dominated by organisms of the *Dolichospermum* genus, which tend to float at the surface and impact both water quality and the recreational use of the lake.

Here we use multivariate linear regression to identify the most relevant environmental factors (meteorological forcing, inflows/outflows, lake level, water quality parameters) affecting the biovolume of cyanobacteria and other algae during blooms. For such an analysis we use water quality data collected by the local authorities with a near-monthly frequency during the ice-off period and discharge data of the main tributary and of the hypolimnetic withdrawal registered on a continuous basis by automatic gauging stations.

Based on the results, we propose a theoretical model to explain the development of *Dolichospermum* blooms in terms of the dominant physical transport processes and environmental factors. Then, a hydrodynamic three-dimensional model (Delft3D) of the lake is implemented for testing the theoretical model. A moderately buoyant tracer is introduced in the epilimnion as proxy of the *Dolichospermum* organisms and its residence time is examined to analyse the role of the hypolimnetic withdrawal on the dominant transport pathways.

## Results and discussion

When applied to all types of blooms, the multivariate linear regression analysis does not reveal any significant relation with hydraulic variables. Conversely, a trend is highlighted for the *Dolichospermum* biovolume, but limited to intense blooms solely, when *Dolichospermum* biovolume is negatively correlated with the difference  $\Delta Q$  between the inflowing discharge from the main tributary and the outflowing discharge through the hypolimnetic withdrawal during the weeks preceding the bloom. Such difference can be considered as a proxy of the outflow through the lake

natural outlet, hence of the water volume renewed in the surface layer. No significant correlations are found between  $\Delta Q$  and other types of phytoplankton monitored in this lake.

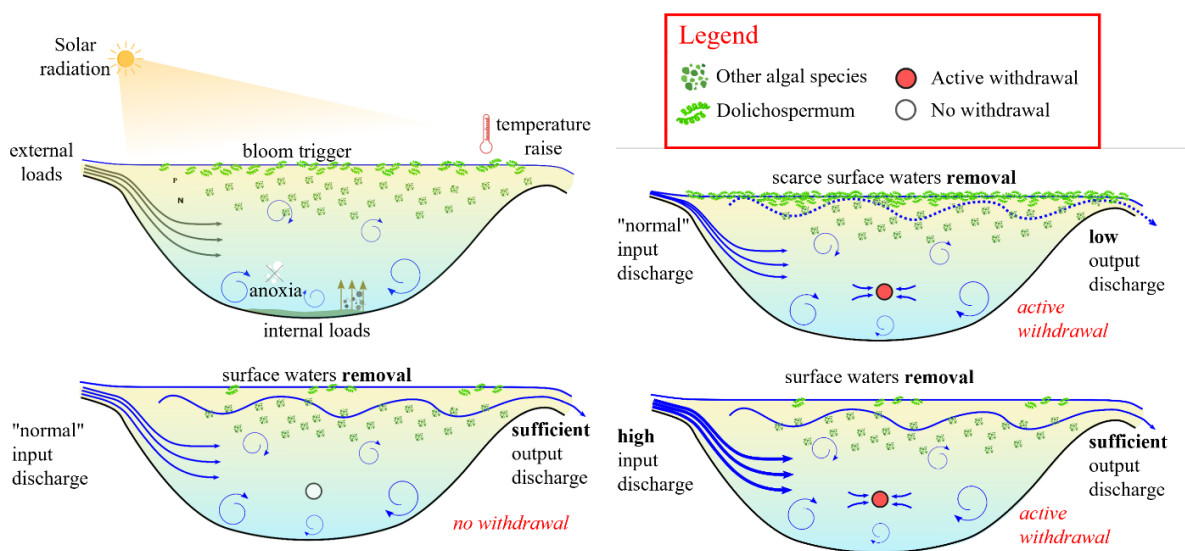


**Figure 1.** Scheme of the theoretical model of *Dolichospermum* blooms evolution hypothesized for Lake Serraia.

The correlation found suggests that enhancing the natural outflow, which implies increasing the flushing of the lake surface layer, may favour the removal of phytoplankton biomass during intense surface *Dolichospermum* blooms (Figure 1). This is confirmed by numerical simulations where  $\Delta Q$  is modulated by activating or deactivating the deep withdrawal: the modelled concentration of substances confined to the surface layers decreases slightly faster when  $\Delta Q$  is larger, thus supporting the results of the statistical analysis.

These results suggest that modulating the withdrawal might contribute to mitigate the intensity of surface *Dolichospermum* blooms in this lake, once they have been initiated and are developing. However, it cannot prevent the occurrence of these blooms, which are essentially triggered by nutrients, temperature and light conditions, nor affect the blooms of other types of phytoplankton that do not float at the surface.

## REFERENCES

- Toffolon, M., Ragazzi, M., Righetti, M., Teodori, C. R., Tubino, M., Defrancesco, C., & Pozzi, S. (2013). Effects of artificial hypolimnetic oxygenation in a shallow lake. Part 1: Phenomenological description and management. *Journal of Environmental Management*, 114, 520-529, DOI: 10.1016/j.jenvman.2012.10.062.

# Suspended particulate aggregation in a large, oligotrophic, freshwater lake following wildfire deposition

K. Larrieu<sup>1,2\*</sup>, Y. Song<sup>3</sup>, M. Rau<sup>4</sup>, A. Forrest<sup>1,2</sup>, and S.G. Schladow<sup>1,2</sup>

<sup>1</sup> Department of Civil and Environmental Engineering, UC Davis, Davis, California, USA

<sup>2</sup> UC Davis Tahoe Environmental Research Center, Incline Village, Nevada, USA

<sup>3</sup> Department of Mechanical Engineering, Penn State University, Pennsylvania, USA

<sup>4</sup> Department of Mechanical and Aerospace Engineering, George Washington University, Washington DC, USA

\*Corresponding author, e-mail [kglarrieu@ucdavis.edu](mailto:kglarrieu@ucdavis.edu)

## KEYWORDS

Suspended particulate matter; aggregation; settling; wildfire impacts; autonomous underwater vehicles

## Introduction

Freshwater lakes across the globe are impacted by increased nutrient and particulate loading rates which can lead to undesirable shifts in trophic state and water quality. In response, great efforts are taken by stakeholders to ensure that activity within a watershed does not contribute to degraded water quality. These concerns are especially prominent for Lake Tahoe, a uniquely large, deep, clear, historically ultra-oligotrophic alpine freshwater lake subjected to disturbances which increase allochthonous particulate loading such as wetland degradation, urban development, increasing severity and frequency of wildfires, and decreasing snowpack. All of these factors indicate that understanding suspended particle dynamics in the epilimnion and metalimnion of Lake Tahoe under changing environmental conditions is critical for maintaining the lake's renowned clarity and water quality. Fine ( $<10 \mu\text{m}$ ) particulate matter is especially concerning since smaller particles have lower sedimentation rates and scatter light more efficiently than larger particles. This combination of high residence time and scattering efficiency means that fine particulate matter can dominate impact on water clarity and photic depth, even when fine particles are present in relatively low volumetric abundance.

## Materials and methods

We present autonomous underwater glider-based observations of particle size distributions, chlorophyll-a, and CTD data in Lake Tahoe following episodic atmospheric deposition of wildfire smoke particulates from the 2021 Caldor Fire and 2022 Mosquito Fire. Additional measurements using a LISST-200X modified with a variable-speed pump assembly help to assess the presence of particle aggregates *in situ* (Ackleson and Rau, 2020). By tracking changes in the *in situ* particle size distribution under varying turbulent shear rates, we can estimate the size, strength, prevalence, and composition of particle aggregates which may be present in the water.

## Results and discussion

Glider-based observations indicate that fine particulates deposited at the surface were removed from the water orders of magnitude faster than would be predicted by simple settling (e.g. Stokes settling). Additionally, the sharpest gradient in particle concentrations closely coincides with the deep chlorophyll-a fluorescence maximum, suggesting the deep chlorophyll-a layer plays a role in controlling the residence time of fine suspended particulates (Figure 1).

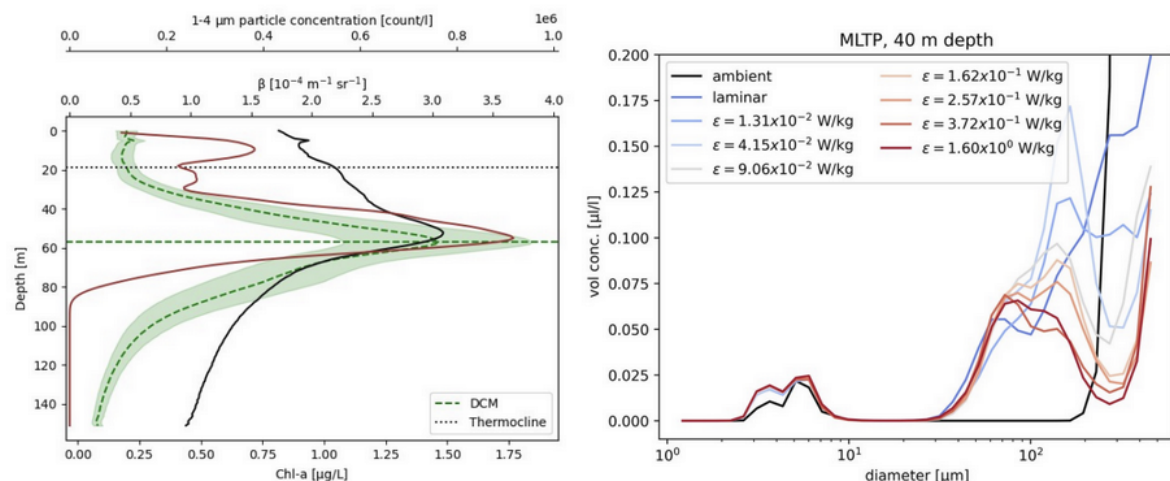


**Figure 1.** Left: Summer 2022 averaged glider profiles of chlorophyll-a (green line, with shaded standard deviations), optical backscatter (black line), and fine particle concentrations (brown line). Horizontal lines also indicate depths of the thermocline and deep chlorophyll-a maximum (DCM). Right: 2022 volumetric particle size distributions at 40 m depth at the mid-lake profiling location. Particle size distributions shown in the ambient condition (black line), and under progressively increasing levels of turbulence (blue to red lines).

Without exposure to strong shear (i.e. under ambient conditions), particle size distributions are dominated by size ranges 100 μm and greater. However when subjected to variable shear rates, shifts in the size distributions indicate that aggregates progressively breakup into significantly smaller constituent primary particles, with resultant size distributions and concentrations consistent with those of measured concentrations of the dominant phytoplankton taxa. Comparing observations between nearshore and mid-lake sites also suggest disparate particulate characteristics between these two locations. Nearshore particulate matter concentrations were greater overall, but with lower proportions of particle aggregates relative to the mid-lake station. These results hint at possible diatom-triggered aggregation of fine particulates in the epilimnion and metalimnion playing a significant role in fine particulate sequestration for the system as a whole. Lastly, ongoing developments of additional experiments and modeling efforts are discussed.

## REFERENCES

- Ackleson, S. G., and Rau, M. J. (2020). A method to measure marine particle aggregate disruption in situ. *Limnology and Oceanography: Methods*, **18**(11), 644–655. <https://doi.org/10.1002/lom3.10391>

# Climate change impacts on aquatic deoxygenation

K. Rose<sup>1\*</sup> and S. Jane<sup>2</sup>

<sup>1</sup>*Department of Biological Sciences, Rensselaer Polytechnic Institute*

<sup>2</sup>*Department of Natural Resources and the Environment, Cornell University*

\*Corresponding author; e-mail [rosek4@rpi.edu](mailto:rosek4@rpi.edu)

## KEYWORDS

Dissolved oxygen, climate change, lake stratification, mixing, temperature

## Introduction

The concentration of dissolved oxygen is an essential variable regulating the chemistry and biology of waterbodies, including both freshwater and marine ecosystems. This concentration is regulated by many factors, including water temperature, gross primary production, ecosystem respiration, and atmospheric exchange. Quantifying rates of change in dissolved oxygen is essential for understanding the impacts of climate change on processes such as greenhouse gas emissions, nutrient cycling, and food web dynamics.

## Materials and methods

We compiled and analysed >400 lakes dissolved oxygen and temperature data sets. We used government, academic, and non-profit sources to compile this data set, including soliciting data from collaborators in GLEON, the Global Lake Ecological Observatory Network. Nearly all lakes were in the temperate zone (23.5° to 60° latitude north and south). We included lakes in the dataset if there was at least one annual profile during the peak summertime stratification (defined as the late summer period, from 15 July to 31 August for northern hemisphere lakes, and 15 January to 28 February for southern hemisphere lakes) for at least fifteen years. In total there were 45,148 dissolved oxygen and temperature profiles spanning 1941 to 2017. Individual lake datasets ranged in sampling frequency and observation period length; there was a median of 2.1 profiles per year and 23 years of data per lake. We used R LakeAnalyzeR to define the depth and occurrence of a hypolimnion in each profile (Read et al. 2011). We also calculated trends in air temperature near each lake over the same time period of observation.

## Results and discussion

Our analyses showed that lake DO concentrations have declined in both surface waters and deep waters over the period 1980 to 2017 by 0.45 and 0.42 mg l<sup>-1</sup>, respectively (Jane et al. 2021). These rates represent losses of 5.5% and 18.6% for surface and deep waters, respectively. These rates are substantially greater than those observed for the oceans, where total water-column DO has declined about 2% since 1960 (Schmidtko, Stramma, and Visbeck 2017).

Epilimnetic deoxygenation was primarily associated with reduced solubility at higher temperatures, with epilimnetic water temperatures increasing by 0.39 °C decade<sup>-1</sup> over the study period and median air temperatures warming at 0.30 °C decade<sup>-1</sup>. Hypolimnetic deoxygenation was not associated with changes in temperature and oxygen solubility. Deep-water temperatures were essentially unchanging over the study period (median trend: (-0.01 °C decade<sup>-1</sup>)). Instead, hypolimnetic deoxygenation was associated with stronger and longer seasonal stratification and water clarity losses. Stratification strength increased in 84% of lakes and was also correlated with the duration of stratification (Jane et al. 2022). Overall, lakes increased in stratification duration by 3.7 days decade<sup>-1</sup>, with shifts in both the onset (1.2 days decade<sup>-1</sup>) and breakdown of stratification (2.5 days decade<sup>-1</sup>). Separately, water clarity losses exceeding 1 m were associated with substantial reductions in deep-water DO saturation, however overall median trends in clarity were stable.

Median seasonal hypolimnetic oxygen depletion rates were essentially unchanged, indicating potentially limited impacts of increased biological respiration contributing to widespread lake

deoxygenation. These increases in the duration of stratification and associated deoxygenation have driven substantial increases in the volume of low-oxygen waters. Lakes have experienced summertime increases in the amount of low oxygen water by 0.9-1.7% per decade, depending on the threshold concentration examined. The duration of seasonal thermal stratification is predicted to continue to increase due to climate change (Woolway et al. 2021). As a result, lake deoxygenation is likely to become an even more pervasive and severe issue.

Because the concentration of dissolved oxygen regulates factors such as aquatic carbon cycling, nutrient cycling, and biodiversity, widespread deoxygenation in both lakes and in marine ecosystems has the potential to alter major Earth-system processes and should be considered among Earth's Planetary Boundaries (Rockström et al. 2009). The fact that lake deoxygenation is driven primarily by a longer stratified season and not watershed-specific processes is a challenge to the efficacy of local management efforts.

## REFERENCES

- Jane, Stephen F., Gretchen J. A. Hansen, Benjamin M. Kraemer, Peter R. Leavitt, Joshua L. Mincer, Rebecca L. North, Rachel M. Pilla, et al. (2021). Widespread Deoxygenation of Temperate Lakes. *Nature* **594** (7861): 66–70. <https://doi.org/10.1038/s41586-021-03550-y>.
- Jane, Stephen F., Joshua L. Mincer, Maximilian P. Lau, Abigail S. L. Lewis, Jonathan T. Stetler, and Kevin C. Rose. (2022) Longer Duration of Seasonal Stratification Contributes to Widespread Increases in Lake Hypoxia and Anoxia. *Global Change Biology*, December, gcb.16525. <https://doi.org/10.1111/gcb.16525>.
- Read, Jordan S., David P. Hamilton, Ian D. Jones, Kohji Muraoka, Luke A. Winslow, Ryan Kroiss, Chin H. Wu, and Evelyn Gaiser (2011). Derivation of Lake Mixing and Stratification Indices from High-Resolution Lake Buoy Data. *Environmental Modelling & Software* **26** (11): 1325–36. <https://doi.org/10.1016/j.envsoft.2011.05.006>.
- Rockström, Johan, Will Steffen, Kevin Noone, Åsa Persson, F. Stuart III Chapin, Eric Lambin, Timothy M. Lenton, et al. (2009). Planetary Boundaries: Exploring the Safe Operating Space for Humanity. *Ecology and Society* **14** (2): art32. <https://doi.org/10.5751/ES-03180-140232>.
- Schmidtko, Sunke, Lothar Stramma, and Martin Visbeck (2017). “Decline in Global Oceanic Oxygen Content during the Past Five Decades.” *Nature* **542** (7641): 335–39. <https://doi.org/10.1038/nature21399>.
- Woolway, R. Iestyn, Sapna Sharma, Gesa A. Weyhenmeyer, Andrey Debolskiy, Małgorzata Golub, Daniel Mercado-Bettín, Marjorie Perroud, et al. (2021). “Phenological Shifts in Lake Stratification under Climate Change.” *Nature Communications* **12** (1): 2318. <https://doi.org/10.1038/s41467-021-22657-4>.

## Observing and predicting the global coastal ocean

N. Pinardi<sup>1\*</sup>

<sup>1</sup>*UN Decade Collaborative Center for Coastal Resilience, Alma Mater Studiorum University of Bologna*

\*Corresponding author; e-mail [nadia.pinardi@unibo.it](mailto:nadia.pinardi@unibo.it)

Coastal areas are where most of the world's population lives and where the response to the UN Decade's challenges will have the largest impact. The concept of the 'Global Coastal Ocean' is transformational, as it highlights the phenomena that control how land and offshore ocean waters interact to create a complex system, strongly impacted by human activities on both local and global levels. Coastline geometries produce the sea level response to multiple forcing factors and regulate the deep ocean circulation through the dissipation of energy on the shelf. Thus, the global coastal ocean contains processes that are key for the ocean climate. The presentation will overview the state-of-the-art operational forecasting from the global ocean to the coasts and the system technological components. The UN Decade Programme CoastPredict (<https://www.coastpredict.org/>) is planning the improvements of global and basin-scale operational ocean forecasting that have made open and free information available at kilometric scales. These capabilities enable the design of integrated observing and forecasting systems for the coastal areas.

# Physical and ecological effects of climate change on a eutrophic lake

R. Schwefel<sup>1\*</sup>, S. Jordan<sup>1</sup>, S. Krishna<sup>2</sup>, M. Hupfer<sup>1</sup>

<sup>1</sup>*Leibniz-Institute of Freshwater Ecology and Inland Fisheries, Berlin, Germany*

<sup>2</sup>*Helmholtz-Zentrum Hereon, Geesthacht, Germany*

\*Corresponding author, e-mail [robert.schwefel@igb-berlin.de](mailto:robert.schwefel@igb-berlin.de)

## KEYWORDS

Climate Change; Numerical Modelling; Lake Arendsee

## Introduction

In this study, the impact of climate change on the thermal structure of lakes and resulting consequences for the lake ecosystem will be investigated on the example of Lake Arendsee. Lake Arendsee is a groundwater-fed lake located in north-eastern Germany. With a surface area of 5.1 km<sup>2</sup> and a maximum depth of 49 m, Lake Arendsee is one of the largest lakes in northern Germany. Due to two large caving-in events in the Middle Ages, it consists of one large elliptical deep basin with steep slopes, resulting in a comparatively deep mean depth (~28 m) compared to other lakes in this region. The lake has been severely eutrophicated since the 1950s resulting in annual mean TP levels of up to 200 µg/L in 2009 accompanied by extensive developments of cyanobacteria and low transparencies. In the recent past, total phosphorus concentrations decreased only slowly to approximately 170 µg/L, rates of oxygen depletion remained high and large parts of the hypolimnion become anoxic during summer. Regular long-term monitoring data are available since the end of the 1960s, high-frequency monitoring is established since 2012. The combination of strong anthropogenic eutrophication and a wealth of monitoring data makes Lake Arendsee a perfect site to study the combined impact of direct man-made changes and climate change.

## Methods

We analysed long-term monitoring data since the 1960s in combination with high-frequency data since 2012 from a mooring equipped with temperature and oxygen loggers and an automatic profiler measuring various parameters several times per day. In addition, we ran a set of 1D numerical models (Flake, GOTM, and Simstrat) to assess the impact of climate change. As meteorological forcing, we used the data from the nearest meteorological station for calibration and validation and a set of predictions based on different combinations of global circulation models and regional climate models for three different emission scenarios (“DWD-Kernensemble” RCP 2.6, 4.5, RCP 8.5; 5 to 6 model combinations per emission scenario). GOTM will be coupled with the biogeochemical model ERGOM.

## Results and discussion

The long-term monitoring data show increasing trends in surface temperatures with highest increases in late spring/early summer and autumn. (~0.7 °C/Decade compared to 0.02 - 0.04 °C/Decade during other seasons). The average trend is at the upper end of the predictions by Flake based on the reference period 1970-2005 (in average 0.35 °C/Decade ranging from 0.09°C/Decade to 0.61°C/Decade depending on the climate model). In contrast, bottom temperatures showed no increase at all which is in line with global observations (Pilla et al. 2020). As a result, model results show an increase in the stratified period during summer. While the increase in surface temperatures is comparable to other dimictic German lakes (Figure 1a), the extension of summer stratification in deeper lakes like Lake Arendsee is higher compared to more shallow lakes.

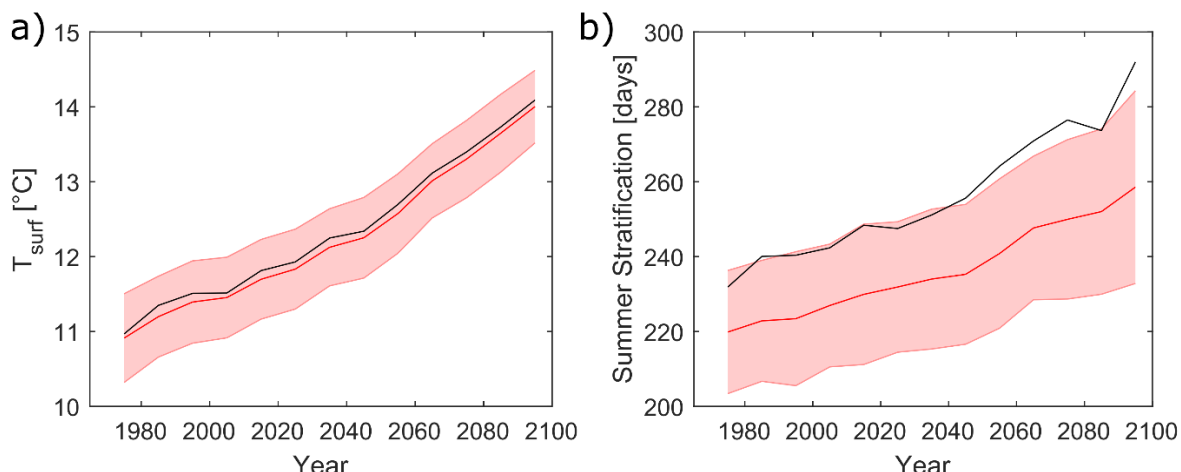


**Figure 1:** (a) Surface temperatures according to the IPCC emission scenario RCP 8.5 (average over all considered climate models) in Lake Arendsee (black) and in a set of 11 dimictic German lakes (mean value as red line with standard deviation as shaded red area). (b) same as panel a) for the duration of summer stratification.

The response of the ecosystem on these changes is complex. Observations confirm that higher temperatures increase the productivity in spring, but later in the year, Chl-A becomes anticorrelated with temperatures. This is likely due to reduced transport of nutrients through a more stable thermocline. Areal hypolimnetic oxygen depletion (measured below 15 m) increased until the decade 200-2010 and is falling slowly since approximately 2010. However, oxygen consumption in the metalimnion increased in the recent past and in 2019 and 2020, exceptionally high oxygen depletion rates were measured. The reason for this increase is not fully understood yet. Despite tendentially sinking depletion rates, the increase in the stratified period in the future has the potential to intensify the problem of bottom hypoxia and the duration during which reduced substances can diffuse out of the anoxic sediment in summer (anoxic age; LaBrie et al. 2023).

## REFERENCES

- LaBrie, R., M. Hupfer, and M. P. Lau. (2023). Anaerobic duration predicts biogeochemical consequences of oxygen depletion in lakes. *Limnology and Oceanography Letters*. doi:10.1002/lol2.10324
- Pilla, R. M. et al. (2020). Deeper waters are changing less consistently than surface waters in a global analysis of 102 lakes. *Sci Rep* **10**:20514. doi:10.1038/s41598-020-76873-x

# Ranking the meteorological factors influencing lake surface water temperature across different climates

A. Yousefi<sup>1\*</sup>, S. Piccolroaz<sup>1</sup>, M. Amadori<sup>1,2</sup> and M. Toffolon<sup>1</sup>

<sup>1</sup>Department of Civil, Environmental and Mechanical Engineering, University of Trento, Trento, Italy

<sup>2</sup>CNR-IREA, Institute for the Electromagnetic Sensing of the Environment, Milano, Italy

\*Corresponding author; e-mail [azadeh.yousefi@unitn.it](mailto:azadeh.yousefi@unitn.it)

## KEYWORDS

Lake Surface Water Temperature; Machine learning; Globolakes; CCI; Climate change.

## Introduction

Predicting lake surface water temperature (LSWT) has become important for assessing the trend of global warming and its effect on lacustrine environment. Data-driven models, and in particular machine learning (ML) methods, are more flexible than physically-based models because they do not need to assume a well-defined conceptual model of the physics of the lake. However, they typically require a large number of observations for their training and testing. Exploiting the flexibility of ML models and the increasing access to LSWT observations also thanks to remote sensing, we investigate the influence of different meteorological variables on LSWT in around 2000 lakes worldwide using Backpropagation Neural Network (BPNN) as a ML approach. The accuracy of the prediction is also investigated to determine for the suitability of such method in cases with low numbers of valid data from remote sensing time series.

## Materials and methods

The LSWT is retrieved from the ESA-CCI dataset providing long-term global LSWT data (<http://cci.esa.int/lakes>). LSWT time series for 2024 lakes are obtained by spatially averaging the LSWT maps based on quality flags. As features (inputs) time series, seven meteorological variables are obtained from ERA5 reanalysis (<https://www.ecmwf.int/en/forecasts/dataset/ecmwf-reanalysis-v5>): air temperature 2 m above the lake surface (AT), wind speed (WS), air pressure (AP), rainfall (R), snowfall (S), specific humidity (SH), longwave and shortwave radiations (LWR and SWR). To obtain a more accurate representation of the variables affecting LSWT, we smooth these time series by weight averaging based on their positive autocorrelation lag. In order to account for the effect of seasonality, the day of the year (DOY) is also used as an additional feature considering  $\sin(\text{DOY})$  and  $\cos(\text{DOY})$  (Yousefi and Toffolon, 2022). The lakes are classified into 5 regions based on the Köppen climate classification in tropical, dry, temperate, continental, and polar climates. We employ BPNN (Chen et al., 2011) for predicting LSWT from ERA5 inputs. The ranking of the features is then accomplished by randomly shuffling the single features and evaluating the deterioration of the model's performance in each lake. The results are then grouped by climate regions.

## Results and discussion

The performance of the BPNN using all features (Figure 1, right) is satisfactory in many cases (a reasonable target for daily RMSE is between 1 and 2°C). The median of RMSE for training and test set is 1.60 and 1.65°C, respectively. The results exhibit lower accuracy in the snow and polar regions likely because of the lowest amount of available LSWT data due to cloudiness.

These preliminary findings, hopefully with further refinements of the modelling process that may lead to improved accuracy and robustness in the results, will be used to assess if the most influential features change depending on the climate region.

The feature importance analysis (Figure 1, left) revealed that  $\sin(\text{DOY})$  and  $\cos(\text{DOY})$  are the most influential features in all regions, suggesting that the climatological year is already a good predictor

in many climate regions, given the strong seasonal variability of LSWT. AT appears to be dominant as often assumed except for tropical region. Within temperate regions, AT assumes significant importance as the 3<sup>rd</sup> most influential predictor, owing to its heightened sensitivity to LSWT in comparison to other regions (e.g., Piccolroaz et al., 2020). Further influential factors are LWR and SH. Other features, like snowfall and rainfall, are not influential (Fujisaki-Manome et al., 2020). These preliminary findings, hopefully with further refinements of the modelling process that may lead to improved accuracy and robustness in the results, will be used to assess if the most influential features change depending on the climate region.

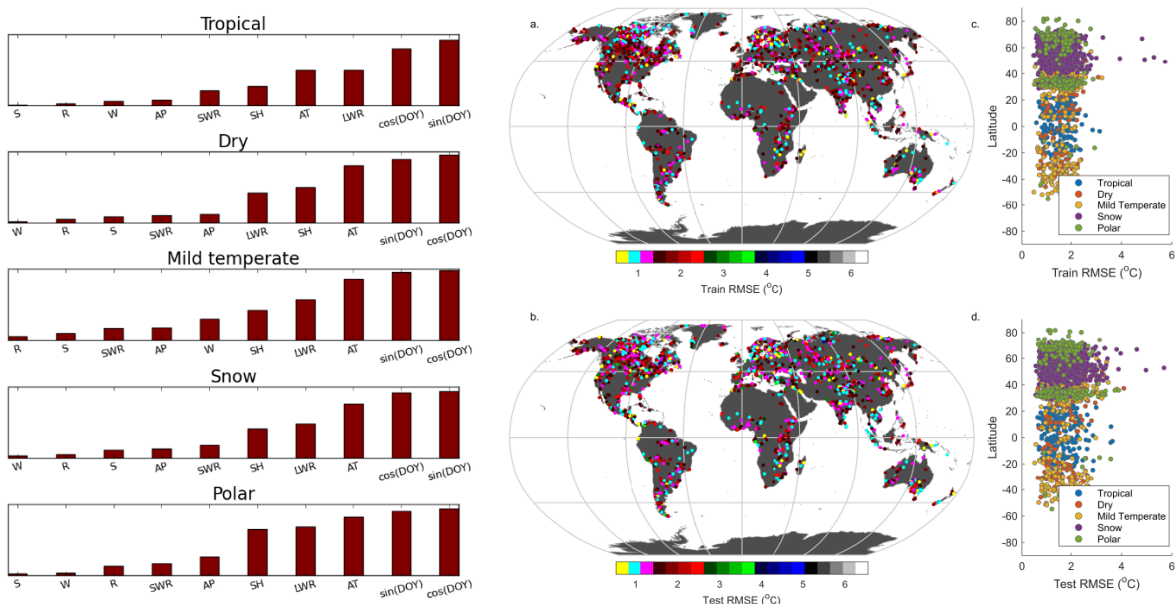


**Figure 1.** The feature importance of meteorological data in Köppen regions obtained by the BPNN model (left), and RMSE of the BPNN model for both training (a and c) and test (b and d) sets (right).

## REFERENCES

- Chen, H. L., Yang, B., Wang, G., Liu, J., Xu, X., Wang, S. J., & Liu, D. Y. (2011), A novel bankruptcy prediction model based on an adaptive fuzzy k-nearest neighbor method, *Knowledge-Based Systems*, 24(8), 1348-1359, doi:10.1016/j.knosys.2011.06.008
- Fujisaki-Manome, A., Anderson, E. J., Kessler, J. A., Chu, P. Y., Wang, J., & Gronewold, A. D. (2020). Simulating impacts of precipitation on ice cover and surface water temperature across large lakes. *Journal of Geophysical Research: Oceans*, 125(5), e2019JC015950. <https://doi.org/10.1029/2019JC015950>
- Piccolroaz, S., Woolway, R. I., & Merchant, C. J. (2020), Global reconstruction of twentieth century lake surface water temperature reveals different warming trends depending on the climatic zone. *Climatic Change*, 160(3), 427-442, doi:10.1007/s10584-020-02663-z
- Yousefi, A., & Toffolon, M. (2022), Critical factors for the use of machine learning to predict lake surface water temperature, *Journal of Hydrology*, 606, 127418, doi:10.1016/j.jhydrol.2021.127418

# Long-term evolution of European perialpine lakes water resources under management factors

L. Hinegk<sup>1\*</sup>, L. Adami<sup>1</sup>, M. Tubino<sup>1</sup>

<sup>1</sup> Department of Civil, Environmental and Mechanical Engineering,  
Università degli studi di Trento, Trento, Italy

\*Luigi Hinegk, e-mail [luigi.hinegk@unitn.it](mailto:luigi.hinegk@unitn.it)

## KEYWORDS

European perialpine lakes; lake levels and outflows; water management; lake regulation; historical analysis.

## Introduction

Multiple water uses and their long-term changes are a distinctive feature of several European perialpine lakes, which were mostly dammed during the second half of the XX century to effectively address changes mainly in hydropower production, irrigation water needs and flood control. Very few of these lake systems succeeded in maintaining their natural conditions. In this regard, strong alterations of the river flow regime have been observed in highly regulated systems through dam operations and water management policies in compliance of the high number of water demands (e.g., Vicente et al., 2017). Comparative studies that also include the historical evolution of the lake water level alongside with the lake outflow are however limited in the European perialpine context, and even less studies have considered lake's alterations starting from a distant past, i.e. the XIX century. Given the highly value of the water resources and the fundamental role of management policies to sustain the high number of water ecosystem services in the area (Salmaso et al., 2018), here we drew attention to the long-term regime of lake levels and outflows for some of the highest regulated lakes of the European perialpine context (i.e. lakes Maggiore, Como, Iseo, Garda alongside with lakes Lugano, Geneva and Zürich) to investigate the multiple drivers of alteration of their pre-regulation regime.

## Materials and methods

The daily data of lake levels and outflows were collected by consulting both online sources and historical documents. A large number of historical data of the Italian lakes were copied by hand from the scanned documents of the Italian Annual Hydrology books and Hydrological Bulletins (Servizio Idrografico, 1917). Such data were integrated by exploring different database (e.g., the Global Runoff Data Centre portal), existing works (e.g. Ranzi et al., 2018 for Lake Como) and contacting national and regional agencies (e.g., the Federal Office for the Environment of Switzerland). The resulting database enabled to analyse data since the XX century, reaching back the second half of the XIX century for several of the lakes considered (i.e. lakes Garda, Como, Zürich and Maggiore). On such basis, we tested the statistical significance of the data collected (e.g. implementing the non-parametric Mann Kendall method), also analysing data at the seasonal scale to consider the influence of other factors than dam construction on lake levels and outflows variation.

## Results and discussion

An example of massive modifications caused by dam construction is presented for Lake Garda in Figure 1. The lake impoundment in 1951 determined a storage-like functioning pattern of the post-regulation lake levels, with high values recorded from January to March (winter season) and significant low values registered during the summer season to support the large irrigation water requirements within the downstream basin. Similar results were observed for the other Italian lakes considered, revealing the common dam management policies that characterize the Po River basin. Other drivers than dam construction of the lake levels and outflows variation are revealed by Lake

Geneva, with consistent changes since the 1970s attributed to the hydropower plants construction and the related concession contracts (Ruiz-Villanueva et al., 2015) or by Lake Zürich, which management policies highlights the importance of considering flood events.

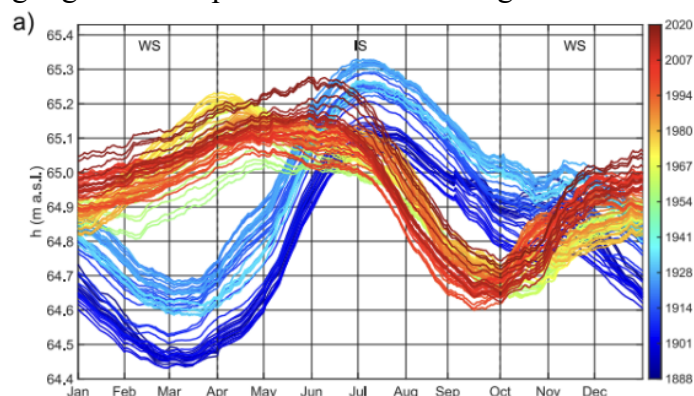


**Figure 1.** Daily annual cycle of Lake Garda water levels over the period 1888-2020. IS = Irrigation Season (1<sup>st</sup> April-30<sup>th</sup> September). WS = Winter Season (1<sup>st</sup> October-31<sup>th</sup> March).

Our first results outline multiple causes in the alteration of the lake levels and outflows for several European perialpine lakes, with major shifts of the annual cycle caused by lake impoundment, changing water management policies or increasing hydraulic infrastructures within the basin. These findings additionally pose into question the role of climatic factors in both the short and long-term variations of lake levels and outflows and stress the need of a detailed quantification of the main water requirements that characterise such regulated systems to design future sustainable water management policies.

## REFERENCES

- Ranzi, R., Michailidi, E. M., Tomirotti, M., Crespi, A., Brunetti, M., and Maugeri, M. (2020). Multi-century (1800-2016) meteo-hydrological series for the Adda river basin (Central Alps). PANGAEA
- Ruiz-Villanueva, V., Stoffel, M., Bussi, G., Francés, F., and Bréthaut, C. (2015). Climate change impacts on discharges of the Rhone River in Lyon by the end of the twenty-first century: model results and implications. *Reg. Environ. Change*, **15**(3):505–515.
- Salmaso, N., Anneville, O., Straile, D., and Viaroli, P. (2018a). European large perialpine lakes under anthropogenic pressures and climate change: present status, research gaps and future challenges. *Hydrobiologia*, **824**(1):1–32.
- Servizio Idrografico - Ministero dei Lavori Pubblici (1917). Annali idrologici - parte prima e seconda. *Annali idrologici*.
- Vicente-Serrano, S. M., Zabalza-Martínez, J., Borràs, G., López-Moreno, J. I., Pla, E., Pascual, D., Savé, R., Biel, C., Funes, I., Martín-Hernández, N., et al. (2017). Effect of reservoirs on streamflow and river regimes in a heavily regulated river basin of northeast Spain. *Catena*, **149**:727–741.